



**Politecnico
di Torino**

**HE^{VD}
IG**

Master's degree course in Environmental and Land Engineering, specialist
pathway in Natural Hazards and Civil Protection

Master's Thesis

Vulnerability assessment of buildings to landslide

Supervisors:

Dr. Daniele MARTINELLI

Prof. Erika PRINA HOWALD

Candidate:

Laura FRANCONI

Academic Year 2021/2022

ACKNOWLEDGEMENTS

Firstly, I would like to thank my professor Daniele Martinelli who proposed this thesis at the Haute Ecole d'Ingénierie et de Gestion du Canton de Vaud- HEIG-VD, in Yverdon-Les-Bains, Switzerland; he was always helpful and kind in supporting and giving me explanations about my work. I sincerely thank Professor Erika Prina Howald for providing me this opportunity to do my thesis abroad; this experience allowed me to grow up both academically and personally/culturally. I am very grateful to Torche Jérémy and Tanja Miteva who closely welcomed, encouraged and motivated me in this experience.

Furthermore, I would like to thank Simone, Mattia, Giovanni for the moments of leisure but also of intense work and study spent together in Yverdon-les-Bains; thanks to all collaborators, all people I met at work and in the residence where I was staying, always very kind, helpful and friendly.

I would like to sincerely thank my boyfriend Andrea who helped, endured, and supported me during my thesis and in my daily life. I thank infinitely Claudia, Laura, and Anna for their support, for the wonderful times we spent together, for always being there despite the distance, for true friendship born in high school. I would like to thank all my friends in Turin with whom I have spent the most leisure moments, the best evenings, the better holidays; all the friends I have met at university since my early years, who have accompanied me throughout this entire path, sharing moments of crazy study but also of great fun.

Last but not least, I express all my gratitude to my entire family, my parents, my grandparents, my sisters and my brother for always believed in me, encouraged, supported and helped me to achieve my objectives.

ABSTRACT

Natural hazards such as floods, landslides, debris flows, earthquakes and fires cause a great number of disasters worldwide every year. Loss of life, physical and economic damage to facilities and infrastructures lead to large yearly monetary losses; in Switzerland, from 1972 to 2021, damage resulting from floods, landslides, debris flows and rockfalls amount to approximately CHF 300 million per year. Climate change, settlement development and increasing land use are some of the main triggers of natural hazards.

The interaction between landslide phenomena, urban and non-urban areas with annexed facilities and infrastructures, has become more relevant in recent years, where there are considerable losses related to the social and economic impact of the affected areas. Permanent landslides, among all the different typologies, generally have a lower probability to produce catastrophic events, but they can lead structural damage to buildings and infrastructures. This is the reason for the great interest of the scientific communities in identifying the most suitable solutions for risk mitigation associated with this type of phenomena.

The present thesis contains an initial introduction in which landslides are classified according to type, triggers and impact, followed by a review of the existing literature on the cases analysed to date. The aim of this thesis is the vulnerability analysis about selected building typologies exposed to the action of permanent landslides. Four building locations on the landslide body were chosen, using the necessary simplifications: the top part (A), the central part (B), the boundary between the moving mass and the stable slope (C) and the foot of the landslide (D); a vulnerability analysis was carried out on each one, the evaluation of which is based on the definition of intensity (I) and resistance parameter (R). The methodology developed results in vulnerability curves reported both by type of building considered and by its position within the landslide body.

The method was applied to four case studies located in the SOUTH-WEST part of Switzerland: Hohberg Landslide, Converney-Taillepiep Landslide, Pont Bourquin Landslide and La Frasse Landslide; the latter refer to permanent landslides moving at a rate of a few cm/years, which evolve, periodically and depending on the triggering cause, into earth and mud flows or rockfall phenomena.

The results show how the four case studies considered validate the proposed methodology as they fall within the range of values used to construct the vulnerability curves.

SOMMARIO

I pericoli naturali come alluvioni, frane, colate detritiche, terremoti, incendi, provocano ogni anno numerose catastrofi a livello mondiale. La perdita di vite umane, i danni fisici ed economici a strutture e infrastrutture portano annualmente ad ingenti perdite di denaro; si stima che in Svizzera dal 1972 al 2021, i danni indotti da alluvioni, frane, colate detritiche e caduta massi abbiano causato un deficit annuale di circa 300 milioni di franchi. Il cambiamento climatico, lo sviluppo degli insediamenti e il crescente sfruttamento del territorio sono alcune tra le maggiori cause scatenanti dei pericoli naturali.

L'interazione tra fenomeni franosi, aree urbane ed extra urbane con annesse strutture e infrastrutture, è diventata maggiormente rilevante negli ultimi anni, dove si contano ingenti perdite legate all'impatto sociale ed economico delle aree colpite. Le frane permanenti, tra tutte le diverse tipologie esistenti, hanno generalmente una probabilità minore di generare eventi catastrofici, ma possono comportare danni strutturali ad edifici ed infrastrutture; questo è il motivo per cui c'è un grande interesse da parte delle comunità scientifiche nell'identificazione delle strategie più appropriate per la mitigazione dei rischi associati a questa tipologia di fenomeni.

La presente tesi contiene una prima parte introduttiva dove si classificano le frane sulla base della tipologia, delle cause di innesco, dell'impatto, per procedere con una revisione della letteratura esistente sui casi analizzati fino ad oggi. L'obiettivo della tesi è l'analisi di vulnerabilità di alcune tipologie di edifici esposti all'azione di frane permanenti. Si sono scelte, adottando le dovute semplificazioni, 4 collocazioni degli edifici sul corpo frana: la parte sommitale (A), la parte centrale (B), il confine tra massa in movimento e il pendio stabile (C) e il piede della frana (D); per ognuna di esse si è svolta l'analisi di vulnerabilità la cui valutazione è basata sulla definizione dell'intensità (I) e del parametro di resistenza (R). La metodologia sviluppata ha come risultato le curve di vulnerabilità riportate sia per tipologia di edificio considerato che per posizione di quest'ultimo all'interno del corpo frana.

Il metodo si è applicato a quattro casi studio collocati nella parte SUD-OVEST della Svizzera: Hohberg Landslide, Converney-Taillepied Landslide, Pont Bourquin Landslide e La Frasse Landslide; quest'ultimi fanno riferimento a frane permanenti

in movimento con una velocità di pochi cm/anno, che evolvono, periodicamente e a seconda della causa innescante, in colate di terra e fango o in fenomeni di caduta massi. I risultati dimostrano che i quattro casi studio considerati validano la metodologia proposta in quanto ricadono nel campo di valori utilizzato per la costruzione delle curve di vulnerabilità.

LIST OF FIGURES

Figure 1: Nomenclature used to define different parts of a landslide.....	5
Figure 2: Diagram of hazard levels as a function of probability and intensity, BAFU 2015	13
Figure 3: View of the Leysin plateau from the Rhone valley. The syncline is visible, as are the limestone lamellae on the rear flank, (Matti, Tacher et Commend 2012).....	21
Figure 4: Both pictures, in the upper part, show wooden chalets, while the picture in the lower part shows wooden chalets with concrete foundation, destroyed by the landslide, source: La Liberté.....	22
Figure 5: Cantonal Cartographic Map legend in which landslides are divided according to speed and then again divided according to depth, source: Guichet cartographique cantonal, Canton de Vaud	23
Figure 6: Illustrates Monte Toc, volume of landslide involved and the location of the Vajont dam.....	26
Figure 7: Masonry buildings affected by cracks and deformations, in 2005 compared to 2011	26
Figure 8: Severe damage to buildings, roadways, and infrastructure caused by large landslide in Stazzone quarter (a,b), in Riana quarter (c,d) e in san Benedetto porcaro quarters (e,f).....	27
Figure 9: Buildings (a,b,c) and roads (d) affected by deformations due to landslide mouvement.....	29
Figure 10: Area related to the Monte La Saxe landslide, in the municipality of Courmayeur	30
Figure 11: Two images that show the houses destroyed by the 2001 earthquake in San Salvador.....	32
Figure 12: The left-hand image shows a wooden house destroyed by the landslide, the right one representing Oso landslide volume	33
Figure 13: There are houses, made of stone and masonry, visibly damaged by landslide body	34
Figure 14: Examples of stone and masonry buildings in the Krini village	36
Figure 15: Gjedrum landslide,Norway, 30 December 2020, source: BBC news.....	37
Figure 16: Houses and flats damaged by the Gjedrum landslide, source: BBC news.....	37
Figure 17: Schematic section showing the most relevant part of the Landslide body, (Bonnard, Forlati and Scavia 2003).....	41
Figure 18: Landslide velocity scale, source: (Hungr, Leroueil et Picarelli 2013)	43
Figure 19: Characteristics of Lungro Landslides, source: (P. G. Peduto D. 2016)	44

Figure 20: Integral decline state of the case study building: (a) the back wall of the building with an inclination of 1.0 %, (b) the front wall of the building with an inclination of 0.8 %, (c) the front wall of room) with an inclination of 0.7 %, (source: (Chen, et al. 2020)).....	49
Figure 21: Examples of threshold value of foundation displacement for different structures, source: (Li, et al. 2010).....	49
Figure 22: The 4 chosen building positions that represent respectively: A building located on the crown of the landslide body, B building located on the lateral edge of the landslide body, C building located in the middle of the landslide body and D building located at the foot of the landslide body.....	51
Figure 23: An example of a vulnerability curve.....	68
Figure 24: Vulnerability curves obtained for case A when the depth of the sliding surface is less than 2 metres	70
Figure 25: Vulnerability curves obtained for case A when the depth of the sliding surface is assumed between 2 and 5 metres	70
Figure 26: Vulnerability curves obtained for case C when the depth of the sliding surface is assumed between 5 and 30 metres	71
Figure 27: Vulnerability curves obtained for case C when the depth of the sliding surface is higher than 30 metres.....	71
Figure 28: Chalet vulnerability curves obtained for case B	72
Figure 29: Residential villa vulnerability curves obtained for case B	73
Figure 30: Residential building vulnerability curves obtained for case B	73
Figure 31: Vulnerability curves obtained for case D when the maintenance state is very poor	74
Figure 32: Vulnerability curves obtained for case D when the maintenance state is medium	75
Figure 33: Vulnerability curves obtained for case D when the maintenance state is very high	75
Figure 34: Local tectonic context of the Hohberg landslide area, (Dapples 2002)	78
Figure 35: Vulnerability curves and indicators obtained for case A when the depth of the sliding surface is assumed between 2 and 5 metres.....	79
Figure 36: Chalet vulnerability curves and indicators obtained for case B	83
Figure 37: Location of La Frasse Landslide with subdivision in 5 main portions, (Matti, Tacher et Commend 2012).....	84
Figure 38: Vulnerability curves and indicators obtained for case C when the depth of the sliding surface is assumed to be higher then 30 metres	86
Figure 39: Pont Bourquin landslide area, near les Diableres, (Jaboyedoff, et al. 2015)	87

Figure 40: Vulnerability curves and indicators obtained for case D when the maintenance state is very poor	89
Figure 41: Vulnerability curves and indicators obtained for case D when the maintenance state is medium	90
Figure 42: Vulnerability curves and indicators obtained for case D when the maintenance state is very high.....	90
Figure 43: Les Diableres village, located in the municipality of Ormont-Dessus, Canton of Vaud, Switzerland	91
Figure 44: Physical vulnerability curves of buildings with different parameters: (a) length and (b) width, source (Chen, et al. 2020)	93

LIST OF TABLES

Table 1: Description of the terms used to illustrate different parts of a landslide	5
Table 2: Landslide classification based on type of movement and type of material developed by Hungr, et al. 2013	7
Table 3: Classification of landslide causal factors, Mihail E. Popescu , Technology Illinois Institute, Chicago, USA	10
Table 4: Classification of landslide remedial measures, Mihail E. Popescu , Illinois Institute of Technology, Chicago, USA	11
Table 5: General factors considered in vulnerability assessment.....	17
Table 6: Factors involved in building vulnerability estimation	18
Table 7: Values of depth, area and number of buildings on the landslide bodies	23
Table 8: Summary of the selected historical landslides	38
Table 9: Summary of structures vulnerable to landslides proposed in the following work.....	42
Table 10: Classification of foundation depth compared to landslide debris depth, (Li, et al. 2010)	45
Table 11: Velocities and related damage that may affect buildings and interior spaces, (Egli 2005)	45
Table 12: Depth classification of landslide, source: (Parkash 2020)	46
Table 13: Evaluation of classes of failure surface depth and of the landslide velocity presented in this work.....	46
Table 14: Threshold value of building inclination where H denotes the building height which is calculated from the outdoor ground (Ministry of Housing and Urban–Rural Development of PRC, 2016), source: (Chen, et al. 2020)	48
Table 15: Parameters chosen in this work, for each of the 4 building locations on the landslide body.....	51
Table 16: Conventional damage severity scale, source: Mercalli's scale (DRM 1990)	53
Table 17: Damage assessment, based on speed, proposed in this work for cases A, B and C	53
Table 18: Damage assessment, based on impact pressure, proposed in this work for cases D	54
Table 19: 4 speed ranges used for the construction of vulnerability curves.....	58
Table 20: 4 debris depth ranges used for the construction of vulnerability curves.....	58
Table 21: Intensity classification provided by this work, cases A, B and C	59
Table 22: Height values and their sources.....	60
Table 23: Velocity ranges and their sources	60
Table 24: Intensity classification provided by this work, case D	60

Table 25: Failure surface depth ranges considered in this work.....	63
Table 26: Scores relating to the type of building construction material used in this work	63
Table 27: Scores relating to the building inclination used in this work.....	65
Table 28: Scores relating to the number of floors/height used in this work	65
Table 29: Scores relating to the type of building construction material used in this work	66
Table 30: Scores relating to the maintenance state used in this work.....	67
Table 31: Explanation of the vulnerability curve legend cases A and C	68
Table 32: Explanation of the vulnerability curve legend case B	69
Table 33: Explanation of the vulnerability curve legend case D	69
Table 34: Data used in the methodology application for case A , landslide crown.....	79
Table 35: Data used in the methodology application for case D , landslide toe	79
Table 36: Data used in the methodology application for case C , landslide central part.....	82
Table 37: Data used in the methodology application for case D , landslide toe	82
Table 38: Data used in the methodology application for case C , landslide central part.....	85
Table 39: Data used in the methodology application for case D , landslide toe	85
Table 40: Data used in the methodology application for case C , landslide central part.....	89
Table 41: Data used in the methodology application for case D , landslide toe	89

TABLE OF CONTENTS

ACKNOWLEDGEMENTS.....	i
ABSTRACT.....	ii
SOMMARIO.....	iv
LIST OF FIGURES.....	vi
LIST OF TABLES.....	ix
TABLE OF CONTENTS.....	xi
Chapter 1: INTRODUCTION.....	1
1.1 Aim of this work	1
1.2 Preface	2
1.3 Landslide	3
1.3.1 Landslide classification	6
1.3.2 Landslide causes	9
1.3.3 Landslide impact and remedial measures.....	10
1.3.4 Landslide hazard management in Switzerland	12
1.4 Landslide Risk and Vulnerability	13
1.4.1 Vulnerability Factors.....	16
Chapter 2: LITERATURE REVIEW	19
2.1 Historical studies.....	19
2.2 Landslide in Switzerland.....	19
2.2.1 La Frasse Landslide, Vaud Alps, 1990	20
2.2.2 Falli-Hölili Landslide, Fribourg, 1994.....	21
2.2.3 Landslide Geodata of the Canton of Vaud, (Federal Office of Topography)	22
2.3 Landslide in Italy.....	24
2.3.1 Deep gravitational deformation of Cassas slopes (Val di Susa Italy) ..	24

2.3.2	Vajont Landslide, Longarone, 1963	25
2.3.3	Slow-moving landslide of Lungro, Calabria (Southern Italy)	26
2.3.4	Large landslide affected the urban centre of San Fratello, Sicily (Southern Italy)	27
2.3.5	Deep gravitational deformation of the eastern slope of the Amiata mountain in Southern Tuscany 2011	28
2.3.6	Mont de La Saxe landslide in the municipality of Courmayeur	29
2.4	Landslide worldwide	31
2.4.1	Séchilienne Landslide	31
2.4.2	Landslide in Santa Tecla, near San Salvador 2001	32
2.4.3	Hazel Landslide, Oso, United the States	33
2.4.4	North Salt Lake Slide, Utah 2014	34
2.4.5	Active Landslides in Achaia, Peloponnese, Greece	35
2.4.6	Gjerdrum landslide, Norway, 2020	36
2.5	Summary of selected landslides	38
Chapter 3: LANDSLIDE TYPE		39
Chapter 4: PARAMETERS INVOLVED IN VULNERABILITY AND DAMAGE ASSESSMENT		42
4.1	Types of buildings structure vulnerable to landslide	42
4.2	Parameters involved in buildings vulnerability	43
4.2.1	Landslide body parameters	43
4.2.2	Building parameters	47
4.2.3	Damage assessment	52
Chapter 5: METHODOLOGY		55
5.1	Intensity	56
5.1.1	Evaluation of Landslide Intensity and parameters used in the proposed methodology	57
5.2	Vulnerability function	61

Chapter 6: VULNERABILITY CURVES	68
6.1 Results	69
Chapter 7: CASE STUDIES.....	76
7.1 Hohberg Landslide (FR)	76
7.1.1 Study area and available dataset.....	76
7.1.2 Geological Context.....	77
7.1.3 Results	78
7.2 Converney-Taillepiep Landslide	80
7.2.1 Study area and available dataset.....	80
7.2.2 Hydrogeological Context	81
7.2.3 Results	82
7.3 La Frasse landslide	83
7.3.1 Study area and available dataset.....	83
7.3.2 Hydrogeological Context	85
7.3.3 Results	85
7.4 Pont Bourquin landslide, Les Diablerets.....	86
7.4.1 Study area and available dataset.....	86
7.4.2 Geological Context.....	88
7.4.3 Results	89
Chapter 8: CONCLUSIONS.....	92
APPENDIX.....	95
REFERENCES.....	96

Chapter 1: INTRODUCTION

1.1 Aim of this work

This work analyses the vulnerability assessment of buildings to landslides. To accomplish the aim, firstly existing literature will be resumed to analyse types of building structure vulnerable to landslide; this thesis also contains a small section on historical studies previously made about landslide, buildings exposed to landslide risk and landslide intensity.

The objectives of this work are:

- Information gathering and analysis of input data
- Study of landslide hazard phenomena and its constraints
- Establish a brochure of type of building structure vulnerable to landslides
- Establish one or more parameters in order to classify intensity and landslide vulnerability
- Construction of vulnerability curves for all different predefined types of building structure to landslides

This work develops within a programme of two-year degree course of Natural Risks and Civil Protection, Department of Environmental and Land Engineering of the Polytechnic Institute of Turin. This master's thesis, elaborated at the university Haute Ecole d'Ingénierie et de Gestion du Canton de Vaud (HEIG-VD) in Yverdon les Bains (Switzerland), marks the end of two-year of study. It is performed in order to obtain the Master Degree in Environmental and Land Engineering.

1.2 Preface

Regarding natural hazard, landslides have one of the highest impacts worldwide in terms of loss of life, damage to public or private buildings, infrastructures, agricultural lands and economic activities. Population growth, hence more buildings in at-risk areas, climate change and intensification of land use have only increased the risk in recent years. Consequently, a rise in the frequency and intensity of natural disasters can be expected in the future: melting of glaciers and thawing of permafrost due to climate change threatens to displace huge amounts of soil, rock and stone, seriously endangering settlements and communication routes downstream (*Swiss Federal Institute for Forest, Snow and Landscape Research, WLS*). In 2021, for example, floods, landslides, debris flows and rockfalls caused damage in Switzerland of around CHF 300 million. This is the highest amount recorded since 2007.

An agency responsible for monitoring natural hazards and implements strategies to improve risk science is the *U.S.G.S. Natural Hazards Science Strategy*. There is an operations centre that continuously monitors natural hazards including landslide-prone areas. The *USGS* is considered to be at the forefront of hazard science because it has a team of scientists with expertise in many different fields and gathers information from academic partners worldwide.

From data analysis of the *Federal Office for the Environment*, the damage costs in Switzerland caused by floods, debris flows, landslides and collapse events between 1972 and 2020 amount to approximately CHF 300 million per year. Most of the damage was caused by single large flood events: i.e., 2005 flood, caused losses of CHF 3 million. The degree of damage is not only strongly influenced by land use (value and vulnerability of threatened objects), intensity and phenomenon size, but also by the measures taken to protect people, environment and property from natural hazards (*FOEN*).

Natural events can cause fatalities. The number of injuries depends on the event's magnitude, the individual's behaviour and the protective measures against natural hazards. It is therefore an indicator of the effectiveness of preventive measures for protection against natural hazards and of the appropriate behaviour towards danger on the population concerned. In the period 1946-2021, floods caused 125

deaths, debris flows 24, landslides 55 and collapse processes caused 96 deaths. On average, there have been 2.7 deaths each year since 1946 as a result of floods, debris flows and landslides, and 1.3 fatalities due to collapse processes (FOEN).

Several studies (Glade (2003); Soldati, et al. (2004); Imaizumi, et al. (2008); Borgatti et Soldati (2010); Gariano and Guzzetti (2016)) emphasise the importance of anthropogenic disturbance (land-use change), which could be more damaging to the future landslide incidence than climate change, despite the authors highlight significant uncertainties surrounding climate–landslide interaction. The analysis by Froude and Petley (*The global phenomenon of fatal landslides from 2004 to 2016*) showed that fatal landslides can be triggered by several causes: human activity (construction on hazardous terrain), illegal hill cutting, mining, etc.

Future research is needed to assess the economic, environmental and social impact that occurrence of a landslide produces; in this thesis, the landslide impact on buildings will be analysed.

1.3 Landslide

Landslide, also called landslip, is defined as movement of mass of rock, earth or debris down a slope, (Cruden 1991). Landslide is a type of "mass wasting," which refers to any down-slope movement of soil and rock under the direct influence of gravity, (U.S.G.S. Natural Hazards Science Strategy).

Landslide is a dynamic system developing in three main phases: the history of a mass movement comprises pre-failure deformations, failure and post failure displacements (Skempton and Hutchinson 1969). "*Failure is the single most significant movement episode in the known or anticipated history of a landslide, which usually involves the first formation of a fully developed rupture surface as a displacement or strain discontinuity*", definition given by Leroueil, et al. (1996). The failure phase can evolve into sliding, falling or flowing; this kinematic change is very relevant for the post-failure behaviour and destructiveness of the landslide. During the collapse, there is an overall loss of strength, which affects speed movement of the landslide post-failure.

A landslide occurs when shear stresses within a slope exceed shear strength of the material layers it is composed of. Shear stresses can be built up within a slope by different process: oversteepening of the base of the slope, rise in the groundwater table, slope loading due to inflow of water or debris accumulation on the slope's surface. While shear strength is mainly dependent on two factors: frictional strength, which is the resistance to movement between the slope material's interacting constituent particles, cohesive strength, which is the bonding between the particles and their spatial disposition.

Landslide can occur:

- in many materials with different mechanical properties: from hard rock to soft soil
- in different geographical contexts: from regions characterized by intense rainfall to arid zones
- in a wide range of geological and morphological settings
- with velocity ranges varying between mm/years and m/s
- with different types of movements
- involving a volume ranging between some m³ to hundreds of millions of m³

The following figure (*Figure 1*) shows the terms used to define a landslide; landslides may have common identifying characteristics, although there are several exceptions with very different features. The landslide begins with a displacement that causes an absence of material upstream, zone of depletion, and an accumulation of material downstream, accumulation zone. Many landslides present escarpments or scarps. The main scarp marks the upstream extension of the landslide and provides the visible part of the rupture surface. The landslide breaking surface is the boundary between the moving landslide body and the underlying geological material. Transverse cracks are formed when landslide's toe moves forward faster than the rest of landslide, resulting in tensional forces. Transverse ridges develop on the landslide edges where material is pushed upwards in a ridge structure. The toe of the landslide marks the end of the moving material, it indicates the maximum distance covered by the landslide. All descriptions of the terms used to define the landslide component parts are given in *Table 1*.

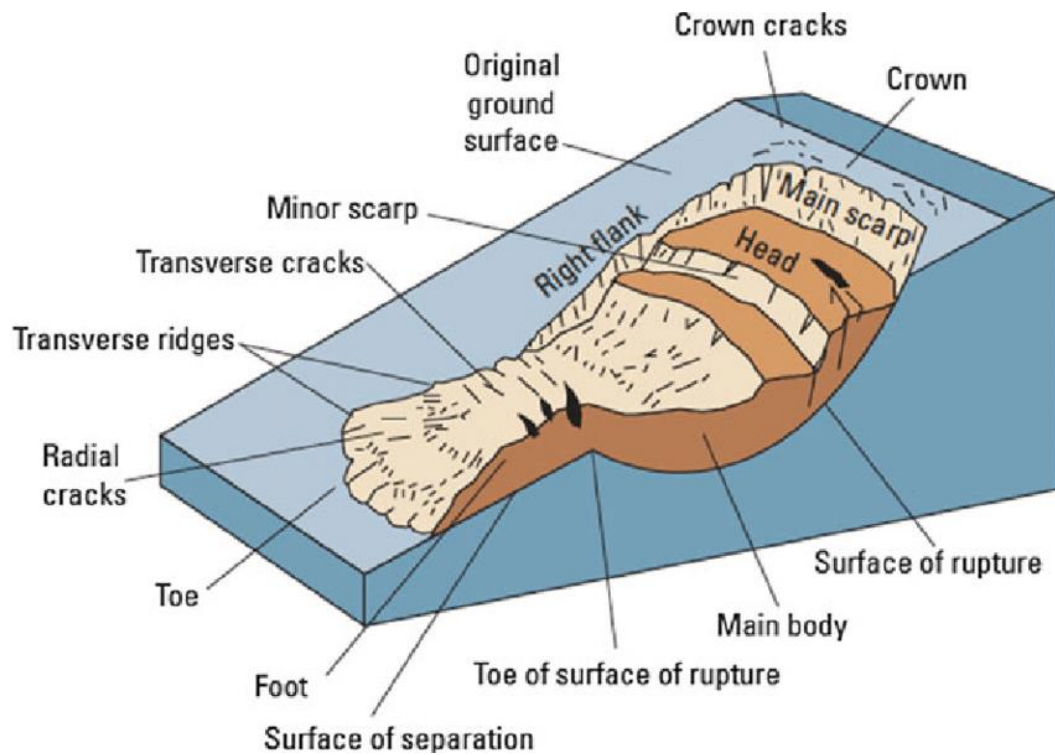


Figure 1: Nomenclature used to define different parts of a landslide

Table 1: Description of the terms used to illustrate different parts of a landslide

PARTS	DESCRIPTION
Crown	Undisturbed material located upstream the escarpment
Main Scarp	Is the visible part of the landslide surface. Steep slope on the top edge of the landslide body, generated by the movement of material detached from the undisturbed ground
Right Flank	Stable slope side describing the left and right lateral extension of the landslide body.
Rupture Surface/Slide Surface	Is the failure surface, the surface down which the material moves, representing the lower movement limit below the original ground surface
Main Body	Massive part of the landslide overlying the failure surface
Tension Cracks	Tension releases predicting landslide movement, usually found in the central part of the landslide body
Separation Surface	Part of the initial ground surface that is now overgrown by landslide material
Toe	The sloping end of the slide. The furthest part of the slide from the main escarpment

1.3.1 Landslide classification

Landslide classification is a difficult matter because it is based on several discriminating factors that sometimes are very subjective. The most widely used landslide classification system in the English language is the one defined by D.J. Varnes. Over time, the authors did not propose new classifications, but introduced modifications to that of Varnes, (Varnes 1954), to reflect recent developments in the understanding of landslide phenomena, materials and mechanisms involved. First modifications date back to 1978, Varnes (1978), and 1966, (Cruden & Varnes 1966) where updates were proposed regarding materials and movement mechanisms. Cruden & Varnes proposed separate names for the movement mode during each stage of a given landslide but we need practical statement to give a traditional terminology to a complex process. The number of classes in which it is possible to divide different landslides should be reasonably small to make the system simple and easy to use and review, (Hungr, Leroueil et Picarelli 2013). In England, Hutchinson (1968, 1988) developed a classification system primarily based on failure and propagation mechanisms together with material, morphology, water content, etc. An attempt to correlate Hutchinson's and Varnes' classifications was published by Hungr in 2001.

In the proposed new version of the landslide classification system (Hungr, Leroueil et Picarelli 2013) the term "landslide" encompasses six modes of slope movement:

- Falls
- Topples
- Slides
- Spreads
- Flows
- Slope deformation

This landslide classification and the types of material related to this subdivision can be seen in *Table 2*.

Table 2: Landslide classification based on type of movement and type of material developed by Hungr, et al. 2013

TYPE OF MOVEMENT	TYPE OF MATERIAL	
	Rock	Soil
Fall	Rock/ice fall	Boulder/debris/silt fall
Topple	Rock block topple	Gravel/sand/silt topple
	Rock flexural topple	
Slide	Rock rotational slide	Clay/silt rotational slide
	Rock planar slide	Clay/silt planar slide
	Rock wedge slide	Gravel/sand/debris slide
	Rock compound slide	Clay/silt compound slide
	Rock irregular slide	
Spread	Rock slope spread	Sand/silt liquefaction spread
		Sensitive clay spread
Flow	Rock/ice avalanche	Sand/silt/debris dry flow
		Sand/clay/silt/debris flow slide
		Debris/Mud/Earth/Peat flow
		Debris flood
		Debris avalanche
Slope deformation	Mountain slope deformation	Soil slope deformation
	Rock slope deformation	Soil creep
		Solifluction

Fall: rocks or boulders falling, bouncing, rolling from steep slopes or cliffs; the block is detached by separating from the intact rock along discontinuities, fractures or bedding planes; this movement may be triggered by gravity, by water freezing that increases in volume within the cracks and results in the block's detachment, by mechanical weathering.

Topple: mass of soil or rock which, under the action of gravity, the thrust exerted by adjacent units or the liquid circulating in fractures, performs a forward rotation about a point below the centre of gravity.

Slide: sliding of a mass of soil or rock down a slope; this sliding can occur either on the failure surface or in areas of intense shear deformation. The slipping can be translational when the landslide body moves on a planar surface or rotational when the surface is concave upwards.

Flow: movement of dry or fully saturated material with velocities similar to those of a viscous fluid; it usually occurs along shear surfaces that are, however, short-lived.

Spread: this phenomenon occurs when underneath a coherent material, such as rock or soil, there is a loose cohesionless material that becomes saturated and liquefies, creating fractures, rotations, slides, translations, subsidence, in the overlying coherent material.

Slope deformation: is a deep gravitational deformation that moves with slow velocities, hard to measure; it occurs in high mountains on steep slopes or escarpments, with fractures or bulges; it is difficult to identify a well-defined failure surface.

The above classification does not contain a separate class of complex landslides that are a combination of two or more main types of mechanisms. For example, rotational (or planar or compound) slide-earthflow is a relatively small landslide, where a sliding failure provides the source to an earthflow of limited extent. Therefore, it is simpler to give a composite name than to subdivide movements into sliding and flowing. Another classification of landslides can be made in relation to the state of activity and its evolution over time (*Varnes 1978*) and space (*Cruden & Varnes 1993*). Over time, it is possible to subdivide landslides into seven different states of activity:

- Moving, monitoring
- Moving during the last seasonal cycle, presently inactive
- Reactivated: active after a period of inactivity
- Dormant: inactive since more than one seasonal cycle, re-activation possible
- Abandoned: inactive, no more influenced by original triggers
- Stabilized: inactive after artificial protective measures
- Relict: “paleo-landslide”, inactive, occurred in extinct morpho-climatic settings

In space, it is possible to subdivide landslides into five different states of activity:

- Progressive: failure surface propagates downslope
- Retrogressive: failure surface propagates upslope
- Confined: failure surface does not daylight at the foot
- Moving: landslide body moves without failure surface change
- Widening: failure surface propagates towards landslide flanks

1.3.2 Landslide causes

Trigger causes are represented by an action which starts the movement of a slope. By definition a trigger is an external stimulus such as intense rainfall, snowmelt, storm waves or rapid stream erosion, earthquake, volcanic eruption that creates an immediate response in form of landslide. This is due to rapid increase in stress or reduction in the strength of the slope material.

A general definition of the slope safety factor F_s could concern the ratio between the downslope shear stress with the shear strength of the soil, along an assumed or known rupture surface. Concerning this definition, it is possible to subdivide landslide causes into external causes which result in an increase of shearing stress (geometrical changes, unloading the slope toe, loading the slope crest, shocks and vibrations, drawdown, changes in water regime), and internal causes resulting in a decrease of the shearing resistance (progressive failure, weathering, seepage erosion), (Terzaghi 1950). Varnes highlighted that both external or internal causes can operate together to reduce the shearing resistance or to increase the shear stress.

Actually, it is a chain of events that leads to the development of a landslide; it is more appropriate to discuss causal factors (including both “conditions” and “processes”) than “causes” alone. Casual process may be natural or anthropogenic but effectively change the static ground conditions sufficiently to cause slope failure, (Popescu 1984).

Landslide causes assessment is a complex issue because they are not always investigated in great detail, so it is reasonable to adopt a simple classification system of landslide causal factors. *WP/WLI Working Group on Causes of Landslides (1994)* collected and made available, from simple investigations and in situ observations, data on most known landslides. It was therefore possible to subdivide the causal factors of landslides according to effects and origins; in *Table 3* is shown a classification of landslide causal factors arranged in four main groups according with the tools and procedures necessary for documentation: ground conditions, geomorphological, physical and man-made processes.

Table 3: Classification of landslide causal factors, Mihail E. Popescu , Technology Illinois Institute, Chicago, USA

GROUND CONDITIONS	Plastic weak material or weathered material Jointed or fissured material Adversely oriented mass or structural discontinuities (including respectively bedding, schistosity or flexural shears, sedimentary contacts) Contrast in permeability and its effects on ground water (stiff, dense material over plastic material)
GEOMORPHOLOGICAL PROCESSES	Tectonic or volcanic uplift Fluvial/wave/glacial erosion of the slope toe Erosion of the lateral edges or subterranean erosion Deposition loading of the slope or its crest Vegetation removal (by erosion, forest fire, drought)
PHYSICAL PROCESSES	Intense, short period rainfall or prolonged high precipitation Rapid melt of deep snow Rapid drawdown following floods, high tides or breaching of natural dams Earthquake Volcanic eruption Thawing of permafrost and freeze and thaw weathering Shrink and swell weathering of expansive soils
MAN-MADE PROCESSES	Excavation of the slope or its toe Loading of the slope or its crest Drawdown (of reservoirs) Irrigation and defective maintenance of drainage systems Water leakage from services (water supplies, sewers, stormwater drains) Vegetation removal (deforestation) Mining and quarrying (open pits or underground galleries) Creation of dumps of very loose waste Artificial vibration (including traffic, pile driving, heavy machinery)

Of all the processes mentioned in *Table 3*, those leading to landslides with disruptive effects are: water, mainly heavy rainfall, seismic activity and volcanic activity.

1.3.3 Landslide impact and remedial measures

Within natural hazards, landslides have one of the highest impacts worldwide in terms of loss of life and injury to people as well as damage to public and private buildings, infrastructures, lifelines, agricultural lands and economic activities. Losses, as fatalities, physical asset damage and economic costs, occur when people, buildings, industry, environment are exposed to landslide. In order to assess the impact of a landslide, it is necessary to identify the elements at risk; these can be divided into four main categories:

- People: any person who may be killed, injured, permanently or temporarily
- Buildings: residential homes, public service or industry
- Infrastructures: roads, service activities, including transport, tourism, banking, trade, health etc.
- Environment: flora (forest, air, water, land), fauna (all animal species)

Landslides could be controlled by protective or preventive measures like: modification of slope geometry, drainage, retaining structures and internal slope reinforcement. For Hutchinson (1977), drainage is the measure mainly used for landslide repair, while slope geometry modification is the second most used method. Modification of slope geometry is the most efficient, particularly in deep seated landslides. Previous studies prove that while one remedial measure may be dominant, most landslide repairs involve the use of a combination of two or more major categories. *Table 4* shows a list of landslide remedial measures divided in four main classes.

Table 4: Classification of landslide remedial measures, Mihail E. Popescu , Illinois Institute of Technology, Chicago, USA

MODIFICATION OF SLOPE GEOMETRY	Removing material from the area driving the landslide or adding material to the area maintaining stability Reducing slope angle
DRAINAGE	Surface drains, shallow or deep trench drains, Drainage tunnels, galleries Counterforts of coarse-grained materials Vertical (small diameter) boreholes with pumping or self-draining or vertical (large diameter) wells with gravity draining Sub horizontal or subvertical boreholes Vegetation planting (hydrological effect)
RETAINING STRUCTURES	Gravity retaining walls, gabion walls or crib-block walls Passive piles, piers and caissons Reinforced earth retaining structures with reinforcement elements Retention nets for rock slope faces Rockfall attenuation or stopping systems (rock trap ditches, benches, fences) Protective rock/concrete blocks against erosion
INTERNAL SLOPE REINFORCEMENT	Rock bolts, micro piles or anchors (prestressed or not) Soil nailing Grouting Heat treatment or freezing Vegetation planting (root strength mechanical effect)

1.3.4 Landslide hazard management in Switzerland

In Switzerland, the national platform for natural hazard management is *PLANAT* founded in 1997. Natural hazards are very relevant in Switzerland, as in many places, and they present a significant threat to human life, infrastructure and material assets. The Federal Government envisaged an improvement in their management after the catastrophic events of the 1990s. The existing danger is accentuated by the construction of infrastructure, the expansion of settlements in risk areas and the effects of climate changes. The main factors influencing natural hazard processes are increase in hydro-meteorological events (frequency and intensity of rainfall) and effects of rising temperatures. The fields of intervention concern: flooding in the alpine (PN1) and valley (PN2) environment, torrential (PN3) and rockfall processes (PN4) and forest protection (PN5).

The knowledge and data from phenomena of recent decades form the basis for current laws and for the 'Natural Hazard Strategy in Switzerland' drawn up by *PLANAT*. The general objectives of the strategy are also relevant to the fields of action on adaptation to climate change and can be summarised as follows:

1. Guarantee of a generally accepted level of security on the basis of uniform criteria;
2. Reduction of existing risks and prevention of new risks;
3. Efficient use of instruments for the optimal reduction of existing risks and prevention of new risks.

To ensure homogeneous management of the different types of natural hazards that affect Switzerland (floods, snow avalanches, landslides, etc.), each canton prepares hazard maps that, according to federal law, have to be considered in land-use plans. Each hazard is classified using two main parameters: intensity and probability based on frequency and return period. Each hazard map divides the territory into zones according to five danger levels, shown in *Figure 2*:

1. Red → high danger: people are in danger inside and outside buildings, buildings can be destroyed, no new building areas have been defined in this zone
2. Blue → medium danger: people are in danger outside the buildings, buildings may be damaged

3. Yellow → low danger: almost no danger to people, little damage to buildings
4. Yellow and white → residual danger: same as yellow zone
5. White → no known danger or negligible danger

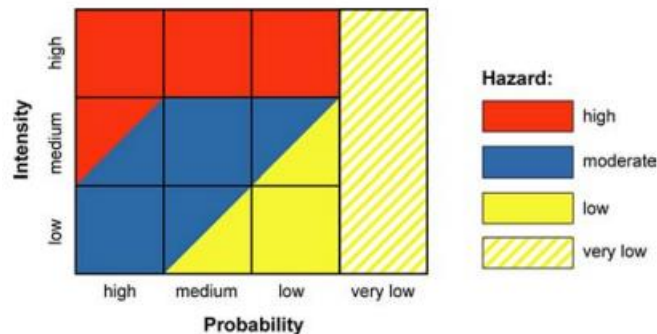


Figure 2: Diagram of hazard levels as a function of probability and intensity, BAFU 2015

These damage levels indicate the degree of danger to people, animals and property. In the case of landslides, i.e. mass movements characterised by a certain speed, people are considered safer inside buildings than outside.

Secondly, the Swiss Confederation has defined various preventive measures in the management of natural hazards in order to avoid or reduce the associated damage:

1. Land-use planning measures has to ensure, on the basis of hazard maps, that the construction of new buildings does not lead to an increase in risk
2. Organisational measures: measures leading to a reduction in the extent of damage
3. Technical measures: protective measures affect the damage by reduction or protection of the elements at risk
4. Biological measures: measures related to natural engineering: works concerning the reduction of bank erosion, grassing, etc.

1.4 Landslide Risk and Vulnerability

Landslide Risk

A first theoretical description is given by Varnes in 1984: “Risk is the probability of a given magnitude multiplied by its consequences”. Since then, many technical and scientific papers have been written on this topic (*Hungr 1981; Hutchinson 1992; Cruden & Varnes 1994; Leroi 1997*). Landslide Risk could be also defined as: measure of the probability and severity of an adverse effect to life, health, property, or

environment; it considers all the consequences of the landslide hazard. The risk value is defined by the following product:

$$R = pi * Val * V$$

Equation 1

Where:

- **V** is the **vulnerability**
- **pi** is the **impact probability**: mathematical product between **hazard** and **exposure**. For static element at risk, the exposure is equal to 1 so the impact probability is equal to the **hazard** (probability that a given potential destructive phenomenon, of a given intensity, occurs in a given time and in a given area).
- **Val** is the **value of the element at risk**: value in terms of cost, public utility, environmental importance for each element at risk. The following types of values are usually considered:
 - **Physical**: cost of the element
 - **Economical**: related to the manufacturing or commercial activities
 - **Social**: related to presence of people of social utility
 - **Environmental**: related to flora and fauna

Vulnerability

Vulnerability is a fundamental component in the evaluation of landslide risk, and its accurate estimation is essential in making a reasonable prediction of landslide consequences. According to the glossary of risk-assessment terms of the *International Society of Soil Mechanics and Geotechnical Engineering*, vulnerability is “the degree of loss to a given element at risk, or set of such elements, exposed to the occurrence of a landslide of a given magnitude/intensity”. It is usually expressed on a scale ranging between 0 (no loss) and 1 (total loss). For real estate, the loss will be damage value compared to the asset amount; for people, it will be the probability that a life will be lost when a damaging event occurs. Vulnerability is linked to the intensity of the phenomenon and to the characteristics of the element at risk. Since vulnerability is considered one of the main elements of risk analysis, many different estimates have been made in the literature. In 1996 Finlay provided some recommended ranges and value of vulnerability of person in open space, in a vehicle

or in a building and he introduced the damage matrix (structural, corporal and functional) for landslide hazard to assess the vulnerability to buildings, road, person. In 2005 Duzgun and Lacasse created a 3D conceptual framework with magnitude (M), scale (S) and elements at risk for assessing vulnerability. In 2008 Remondo estimated vulnerability of transport infrastructure, land resources and buildings from detailed analysis of past damage during 50 years in a specific study area. One method to calculate vulnerability was the ratio between the economic loss divided by the corresponding net values of the exposed elements. Always in 2008 Zezere gave the vulnerability of structures and roads under different slide intensities based on experience of historic data, in combination with the information which structure type, age, number of floors, etc. In 2008, Uzielli quantitatively defined physical vulnerability to landslides as a function of landslide intensity and susceptibility of vulnerable items.

Unlike other natural processes, it is very difficult to assess landslide vulnerability due to the complexity and to the wide range of landslide process. In 2003 Glade highlighted that the different effects included several factors like:

- Temporal probability of people being physically there during the landslide event is variable
- Human beings have a different capacity to deal with the hazardous event
- Presence of warning systems has an influence on people's vulnerability

Research has considered the different impacts due to many different landslide processes: Heinimann in 1999 assessed vulnerability by estimating it for several types of landslide events. Despite research and efforts to estimate the vulnerability of landslide elements, the main limitation of this approach is that most of the data must be assumed.

In fact, two different types of methods can be highlighted in previous studies to assess vulnerability: a qualitative analysis and a quantitative one. Qualitative analysis is very common today and is mainly used in regional medium- and small-scale landslide risk evaluation. There are two main qualitative analysis methods: one is by rating the structure type, use frequency, people density of buildings and the hazard intensity divided into three classes (high, medium or low), (*Cardinali, et al. 2002; Zhang, et al. 1998; Reichenbach 2005*). The other is expressed by

distribution map of economic value based on the land use maps by remote sensing or from the local government, (Tang 2005; Yin 2004). Quantitative analysis on building vulnerability, on the other hand, relies on real or historical data, numerical models or statistical analysis. (Galli & Guzzetti 2007; Bell & Glade 2004; Luo 2000).

1.4.1 Vulnerability Factors

Vulnerability estimation is a complicated matter because it is influenced by many factors; it is analysed by several researchers to understand the elements on which it depends primarily. It is possible to subdivide the vulnerability factors, as mentioned in the *IMIRILAND project* (Bonnard, Forlati and Scavia 2003), in physical, social, environmental and economic components.

Physical vulnerability

This term is defined as the degree of loss of a given element or set of elements at risk when they are impacted by an unstable mass. This impact has to be analysed in terms of structural failure by considering the deformation capacity of the building when it is hit by blocks of rock or a mass moving at a certain velocity. Physical damage depends on several factors including: the state of maintenance of the structures, the material used in their construction, especially if it is wood, which deteriorates easily if not treated properly. Main criteria for determining physical vulnerability value are: phenomenon intensity, the structure state of maintenance together with the type and function of the building and its deformation capacity.

Social vulnerability

This term describes the impact that a hazardous event (landslide) may have on the population, including the temporary or permanent disability that may result along with the psychological consequences of losing home. The factors contributing to the assessment of social vulnerability are: the population's ability to understand the phenomenon reacting with appropriate actions and phenomenon intensity in relation to warning signals.

Environmental vulnerability

The environmental impact that a landslide can have mainly concerns the deforestation of a slope section and damage to flora and fauna. The main criteria for assessing this type of vulnerability are: the intensity of the phenomenon, the

generally destructive effect on nature and the risks to animals, plants and ecosystems.

Economic vulnerability

This term expresses the economic damage resulting from the impact of the landslide body with roads, railway lines, water mains or power lines. If the landslide ends in a lake, it can lead to problems both upstream with flooding and downstream with landslides flowing with very high velocities. The main criteria for assessing this type of vulnerability are: the economic activities affected, the types of services involved such as industry, transport or tourism, traffic and cost linked to the infrastructure blockade.

According to the definition of *International Society of Soil Mechanics and Geotechnical Engineering*, it is possible to define vulnerability as a function on both the typology of the elements at risk (E) and the landslide intensity (I):

$$V = f(I, E)$$

Equation 2

Vulnerability assessment can refer to different subjects such as humans, buildings, environment, infrastructure, etc. The general factors that need to be considered for vulnerability estimation are reported in *Table 5*.

Table 5: General factors considered in vulnerability assessment

GENERAL FACTORS FOR VULNERABILITY ESTIMATION	landslide volume
	landslide run-out
	extent of the area involved
	depth of the landslide failure surface
	resistance ability of the element at risk
	impact energy
	presence of protection elements
	landslide surface displacement
	characteristics of the neighbouring slopes
	slope geology
	presence of water inside the slope
	presence of vegetation
	presence road/railway lines
	presence of lifelines
	presence of buildings with particularly vulnerable populations (hospitals, elderly nursing homes, kindergartens, schools, jails)
	presence of buildings with high economic importance

In this work vulnerability assessment of building to landslide is analysed; several factors, contained in *Table 6*, are therefore involved in building vulnerability evaluation.

Table 6: Factors involved in building vulnerability estimation

<p>FACTORS INVOLVED IN BUILDING VULNERABILITY ESTIMATION</p>	<p>building's type building's location in the landslide body depth of building foundations inclination of buildings foundation material used in the construction of building and foundations (concrete, masonry, timber) material's strength used in building's construction building's construction age building's maintenance state building deformation number of floors of which a building is made up, location of person within the damaged structure people density inside buildings possible presence and size of windows position of the wall impact point detailed geometry of the walls</p>
---	--

In the following chapters, three specific types of buildings will be assessed, taking into consideration the above-mentioned factors; a possible estimation of this parameters will be given in order to obtain a vulnerability assessment by means of vulnerability curves.

Chapter 2: LITERATURE REVIEW

2.1 Historical studies

The analysis of historical studies provides the opportunity to identify landslide-prone areas on the basis of past events and to learn about development of the phenomenon and its possible evolutions. This study is also of great interest for future spatial planning, both in determining the danger areas and in implementing the most suited prevention and protection measures.

The literature review presented in this chapter aims to collect the greatest amount of data about damage caused by landslides to people (injured, dead), environment, and infrastructure (roads, buildings). Historical events relating to different countries worldwide are reported, with the main focus on Italy and Switzerland.

The purpose of this literature review is to clarify which parameters are fundamental in the prevention of landslide damage, and then to focus the subsequent analysis on buildings and on characteristics they must have in order to prevent them. The data on selected landslides will be summarised in *Table 8*, at the end of this chapter, in order to make them easier to analyse.

2.2 Landslide in Switzerland

In Switzerland, unstable areas (including all slide-prone areas) correspond to 6-8% of the surface area. These zones are mainly located in the Alpine and pre-Alpine arc, but are also found in the Jura and the Swiss Plateau (Mittelland). Ground movements include events with volumes ranging between a few m³ to several km³ and velocities varying between mm/years to tens of m/s.

The melting of glaciers and the decreasing stability of permafrost due to thawing and freezing cycles are becoming increasingly frequent. Recently in the Alps, there have been several rock collapses and numerous landslides; many millions of cubic metres of rock have fallen into the valley from Pizzo Cengalo (Bergell valley) in the Grison canton; in addition, the Aletsch glacier, the Moosfluh, is slipping and breaking up. In this context, prevention measures, implementation of safety measures such as protective works and monitoring become increasingly important.

On-site risk assessment is the responsibility of Cantonal authorities; in order to reduce risks associated with natural hazards, together with the Cantons and Municipalities, Federal Government monitors and finances measures within the scope of integrated risk management for natural hazards.

The following is a list of the main landslide events that have taken place in the Canton of Vaud in recent years:

- 1990: Champ Chamot a Belmont, landslide and debris flow
- 1999: La Saussaz a Villars-sur-Ollon, massive landslide threatened dozens of chalets
- 1999-2006: les Roches in Vallamand, major landslides which led to the permanent evacuation of 16 houses and required the securing of the Sugiez-Salavaux cantonal road
- 2001: landslide at Côtes du Lac with a volume of 150000 m³, near Yverdon
- 2002: landslides (volume ranging between 2000 m³ and 1500 m³) in Leysin: closure of Aigle-Leysin line
- 2005: Montreux: several landslides, one of them permanently damages a house
- 2006: many landslides in the Pre-Alps (Ormont-Dessous, Leysin)
- 2007: landslide at Pont Bourquin in Ormont-Dessus, closure of Pillon cantonal road for 1 week
- 2007: many spontaneous landslides in the Pre-Alps (Montreux, Diablerets, Corbeyrier, Veytaux, Villeneuve)
- 2007: Montreux: large landslides threatening homes and the fall of a slope forced closure of Montreux-Glion Road
- 2011: Gryon, landslide above the BVB communication line resulting in its closure

2.2.1 La Frasse Landslide, Vaud Alps, 1990

La Frasse landslide in the Vaud Alps is one of the most unstable areas in the world. This landslide is located downstream of Sepey village (VD), in the municipalities of Aigle and Ormont-Dessous, and affects the cantonal road between Aigle and Sepey. The greatest risks concern: the town and inhabitants of Aigle due to the obstruction of the Grande Eau riverbed, significant deformations of the cantonal road RC 705

connecting Aigle to Le Sepey and, to a lesser extent, the road between Le Sepey and Leysin (RC 709). The landslide has an estimated volume of 40 million m³, a length of approximately 2000 m and a width of 500/1000 m. The speed of landslide movement varies between 15 and 60 cm/year to 350 cm/year during the highest activity periods.

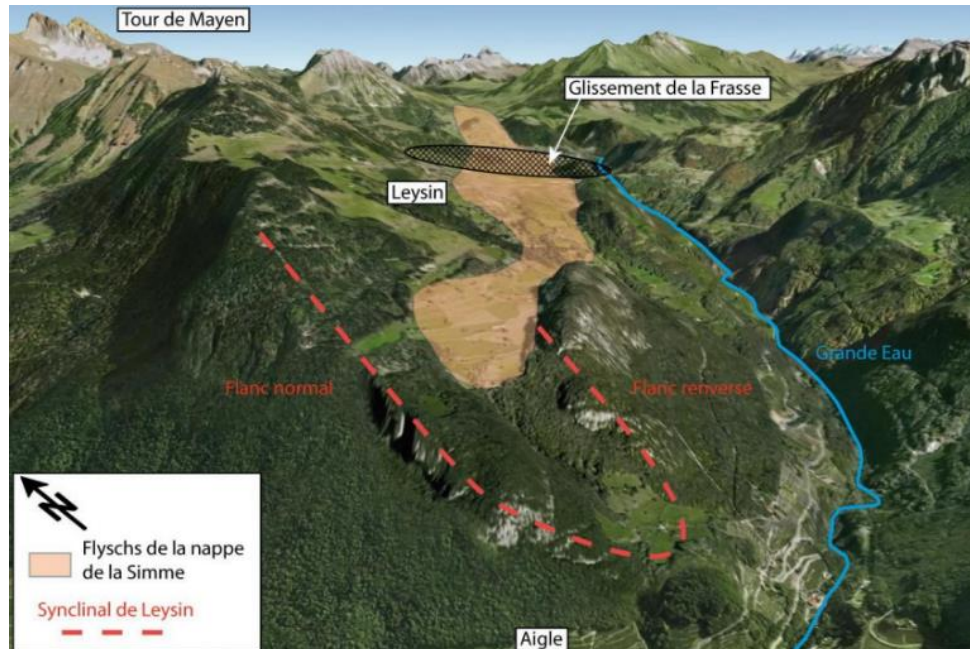


Figure 3: View of the Leysin plateau from the Rhone valley. The syncline is visible, as are the limestone lamellae on the rear flank, (Matti, Tacher et Commend 2012)

The origin of the phenomenon may be the result of:

- presence of a considerable thickness of clayey rocks that are highly sensitive to alteration phenomena (flysch)
- erosion of the layers at the base of the slope due to glacier: when the ice retreats, the flysch begin to slide
- presence of interstitial water, which studies and monitoring have proven to be the driving force behind this phenomenon

2.2.2 Falli-Hölili Landslide, Fribourg, 1994

On 9 July 1994, the village of Falli-Hölili on the heights of Plasselb (FR) was destroyed by a massive landslide. Between 30 and 40 million of cubic metres of earth moved from Schwyberg mountain into the valley. The landslide body was about two kilometres long and 700 metres wide, with a depth of up to 70 metres. The landslide was moving forward with a velocity of about 6 metres per day; 41 houses were

destroyed (shown in *Figure 4*), as well as the hotel, the Falli-Hölili restaurant with a ski lift, campsites and military camps. There were no casualties because the village was evacuated the month before; the first signs appeared in March with several problems with the water pipes; then in April the owners' noticed cracks in their chalets and in June the area was evacuated.



Figure 4: Both pictures, in the upper part, show wooden chalets, while the picture in the lower part shows wooden chalets with concrete foundation, destroyed by the landslide, source: La Liberté

Litology of this area is mainly composed of flysch, an unstable clayey soil common in the Fribourg Pre-Alps. In reality, the ground in this area had already been shifting for thousands of years and had suffered a major landslide in 1612. According to geologists, the 1994 episode was a reactivation of the phenomenon. The Falli-Hölili disaster had an impact on spatial planning: in 1995, the cantonal government decided to declare 500000 m² of building land unbuildable for their high exposure to natural hazards.

2.2.3 Landslide Geodata of the Canton of Vaud, (Federal Office of Topography)

The Cantonal Cartographic Map of the Canton Vaud offers a geoconsultation service in accordance with Article 26 of the cantonal rules on geoinformation (RLGéo-VD). It provides access to a wealth of information in various fields, such as land use, land ownership, buildings, nature reserves, polluted sites or environmental risk.

In the cantonal map guide, landslides are mapped as areas and subdivided into permanent and spontaneous landslides; in the following work, permanent landslides will be analysed. These are subdivided, as can be seen in *Figure 5*, into different groups according to speed and depth, and for some of them, the failure surface depth is also specified.

Glissements de terrain permanents - DUTI

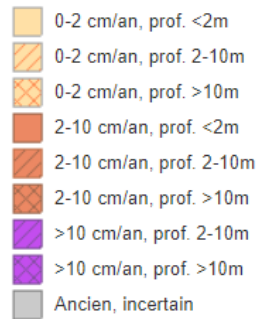


Figure 5: Cantonal Cartographic Map legend in which landslides are divided according to speed and then again divided according to depth, source: Guichet cartographique cantonal, Canton de Vaud

Main data of mapped landslides will be summarised in *Table 7*.

Table 7: Values of depth, area and number of buildings on the landslide bodies

LANDSLIDE NUMBER	DEPTH (m)	AREA (m ²)	BUILDINGS INVOLVED
1	min. 2 max. 4	49268.9	1
2	min. 10 max. 15	157539.5	-
3	min. 4 max. 6	11670	1
4	min. 7 max. 10	70236.3	-
5	min. 2 max. 3	22133.2	1
6	min. 2 max. 3	48848.3	-
7	min. 4 max. 7	105417.1	-
8	min. 4 max. 6	273892.4	-
9	min. 3 max. 5	282820.2	-
10	min. 40 max. 70	247746.5	-
11	min. 8 max. 12	596507	2
12	>10	201854.3	60
13	min. 20 max. 25	267673.7	1
14	min. 8 max. 12	720937.1	5
15	min. 10 max. 15	92591.2	9
16	min. 30 max. 50	1029362	2
17	min. 7 max. 10	949221.5	14
18	20	70140	1
19	15	995493.7	10
20	min. 6 max. 8	16270.8	1

2.3 Landslide in Italy

In Italy, between 1945 and 1990 landslides and floods were responsible for 3488 of the total 7688 fatalities due to natural hazards and cost the national economy some 17 000 million Euro. Hydrogeological instability has increased significantly in recent years: this was revealed in a report by ISPRA (*Higher Institute for Environmental Protection and Research*); according to the data collected, the phenomenon increased in 2021, affecting 94% of municipalities: more than 540000 households and 1300000 inhabitants live in areas classified as landslide-prone. ISPRA in cooperation with the autonomous regions and municipalities has produced an *Inventory of Landslide Phenomena in Italy (IFFI)*. From analysis of the latter, most important factors for triggering landslide phenomena are: short or intense precipitation, persistent rainfall and earthquakes. Therefore, indicators for establishing landslide risk are: very high hazard (P4) high hazard (P3), medium hazard (P2) and low hazard (P1).

The human and economic costs of landslides increased dramatically in recent years so it is necessary to analyse historical data to understand and prevent what might happen in the future.

2.3.1 Deep gravitational deformation of Cassas slopes (*Val di Susa Italy*)

Cassas landslide is located on the right orographic slope of the middle Susa Valley in the Salbertrand municipality, “Gran Bosco” natural park (country of Turin, Piedmont, Italy). The area involved in the upheaval, which develops on the evolution of a deep gravitational deformation, has a surface of approximately 900000 m² over a total width of 1800 m. The landslide top is located near minor watershed at about 2000 m a.s.l., while the landslide foot is placed at about 1000 m in the wide Salbertrand valley flat which was formed by the filling of a landslide dammed lake in locality of Serre la Voute, (*Capello, 1941*). This movement could include a total volume of about 10 to 12 million m³ (*Bonnard, Forlati and Scavia 2003*), with accumulation both on the slope and on the valley floor.

The phenomenon is of great interest due to the presence of infrastructures that are potentially exposed to risk, such as highway A32, connection between Turin and Frejus Tunnel with its service station, Torino-Modane international railroad and Monginevro national road SS 24. Another risk element could be Dora Riparia River.

Causes of landslide triggering may be: fractured material that enables deep water circulation, favourable orientation of secondary discontinuities and heavy rainfall.

In 2014, the sliding plane was measured between 47 and 54 metres. Later a slip surface was identified at a depth of approximately 50 to 60 m in contact with the substrate.

Historical data show that the first record of slope's instability was in 1728; several slope instability events were later registered in the 19th and 20th centuries as a result of huge floods. Actually, the landslide is monitored both topographically and geotechnically, with inclinometers to control the unstable area.

2.3.2 Vajont Landslide, Longarone, 1963

Vajont Landslide is one of the best examples of slow-moving landslide that failed catastrophically in Italy. On 9 October 1963 a huge landslide, about 2 km long, with about 260 million m³ of forest, earth and rock fell from the southern flank of Monte Toc into the lake below. The highest recorded speed reached 110 km/h: in 45 seconds it had completely filled the Vajont lake. The impact moved 115 million of m³ in 25 seconds, of which about 50 million of m³ swept over the 250 m high dam. The impact generated three waves: one went upwards damaging the houses of Casso, one went towards the lakeshore and, through a washout action of the lake itself, destroyed some places in the municipality of Erto and Casso; the third (containing about 50 million cubic metres of water) leapt over the dam edge, which remained intact, and plunged into the narrow valley below.

Triggers could be heavy rainfall or inclination of discontinuities parallel to the slope. Before the landslide that caused the flood, the downward flow of the regolith was 1.01 centimetres per week. In September, this run-off reached 25.4 centimetres per day, until, on the day before the landslide, it achieves 1 metre per day.

The approximately 50 million cubic metres of water that managed to bypass the structure poured into the southern sector of Longarone and devastated the town. The death toll was around 2100 people together with buildings and infrastructure completely destroyed. The figure below (*Figure 6*) shows the landslide volume and allows to understand the dimensions involved.

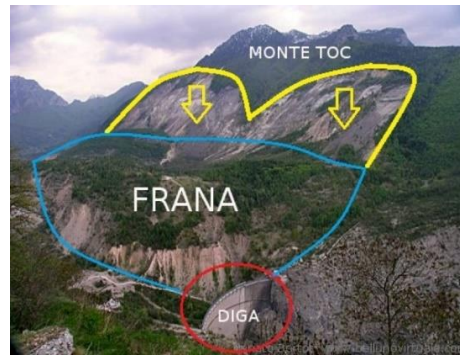


Figure 6: Illustrates Monte Toc, volume of landslide involved and the location of the Vajont dam

2.3.3 Slow-moving landslide of Lungro, Calabria (Southern Italy)

As a result of slow-moving landslide which affected the built-up area for several years, many structures in Lungro's centre are characterized by cracks and deformations, seen in *Figure 7*. This landslide is classified as slide with uncertain boundary, including some minor sliding and flow phenomena. The majority of buildings falling within this area are made of masonry.



Figure 7: Masonry buildings affected by cracks and deformations, in 2005 compared to 2011

The analysis of the available data, (Antronico, et al. 2014) has pointed out that, in 2006–2011 period, an increase in the building degradation was registered in the left portion of the landslide. This complex landslide, with retrogressive character, is 10–20 m deep, but in the historic centre the depth reaches up to 30 m. The measured displacement speed is approximately 10/18 cm/year. Monitoring analysis shows

that masonry buildings can provide less significant and widespread damage than reinforced concrete buildings, which are not a solution to the problem unless coupled with slope stabilisation measures.

2.3.4 Large landslide affected the urban centre of San Fratello, Sicily (Southern Italy)

On February 14 in 2010, a large landslide affected the urban centre of San Fratello town (Sicily Island, Southern Italy), causing severe damage to buildings, roadways, and infrastructure (shown in *Figure 8*), as well as about 2000 evacuees (out of a total population of 4500 inhabitants). This large complex landslide, with an area of more than 1,2 km², represents one of the largest phenomena in Sicily, (*Frodella, et al. 2017*).



Figure 8: Severe damage to buildings, roadways, and infrastructure caused by large landslide in Stazzzone quarter (a,b), in Riana quarter (c,d) e in san Benedetto porcaro quarters (e,f)

Intense and exceptional rainfall events were the main factor that, together with steep slopes and widespread outcropping clay lithotypes, triggered various slope movements. The landslide on February 14th 2010 developed over an elevation difference of 450 m, with a maximum width of 1.5 km and a length of 1.9 km; it can be classified as a complex roto-translational mass movement (*Cruden & Varnes 1996*) of approximately 20×10^6 m³, which mainly involved the silt-clay cover with an average thickness of 10 m, and only limited bedrock. In the upper zone of the landslide, a large crown developed (mainly in the city district areas), while in the middle sector of non-urbanised slope, minor escarpments and tension/traction fractures occurred; the landslide toe developed downstream in a slow earthflow.

2.3.5 Deep gravitational deformation of the eastern slope of the Amiata mountain in Southern Tuscany 2011

The mid-Tuscan ridge is mainly made up of marly limestone and marlstone, overlaid by soils of the 'Tuscan series' made up of evaporites, limestone, marly limestone and jaspers; dozens of independent landslides characterised by different degrees of activity have developed on these soils. They can be traced back to three main areas called: S. Pietro (SP) the northern one, Podere Mezzavia (PM) the southern one and Abbadia S. Salvatore (AS) the central-western one; they cover an extension of more or less 5 km. The slope conformations indicate the existence of landslide movements especially rotational slides; in Varnes' classification, this landslide falls within the group of complex landslides.

S. Pietro (SP)

The main slope is vertical and modelled on the lava flow edges. It presents a notable lateral continuity and, in the central part reaches a height of 160 m, while in the northern part it is about 40 m high in accordance with the progressive thinning of lavas. Upstream of the main slope, there are many open fractures that affect the volcanic rocks and indicate the progressive involvement of this sector in gravitational processes. The main body is made up of many smaller, more superficial landslides; the main sliding plane develops within the Ligurian units and in the distal part also on Pliocene terrain. The thickness of the landslide body is expected to be up to 100 m, depending on the height of the main slope, while the surface movements are less than 30 m thick. Although the activity level of individual landslide bodies is unknown, signs of recent and ongoing activity are evident along the slope given the deformations that have affected some buildings and county roads.

Podere Mezzavia (PM)

The main scarp develops in an arcuate shape from the southern outskirts of the Abbadia San Salvatore settlement to that of Piancastagnaio. The height of the scarp is lower than that of the San Piero landslide, not exceeding 50 metres. The base of the escarpment, modelled on Ligurian soils, is generally covered by a thick layer of colluvial deposits and lava blocks immersed in clayey sediments. The height of the main slope indicates that the minimum thickness of the landslide body is about 100 m, while for secondary gullies the thickness should not exceed 30-40 m. Some

buildings on the southern outskirts of Abbadia were affected by fractures suggesting local movement reactivations. Injuries and deformations are also recorded on provincial road no. 54 with bump creations, depressions and fractures.

Abbadia San Salvatore (AS)

The movement develops upstream of the two landslides described above; the main escarpment, several km long, is oriented approximately NW-SE and about 100 m high. The slope of the mountainside is steep, exceeding 30°, its lack of verticality suggests a long period of degradation. At the slope toe a thick colluvial blanket makes it impossible to assess the nature and age of the deposits.



Figure 9: Buildings (a,b,c) and roads (d) affected by deformations due to landslide movement

2.3.6 Mont de La Saxe landslide in the municipality of Courmayeur

Mont de La Saxe landslide affects the south-western slope of Mont de La Saxe in the municipality of Courmayeur, Aosta Valley. This landslide can currently be considered one of the most critical active landslide phenomena in Italian Alps. Investigations and monitoring, geological studies and numerical modelling have identified various collapse scenarios associated with different sectors of the landslide body, with estimated volumes ranging from 400,000 m³ to 8.3 million m³ in case of total collapse. The area affected by the landslide phenomenon covers a

surface a of approximately 120000 to 170000 m², with a maximum width of 350 m and a maximum length of 500 m, (Figure 10). The landslide body consists of a mass of clayey shale with an average depth of the failure surface between 60 and 70 m from ground level. The main slope of the landslide body is located at an altitude of 1800 m, consisting of a wall of fractured clayey schist; in the zone preceding the latter, there is another rock mass, also characterised by the presence of beating fractures caused by a retrogressive propagation of the sliding surface.

The landslide affects the villages of Entrèves and La Palud, where more than 2000 people reside during high tourist frequency, the access road to the Mont Blanc Tunnel, the access road to Val Ferret, and the Dora di Ferret, with the potential formation of a landslide lake. The landslide has been monitored since 2009 with systems such as GPS, DMS, geodetic topographic network and ground radar.

During the spring 2014 emergency, following the increase in landslide displacement values and the sequence of collapse phenomena, closure of several streets in Courmayeur and evacuation of 80 people from the locality of La Palud was ordered. In January 2011, a rockfall occurred at km 6+800 on the SS26 just before the entrance to the avalanche tunnel. A series of rock elements overtook the latter, impacting on the carriageway and on car passing by causing the death of a French tourist.

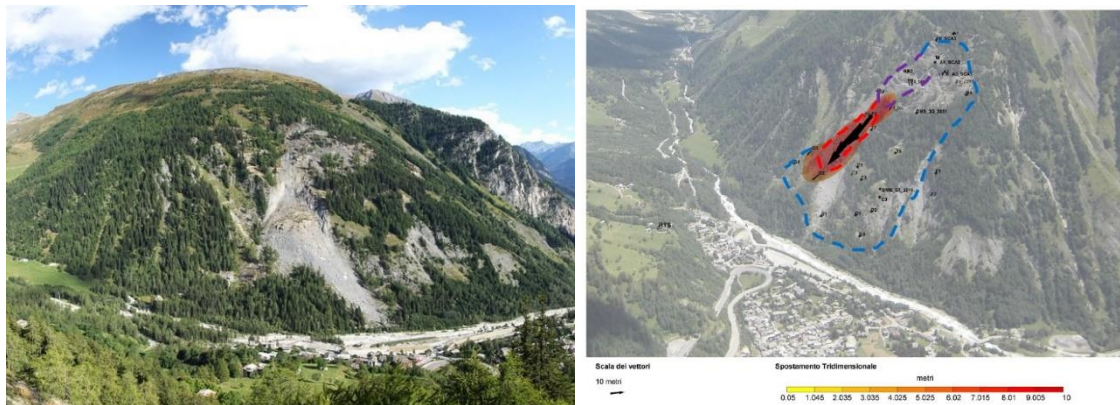


Figure 10: Area related to the Monte La Saxe landslide, in the municipality of Courmayeur

2.4 Landslide worldwide

Landslides occur all over the world and, although the soils on which they take place have different characteristics, the triggering causes are similar and can be grouped into 2 macro-categories: natural predisposing factors (climate change, heavy rainfall, conditions and type of soil affected) and human causes (deforestation, anthropogenic settlement, excavation, slope undermining, anthropisation, etc.).

2.4.1 *Séchilienne Landslide*

The Séchilienne landslide developed on the right side of the Romanche valley, in the Isère Departement of the French Alps; it is one of the major active landslides in France. This landslide occurred on the slope extending from an elevation of 330 m a.s.l. at the valley bottom to 1150 m a.s.l. at Mont Sec. The landslide itself extends from 600 m a.s.l. up to 1130 m a.s.l. over an area of approximately 700000 m².

The first signs of landslide activation, such as the elliptical morphology of the slope and the presence of active screes, date back to 1937/1948. An important reactivation phenomenon was observed in 1980's where rockfalls hit the national road RN91 and the existence of a large slope deformation was recognized. Protective measures were installed after these occurrences: fence with an electrical wire alarm, traffic lights, a dam with a high storage volume capacity.

This landslide can be divided into three main areas:

- Crown body, the most active and disrupted part with the volume of approximately 300000 m³ with a velocity between 0.15 to 1 m/year, periodically releases rockfalls through Les Ruines
- Intermediate zone with a medium activity, a volume of 2/2.5 millions of m³ and velocity of about 0.05/0.15 m/year
- Upper and North-western part with a large slowly moving zone with low velocity of about 0.02 to 0.04 m/year

The main elements at risk are the RN 91 (nearly 10000 vehicles/day), the small village of Ile-Falcon, a paper factory and a small electric power plant. Other zone exposed to secondary phenomena are: in the case of damming and rising water behind the natural dam, the village of Séchilienne, and in the case of overtopping and rapid erosion of the dam, Vizille town, its surroundings and chemical industries.

2.4.2 Landslide in Santa Tecla, near San Salvador 2001

The landslide which devastated Santa Tecla was triggered by a 7.6 magnitude earthquake; the latter led to the liquefaction of the ash deposits near the basal shear surface, at a depth of 15 to 20 m. Before the earthquake struck, Holocene ash deposits at the base of the Las Colinas landslide had probably collected some water, enough to liquefy the ground when the quake began (Harp); beneath these deposits is an ancient impermeable soil layer that acts as an aquiclude, retaining water and creating an aquifer perched within the overlying ash. This deposit can liquefy during seismic tremors, while much of the overlying layers remain dry, (Harp observed that the tip of the landslide tongue was wet while the landslide material from the top of the ridge was dry). Loose debris flowed down the ridge, dragging parts of the forest with it.

At least 450 people were reported dead and 1200 missing after a landslide destroyed part of the San Salvador suburb of Las Colinas. Another landslide killed 10 people travelling by bus along the Pan American Highway near San Vicente. Numerous other landslides slowed down relief efforts, blocking highway, destroy buildings and infrastructures. *Figure 11* shows houses destroyed after the earthquake in San Salvador: it can be seen that these are predominantly built of masonry or concrete.

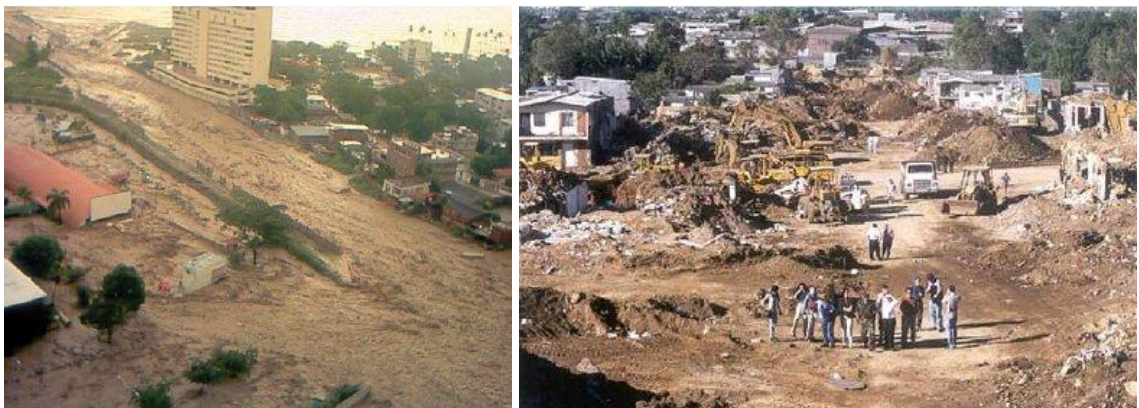


Figure 11: Two images that show the houses destroyed by the 2001 earthquake in San Salvador

2.4.3 Hazel Landslide, Oso, United the States

Oso landslide occurred on March 22 in 2014 and it is the deadliest landslide event in United States. It originated within an approximately 200 m high slope made of unconsolidated glacial and colluvial deposits (deposited by previous landslides). A portion of unstable hill collapsed, sending mud and debris to the south across the North Fork of the Stillaguamish River, flooding a rural neighbourhood, and covering an area of approximately 2.6 km². The mud, soil and rocky debris left by the landslide covered an area 460 m long and 1300 m wide, depositing debris 10 to 20 m deep. The landslide involved a complex sequence of events including rotation, translation, and flow mechanisms and can be referred to as a debris-avalanche flow. It also dammed the river, causing extensive flooding upstream and blocking State Route 530, the main road to the town of Darrington, 26 km east of Oso.

43 people were killed and 49 houses destroyed. *Figure 12* shows: on the left wooden houses destroyed by the landslide, on the right a picture representing Oso landslide. This landslide completely destroyed the Steelhead Haven neighbourhood, as well as several homes located on nearby State Highway 530. Approximately 600 metres of highway were buried from a height of up to 6 m of debris, closing this important east-west communication route for more than 2 months.



Figure 12: The left-hand image shows a wooden house destroyed by the landslide, the right one representing Oso landslide volume

Change in pore pressure and water level are one of the main factors that led to the landslide development, together with erosion at the base of the slope by the river flow. USGS research indicates that the average speed of the landslide was about 65 km/h, with maximum speeds probably even higher. The total size of the Oso landslide was approximately 7.6 million cubic metres of sand, tilt and clay. The

landslide also caused significant economic losses, estimated for more than 50 million dollars.

2.4.4 North Salt Lake Slide, Utah 2014

On August 5th, 2014, a 32 m-tall and 24° inclined hillslope failed behind a North Salt Lake City, Utah neighbourhood, moving 97000 m³ of material down slope and threatening several homes, visible in *Figure 13*. The landslide left an 18-metre-high head slope on the rotational landslide. Twenty-seven families were evacuated immediately, and seven families were warned to stay away from their homes overnight, waiting for the ground to stabilise.



Figure 13: There are houses, made of stone and masonry, visibly damaged by landslide body

The results of the analysis about Parkway Drive Landslide suggest that the characteristics of the Quaternary geological sediments and rock geology underlying the slope, rainfall events and hydrological characteristics of the slope, as well as human modification of the landscape have contributed to the slope destabilisation and played a key role in the slope failure.

The landslide continued to be active after 2014 event, the major movements have been located in the northeast and northwest sections of the toe: with 101.6 cm of downslope movement on the western side and from 279 to 483 cm of downslope movement in the centre of the slide, over the 2014, 2017-time interval.

The main mitigation efforts are: reduce the overall slope and remove material from the head, boulders were placed in the section just below the regraded head scarp, surface drain pipes and shallow canals, were also added to the centre of the slide.

2.4.5 Active Landslides in Achaia, Peloponnese, Greece

The Achaia area has been the focus of different studies concerning landslides and vulnerability over the past decade. The lithological conditions of this area are one of the most decisive parameters for the occurrence of landslides: the highest density is recorded in fluvio-terrestrial and clastic formations of the Pliocene and Pleistocene.

The most common triggering mechanisms are seismicity, steep slopes, highly fractured rocks in the source areas and heavy rainfall. Therefore, increased permeability of rock formations produced by earthquakes (due to strong ground movement and/or cracking) together with events or periods of heavy precipitation are the main triggering factors for landslide events.

The landslide area mainly affects the northern/eastern slopes of Mount Panachaiko, near the villages of Krini, Pititsa. In 1985, a landslide was recorded in soils consisting of marly/clayey sediments overlain by 1.5/2 m of eroded material in the southern part of Krini. This phenomenon is classified as a complex landslide: partly formed by a large earth flow, partly by a translational slide. In addition to large slope collapses, many shallow and small landslides were also observed: these affected flysch cover and marl and clay units. The village of Pititsa lies within the Upper Cretaceous-Paleocene flysch, consisting of sandstone alterations with limestone and marl intercalations. The Pititsa landslide can also be classified as an earthflow with the same characteristics as the main body of the Krini landslide, but mostly retaining lithological homogeneity.

The monitoring data refer to the period 2016-2021; the average velocity of the Krini landslide was found to be 6 mm/year downwards (0.6 cm/year) and 28.7 mm/year (3 cm/year) eastwards. The average speed of the Pititsa landslide was 1.8 mm/year (0.2 cm/year) downwards and 7.7 mm/year (0.8 cm/year) eastwards. The area affected by the Krini landslide is 4080000 m² while the surface of active portion around the village of Pititsa is 800000 m². Examples of buildings that could be affected by the Krini landslide are shown in the *Figure 14*.



Figure 14: Examples of stone and masonry buildings in the Krini village

The main results obtained from the monitoring undertaken on the analysed landslides are:

- the maximum displacement rate is located approximately in the centre of each landslide
- results indicate that there is a correlation between precipitation and landslide movement: for Krini landslide, we found an average delay of 13.5 days between maximum rainfall and maximum displacement
- displacement rates of the active Krini landslide increase after a period of precipitation
- results suggest that the amount of total precipitation may control the increase in the displacement rate of an active landslide
- Krini village is affected by a deep landslide with progressive deformation in the order of dm/cm per year.

2.4.6 Gjerdrum landslide, Norway, 2020

Gjedrum landslide, shown in *Figure 15*, was a quick clay landslide that occurred in the early hours of 30 December 2020 in Ask village, Norway. The latter was triggered by heavy rainfall in the days before the accident, which caused soil movement in this area. Gjedrum landslide involved an area of 300 by 700 metres; heavy rainfall also caused a debris flow affecting an area of 90000 m².



Figure 15: Gjedrum landslide, Norway, 30 December 2020, source: BBC news

Historically, several landslides have occurred in the municipality of interest:

- in 1924 a landslide destroyed several farms and damaged 1600 metres of road
- in 1973 there was another landslide
- in 1980 a landslide affected the lower part of the area analysed
- in 2008 the hydrologist Romerikes Blad warned the municipality of soil erosion and of potential landslides risk

More than 30 buildings were destroyed, in particular residential buildings (houses and apartment blocks, visible in *Figure 16*), more than 1000 people were evacuated, 10 killed and 10 injured.



Figure 16: Houses and flats damaged by the Gjedrum landslide, source: BBC news

2.5 Summary of selected landslides

In the following section, a summary table (*Table 8*) of the selected historical events is reported.

Table 8: Summary of the selected historical landslides

DATE	SITE AND COUNTRY	SLIDING PLANE DEPTH (m)	VOLUME (m ³)	VELOCITY	DAMAGES
1990	Vaud Alps, CH	-	40 million	15-60 to 350 cm/year	Aigle town
09/07/1994	Fribourg, CH	-	30 to 40 million	6 m/day	Falli-Hölly village, an hote and military camps
1999-2006	Champ Chamot Belmont, CH	-	-	-	16 damaged houses
2001	Côtes du Lac, CH	-	150000	-	-
-	Susa Valley, IT	50 to 60	10 million	-	-
09/10/1963	Longarone, IT		115 million	1.01 cm/week to 1 m/day	City of Longarone
2006-2011	Lungro, IT	10-20 up to 30	-	10/18 cm/year	many structures damaged in Lungro's centre
14/02/2010	San Fratello, IT	10	2120	-	buildings, infrastructures
2011-2014	Courmayeur, IT	60 to 70	400000 to 8.3 million	-	La Palud town and the road SS26
1985-2021	Achaia, GR	1.5/2 m		0.2 to 3 cm/year	Krini Village
1937	Séchilienne, FR	-	300000 2/2.5 million	0.15/1 m/year	RN 91 Village of Falcon, Vizille town
2001	Santa Tecla, ES	15 to 20		-	Houses in San Salvador
22/03/2014	Oso, US	10 to 20	7.6 million	65 km/h	49 houses and other structures destroyed
05/08/2014	North Salt Lake, US	20	97000	-	Houses damaged
30/12/2020	Gjedrum, NO	-	90000	-	30 buildings destroy 10 people killed 10 injured 1000 people evacuated

Chapter 3: LANDSLIDE TYPE

In the present thesis between all different types of landslides, from debris flow to complex landslides, slow-moving landslides are analysed. Permanent landslides are involved the evolution of mountainous landscapes since they mobilize large land masses and change their geomorphologic structure. Slow-moving landslide can evolve in multiple phenomena such as: mud or debris flows, lateral spread, rockfall translational and rotational slides. This type of phenomenon is widespread throughout the world; several authors have analysed slow-moving landslides as: Cascini, et al. (2008) Antronico, et al. (2015); Uzielli, et al. (2015) Nicodemo, et al. (2017) Borrelli, et al. (2018) Ferlisi, et al. (2019) in Italy, Clifton, et al. (1986) Brooker and Peck, (1993) Moore, et al. (2006) Barlow, (2000) in Canada, Chen, et al. (2016) Zhang et al. (2018) Dong, et al. (2018) Wang, et al. (2018) in China, Esser (2000) in USA and Jworchan, et al. (2008) in Australia.

Being slow-moving landslides, they are usually deep, thickness higher than 3 m, with a complex subsurface hydrological system that often results in a triggering factor for the movement. They move mainly by friction along shear zones in weak materials or heavily damaged sedimentary layers on slopes that are usually slightly inclined (less than 20°). Masses movement of soil and rock occur in areas that are generally mechanically weak, characterized by high seasonal precipitation. Both materials often have interconnected, clay-rich layers that host the failure surface or subsidence zone. Many times, these phenomena occur in weak materials, such as damaged sedimentary layers, and evolve into earthflow processes; further triggering mechanisms are lateral spreading or frictional sliding. Other materials where slow-moving landslides can occur are highly weathered metamorphic rocks, with absence of clay layers.

It is possible to define these types of landslides as coherent masses of soil and rock sliding down the slope, with velocities ranging between a few mm/year (slow landslides) to a some m/year (intermediate velocity landslides), according to *Varnes' classification*. Velocities are highly variable in time, space and depending on the situ geomorphological context. Following are three examples of monitored landslide velocity ranges:

- La Montagna earthflow, in Italy, displays velocities varying spatially between 0.4 to 92 m/year
- Maca landslide, in Peru, monitored from a single location moves at temporally varying speeds of 0.01 to 10 m/year
- La Frasse landslide, in Switzerland, with a mean annual velocity varying between 20 and 60 cm/year reaching the value of 1 m/year measured during the landslide event.

Thus, velocities for this type of phenomena are highly variable both daily, seasonally and annually; for this reason, it is difficult to define an average landslide body velocity, and some studies report the maximum annual velocity recorded on the central part of the landslide body, (*Lacroix P. 2020*). A speed classification hypothesis used in the methodology developed in the following thesis will be described below.

Permanent landslides develop differently in time and space, damaging roads, infrastructure, facilities, but also environment. They usually do not endanger people but can cause differential settlements or overturning of structures resulting in social and economic damage. They are controlled by external and internal factors such as: seismicity, river cutting, human impact together with type of material and flow of water within the landslide body. The complex kinematics of this type of landslide involve several physical factors such as: mechanical properties of the material (cohesion, friction angle), previous landslide triggering, pore water pressure and dynamic load.

The continuous monitoring of these landslides over long time spans and the improvement of dynamics models is very important to understand how and as a result of which factors the movement is triggered. The continued development of mechanical dynamics models of these types of landslides is useful not only for the complex interactions that drive them, but also because they could be a starting point for rapid landslides such as debris flows.

In this work, therefore, this type of landslide will be studied and the methodology for making vulnerability curves will be developed on it. Simplifications will be made regarding landslide body, it will be divided into 4 main parts: crown on the top of the landslide, main body in the middle part, lower landslide body and landslide toe.

The landslide body subdivided in this way is displayed in *Figure 17*.

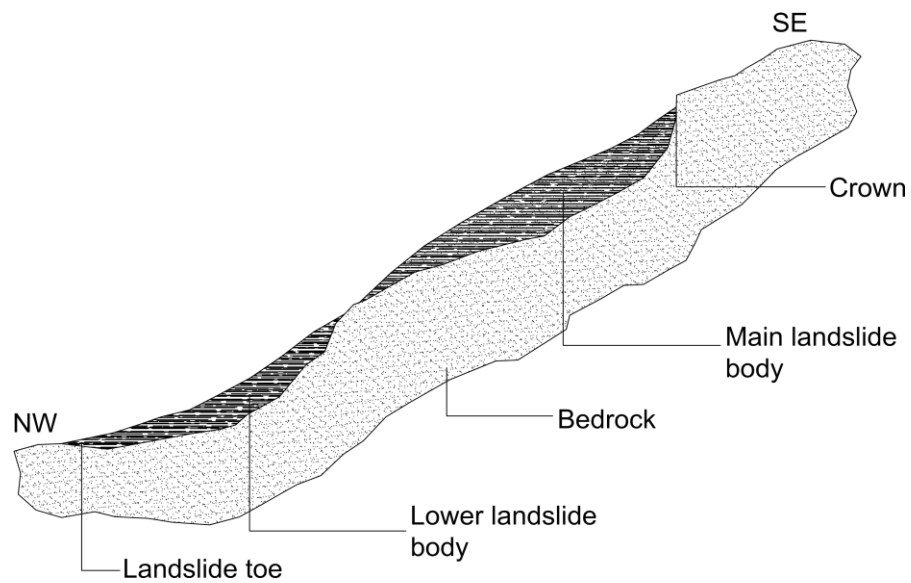


Figure 17: Schematic section showing the most relevant part of the Landslide body, (Bonnard, Forlati and Scavia 2003)

This simplification will make it possible to consider 4 different building locations in the landslide body, according to the degree of damage they may suffer from landslide movement.

Chapter 4: PARAMETERS INVOLVED IN VULNERABILITY AND DAMAGE ASSESSMENT

4.1 Types of buildings structure vulnerable to landslide

In this work, the response of buildings to interaction with landslide body will be evaluated. Firstly, a classification of buildings according to material and number of floors is provided. Buildings are the most concerned elements in landslide risk assessment along with human lives. From literature review, the main buildings damaged by landslides can be grouped into: chalets, residential buildings and residential villas. Chalets are typical mountain buildings, used for both residential and rural purposes. Some of them are completely made of timber, a material mainly used in mountains because it is readily available and an excellent thermal insulator, keeping the house warm in winter and cold in summer. Others have the first floor built in concrete and the second or third (if there is one) in timber; the foundations are always considered to be in concrete; these 2 types of materials will be taken into account for the vulnerability assessment. Residential buildings and villas, on the other hand, are mainly located at the valley bottom, at the base of the slopes, or in towns, meant in the present work as small mountain towns composed of several hamlets also located at high altitudes. They are mainly constructed of concrete, stone and masonry. Some of them are built in both masonry and concrete because, as the article of Lungro (Calabria, Italy) case study points out, reinforced concrete structures do not always guarantee less landslide damage if they are not accompanied by slope stabilisation measures, (Antronico, et al. 2014). On the contrary, masonry buildings, if located in a landslide area with specific features, can suffer not relevant and widespread damage. Table 9 shows the structures analysed in this thesis and classified by building material and number of floors.

Table 9: Summary of structures vulnerable to landslides proposed in the following work

TYPE OF STRUCTURE	TYPE OF MATERIAL	NUMBER OF FLOORS
Chalet	Timber	1
	Timber and Concrete	2,>2
Residential Building	Masonry	4
	Reinforced Concrete	>4
Residential Villa	Masonry	2
	Concrete and Masonry	3

As can be seen in *Table 9*, chalets analysed in the present work have a maximum of two, three storeys and therefore relatively low heights, while residential buildings, mainly located at low altitudes, have a more massive structure, with greater heights to increase living capacity.

4.2 Parameters involved in buildings vulnerability

As introduced in *Section 1.4.1*, parameters involved in vulnerability assessment of buildings to landslides are multiple and can be divided into two broad categories: those referring to buildings and those relating to the landslide body. In this chapter, some of them will be analysed to establish the most relevant ones used in the subsequent methodology for vulnerability assessment. A breakdown of the parameters used according to the building position on the landslide body will be given at the end of this chapter.

4.2.1 Landslide body parameters

Considering, as described in *Section 3*, a slow-moving landslide, only some of the parameters mentioned above will be useful for the characterisation of this landslide movement. For example, the volume of the moving mass, considering a landslide that moves a few centimetres per year, is not taken into account. **Velocity**, on the other hand, is considered by various authors as a fundamental parameter in the landslide classifications: Varnes' classification (1978), reported in *Figure 18*, divides the rate of movement into 7 classes from extremely rapid to extremely slow; in this work, landslides relative to the first 3 classes will be considered.

Velocity Class	Description	Velocity (mm/sec)	Typical Velocity	Probable Destructive Significance
7	Extremely Rapid	5×10^3	5 m/sec	Catastrophe of major violence; buildings destroyed by impact of displaced material; many deaths; escape unlikely
6	Very Rapid	5×10^1	3 m/min	Some lives lost; velocity too great to permit all persons to escape
5	Rapid	5×10^{-1}	1.8 m/hr	Escape evacuation possible; structures; possessions, and equipment destroyed
4	Moderate	5×10^{-3}	13 m/month	Some temporary and insensitive structures can be temporarily maintained
3	Slow	5×10^{-5}	1.6 m/year	Remedial construction can be undertaken during movement; insensitive structures can be maintained with frequent maintenance work if total movement is not large during a particular acceleration phase
2	Very Slow	5×10^{-7}	15 mm/year	Some permanent structures undamaged by movement
	Extremely SLOW			Imperceptible without instruments; construction POSSIBLE WITH PRECAUTIONS

Figure 18: Landslide velocity scale, source: (Hungr, Leroueil et Picarelli 2013)

Within this classification, the first 3 classes refer to slow movements with speeds that have an upper limit of 13 m/month and a lower limit of 15 mm/year.

Another study (P. G. Peduto D. 2016), concerning slow-moving landslides in the urban area of Lungro (Calabria, Italy), reports a distinction between ordinary and critical velocities in relation to different types of material and types of kinematics in the area under study. The velocities (Figure 19) measured in this study have values within the limits of the classification proposed by Varnes.

Velocity [cm/year]		Geomaterial	kinematic_ TYPE
ordinary	critical		
2-4	> 200	detritic-colluvial covers	complex landslide
5-7	> 20		
0.5-5	> 80	deeply weathered and chaotic phyllites	complex landslide
4-20	> 100		
0.5-5	> 40	deeply weathered and chaotic phyllites	landslide zone
0.2-0.5	2-5	weathered and chaotic phyllites	slide

Figure 19: Characteristics of Lungro Landslides, source: (P. G. Peduto D. 2016)

A subdivision of velocities, within the Varnes limits, referring to different depths as proposed in the *Canton Vaud Cartographic Guide*, will be presented later.

A useful parameter to consider is the **depth** of the landslide **failure surface**. This parameter is very relevant in vulnerability assessment of buildings because it allows us to understand whether the landslide body can interact with building foundations. Several studies report classifications related to the depth of the rupture surface and they divide landslide in 4 different classes (Li et Mo 2019), for example:

- CREC (1977) and Qiao et Li (1990): Extremely deep (>50 m), deep (20–50 m), medium deep (6–20 m), shallow (<6 m)
- DZT0218-2006 (2006): Extremely deep (>50 m), deep (25–50 m), medium deep (10–25 m), shallow (<10 m)
- Zhang (2016): Extremely deep (>50 m), deep (20–50 m), medium deep (10–20 m), shallow (<10 m)

Another article, (Li, et al. 2010), gives a classification of landslide depth compared to foundation depth and divides it into 3 classes; it also provides an attempt to vulnerability assessment related to debris depth, as seen in *Table 10*.

Table 10: Classification of foundation depth compared to landslide debris depth, (Li, et al. 2010)

DEPTH OF FOUNDATION (INCLUDING PILES) (m)	LANDSLIDE DEBRIS DEPTH (m)	VULNERABILITY
≤ 2	< 2	1.0
> 2	< 2	0
Less than a landslide depth	2-10	1.0
10-13	2-10	0.5-1.0
> 13	2-10	0.0-0.5
Any	> 10	1.0

The same classification is given by VKF AEAI, which distinguishes: $h < 2$ m for shallow landslides, $2 < h < 10$ m for semi-deep landslides and $h > 10$ m for deep landslides. AEAI, Association des Etablissements cantonaux d'Assurance Incendie, indicates that the determining parameter for permanent landslides is the movement velocity, proposing a subdivision of damage according to the landslide speed, *Table 11*.

Table 11: Velocities and related damage that may affect buildings and interior spaces, (Egli 2005)

VELOCITY (mm/year)	DAMAGE THAT MAY AFFECT BUILDINGS AND INTERIOR SPACES
1÷5	No damage to the building or formation of some cracks depending on the type of building material and type of foundation; slight settlements and ground elevation
10÷50	Formation of many cracks and/or tilting of the building; compaction and compression phenomena lead to visible changes in the soil; underground pipes are damaged
200÷1000	Formation of numerous cracks and/or tilting of the building; settling and compression phenomena cause lasting changes in the soil; underground pipes must be checked annually for their condition

Subdivision presented in *Table 10* is the same as Canton of Vaud Cartographic Guide; In this case, the depth of permanent landslides has a lower limit for shallow landslides being 2 m and an upper limit for deep landslides being 10 m. While in the book “*Training Module on COMPREHENSIVE LANDSLIDES RISK MANAGEMENT (Parkash 2020)*” another classification of landslide depth is provided and it is based on 4 different classes with a lower limit for shallow landslides of 1.5 m, and an upper limit for deep landslides of 20 m.

Table 12: Depth classification of landslide, source: (Parkash 2020)

S. NO.	SLIDE DEPTH BELOW SURFACE		CLASS NAME
		(m)	
1		<1.5	Superficial slide
SS		1.5÷5	Shallow slide
3		5÷20	Deep slide
4		>20	Very deep slide

The depth assessment proposed in this work, *Table 13*, is based on previous studies, cited above, and on the depth classification proposed by the *Cantonal Map Guide*; it is decided to divide the depth of the landslide failure surface into 4 classes and correlate it with the velocity of the landslide movement. These two quantities (depth, velocity) are linked for the subsequent assessment of the building's vulnerability: a greater depth of the failure surface involves larger volumes and if the velocity is relatively high it can lead to even irreversible structural damage.

Table 13: Evaluation of classes of failure surface depth and of the landslide velocity presented in this work

CLASSES	DEPTH OF THE LANDSLIDE		VELOCITY
		FAILURE SURFACE (m)	
1		<2	<10
2		2÷5	10÷30
3		5÷30	30÷100
4		>30	> 100

Another important factor relating to the landslide body is the **surface area** of the affected site, which is useful to understand the number of buildings on the moving mass; it is also necessary to analyse the geology, the presence of water and vegetation in the area under study.

Geology of the slopes have to be analysed in order to know the lithologies involved; many of the case studies consulted for this work (Antronico, et al. 2014), (Frodella, et al. 2017), (Chen, Yin et Dai 2011) contain specific data relating to lithology, hydrology, morphology, mechanical response which, together with photographic and in situ monitoring, help to understand the predisposing factors of slope instability. As written in the book "IMIRILAND PROJECT", (Bonnard, Forlati and Scavia 2003), the first key step in hazard definition and vulnerability characterisation is the qualitative understanding of the possible mechanism of failure with geomorphological and geological constraints, deformations, lithologies

and related boundary conditions. Geological analyses of landslide sites cannot be limited to the 'in situ' geomechanical properties of the landslide area, such as fractures, orientation of discontinuities, but the conditions 'around site' also have to be evaluated.

The presence of **vegetation** can also be an important factor that influences the movement of landslide body. From soil point of view, vegetation, by providing a 'screening' action in sloping terrain, plays a primary role in consolidating slopes and controlling surface erosion. Indeed, the root systems of trees and shrubs harness soil particles, contributing to the formation of a well-structured and mechanically stable horizon. Root systems can stabilise the slope if the failure surface is shallow, but they can also in stabilise it if the failure surface is deep, since they are unable to anchor themselves to a solid layer. The size of the root systems can be approximated to half the height of the tree: by adopting this simplification, it is possible to establish the action that trees can play on moving slopes. The presence of water along the slope is also controlled by trees because it is directed towards the deeper layers, limiting surface runoff phenomena.

Water, within the slope, both moving and static, can cause the slope's stability conditions to change, to the point of being the triggering cause of the landslide movement. Occurrence and circulation of water is therefore an important factor in the formation of the sliding surface; in this thesis, we assume to know the existence of one or more sliding surfaces by analysing their depth.

4.2.2 Building parameters

Concerning buildings several parameters can be considered, but in this work the focus will be on those useful for the vulnerability assessment of buildings to slow-moving landslide. Being a landslide with a velocity of a few cm/years, the visible traces of its movement can be the deformation of the building with the presence, more or less marked, of cracks and fractures, or the progressive structure inclination that would indicate a possible movement of layers on the foundations level. Three of the most important parameters are therefore: the construction material, the depth and the inclination of the **building foundations**. A foundation is defined as the lower part of a structure, designed to evenly distribute the weight of a building and provide a strong footing. As mentioned in a study related to physical vulnerability of buildings affected by slow-moving landslides, (*Chen, et al. 2020*), the

length, width and foundation depth are the three most critical factors that affect the vulnerability. The results of this study demonstrate that the higher the ratio of length to width of the building, the more serious the damage to the building. Likewise, the shallower the foundation, the more severe the damage will be. Referring to the buildings considered in this work, the foundation's depth can be assumed to be approximately equal to:

- greater than 1 m for concrete-built mountain Chalets (at least 1 metre, shallow foundations, because they must anchor themselves under the soil layer that undergoes the freezing and thawing cycles)
- 1 m or greater than 1 m for Residential Villas (shallow foundations)
- foundations of Residential Buildings are usually deep and their depth depends on the type of soil on which the foundation piles are to be built: they must have the foundation placed on a layer with good mechanical properties and have depths ranging from 2 m to 10 m, to more than 10 m (deep foundations)

Another parameter to have regard to is the building ***inclination***; from *Technical Specification for Incline-rectifying of Buildings (JGJ 270-2012; Ministry of Housing and Urban-Rural Development of PRC, 2012)*, (Chen, et al. 2020), is proposed that the incline angle α of the building is the angle between the inclined structure and the vertical plane. A threshold values of building inclination are given in *Table 14*, while *Figure 22* represents the decline states of a building in the case study examined; the inclination refers to the threshold values mentioned in the table below.

Table 14: Threshold value of building inclination where H denotes the building height which is calculated from the outdoor ground (Ministry of Housing and Urban-Rural Development of PRC, 2016), source: (Chen, et al. 2020)

HEIGHT (m)	THRESHOLD VALUE (i_m)
$H \leq 24$	1%
$24 < H \leq 60$	0.7%
$60 < H \leq 100$	0.5%

Given these threshold values, if we assume 10 m as hypothetical building height, the critical horizontal distance between the top and building bottom is approximately 10 cm, assuming that i_m is equal to 1%. In the subsequent methodology parameter definition regarding inclination will be analysed in more detail.



Figure 20: Integral decline state of the case study building: (a) the back wall of the building with an inclination of 1.0 %, (b) the front wall of the building with an inclination of 0.8 %, (c) the front wall of room) with an inclination of 0.7 %, (source: (Chen, et al. 2020))

Another study that deals with building inclinations as a function of material and building height is that related to a quantitative vulnerability estimation, (Li, et al. 2010). In Figure 21 it is possible to visualise for different height ranges of the entire building or just the foundations which threshold value is applicable in relation also to the type of soil.

Deformation features		Foundation soil	
		Medium and low compressive soil	High compressive soil
Masonry structures	Partial inclination of foundation	0.002	0.003
Single-storey frame structure	Settlement (mm)	120 (only for medium compressive soil)	200
Simple shaped high-rise building	Average settlement of foundation (mm)	200	
Common industrial and civil buildings			
Frame structure	Settlement difference between adjacent piles	0.002/	0.003/
Outside columns with masonry wall		0.0007/	0.001/
High-rise building			
$H_g \leq 24$	Integral inclination	0.004	
$24 < H_g \leq 60$		0.003	
$60 < H_g \leq 100$		0.0025	
$H_g > 100$		0.002	
Tower structure			
$H_g \leq 20$	Inclination of foundation	0.008	
$20 < H_g \leq 50$		0.006	
$50 < H_g \leq 100$		0.005	
$100 < H_g \leq 150$		0.004	
$150 < H_g \leq 200$		0.003	
$200 < H_g \leq 250$		0.002	
Tower structure			
$H_g \leq 100$	Settlement of foundation (mm)	400	
$100 < H_g \leq 200$		300	
$200 < H_g \leq 250$		200	

l (in mm) central distance between adjacent piles; H_g (in m) height of building above ground

Figure 21: Examples of threshold value of foundation displacement for different structures, source: (Li, et al. 2010)

Another factor that has to be considered is the presence of any **stabilising interventions**, but in this methodology, we adopt as a simplification the absence of any protective element.

Impact pressure, as shown by several studies, especially in relation to debris flows that move at high velocity and can therefore reach high impact pressures, is a parameter that needs to be considered for risk elements located at the foot of the landslide body. In the studies of Hu, et al. (2012) and Kang, et al. (2016) is illustrated that, with the same landslide intensity, concrete buildings suffer less damage than masonry and timber buildings. It has been shown that timber buildings suffer significant structural damage already at impact pressures between 15 and 30 kPa; whereas an impact pressure of more than 100 [kPa] is required for a reinforced concrete building to sustain irreversible structural damage.

Others two important factors are the **age of construction** and **maintenance state** of the buildings; as defined by the *Swiss Federal Roads Office (ASTRA)*, there are six classes concerning the classification scale of the maintenance status, from (1) good to (5) alarming, including (6) structures for which no information is available. The latter is defined on the basis of criteria relating to physical condition (electrical, mechanical, signs of wear and tear, visible damage), functionality of components and cost-effectiveness. The physical condition of the components is determined by visual inspection, while functionality can only be assessed by operators/users. With regard to the cost-effectiveness criterion, two aspects must be combined: remaining life and availability of spare parts.

As already mentioned at the end of *Chapter 3*, great importance to consider the building locations in the landslide body; in the present thesis 4 different building positions are analysed, summarise with necessary simplifications, the 4 critical situations that may be found in reality.

The 4 chosen **building positions** are shown in *Figure 22*, and represent respectively:

- A. building located on the **crown** of the landslide body
- B. building located on the lateral **edge** of the landslide body (the most critical situation)
- C. building located in the **middle** of the landslide body
- D. building located at the **foot** of the landslide body

The main parameters that will be considered for each of the 4 building positions are reported in *Table 15* and are analysed in *Chapter 5*.

Table 15: Parameters chosen in this work, for each of the 4 building locations on the landslide body

POSITION	PARAMETERS
On the crown (A)	Depth foundation
	Depth of the failure surface
	Building construction material
	Landslide velocity
On the lateral edge (B)	Number of floors (building height)
	Landslide velocity
	Building inclination
	Building construction material
In the middle (C)	Depth foundation
	Depth of the failure surface
	Building construction material
	Landslide velocity
At the foot (D)	Depth of landslide debris
	Landslide velocity
	Material density involved in the landslide
	State of maintenance
	Number of floors (building height)
	Building construction material

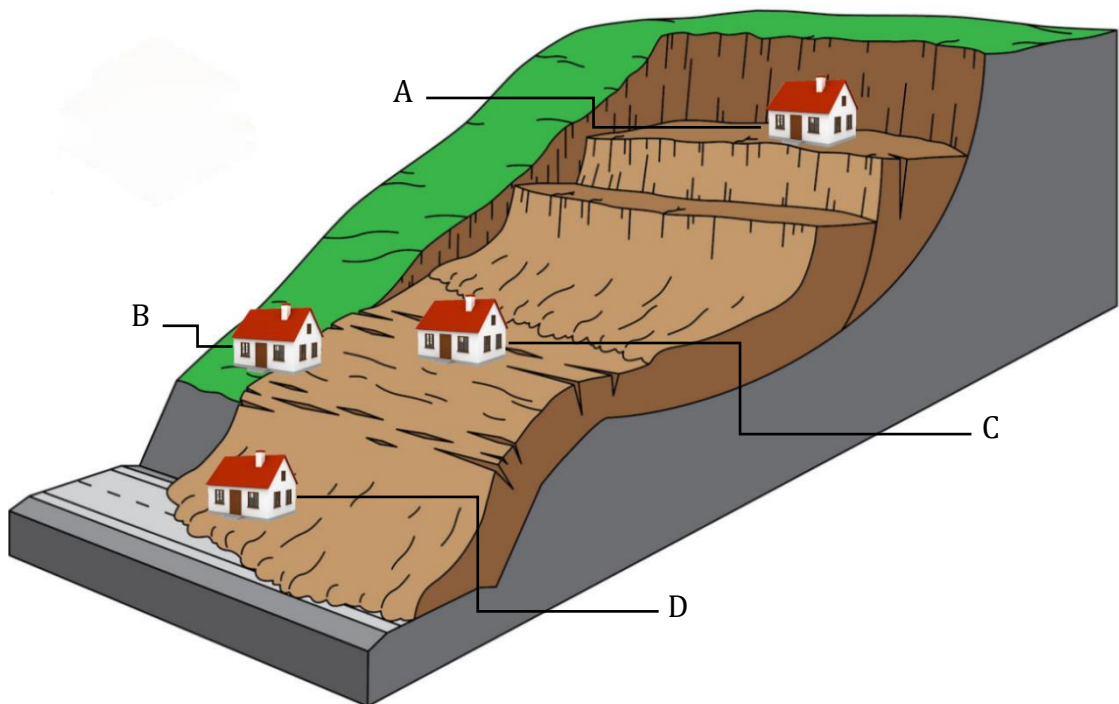


Figure 22: The 4 chosen building positions that represent respectively: A building located on the crown of the landslide body, B building located on the lateral edge of the landslide body, C building located in the middle of the landslide body and D building located at the foot of the landslide body

4.2.3 Damage assessment

The aim of this thesis is to study impact that landslides have on buildings in terms of vulnerability and damage assessment. The buildings considered are all located within the landslide body, those outside the unstable area are not accounted. Damage evolution depend on landslide characteristics, in this case referring to slow-moving landslide. Damages that a building may suffer are manifold and depend on several factors such as landslide intensity and strength of the exposed element. Resistance of risk elements in turn depends on multiple factors, including: the construction material, foundation's depth, the height therefore the number of building storeys, the building age, the mitigation measures implemented on the landslide body, etc. According to the position on the landslide body, the building will suffer different damage: for cases A, B and C the elements most at risk will be the building foundations, while in case D the buildings suffer the impact, so the material, the building height and the impact pressure will become the main parameters. Damage assessment is mainly based on in situ observations to detect extensive cracks, partial or total collapse of the building and distortion or tilting of structures. A building damage assessment for cases A, B, C and another for case D will be given below.

Many classifications have been made according to the level of damage severity. An example is the one proposed by *Geomorphological Services Ltd (1991)* which considers 5 damage classes:

- Negligible: presence of cracks or splits without any deformation visible
- Slight: presence of cracks, some small signs of apparent settlement. Repairs to non-urgent structures
- Moderate: widely persistent cracks. Possible presence of structural component fractures. Settlement may lead to tilting of the structure
- Serious: presence of extensive cracks. Settlement can lead to significant tilting and distortion of the structure. Urgent repairs are needed to make the structures accessible in the future
- Severe: presence of extensive cracks. Settlement can lead to distortion and rotation of structures. If the deformations compromise the structural function of the building, demolition is required and in the worst case, if the movements continue over time, even abandonment of the area.

Other classifications are based on the damage severity scale expressed, in percentage terms, with the building cost. One of these is the conventional damage severity scale, inspired by *Mercalli's scale (DRM 1990)*, which expresses a measure of vulnerability by correlating the damage degree with the phenomenon's intensity and construction characteristics, *Table 16*.

Table 16: Conventional damage severity scale, source: Mercalli's scale (DRM 1990)

CLASSES	CONSTRUCTION VALUE (COST) EXPRESSED IN % TERMS	DAMAGE DESCRIPTION
1	few %	light non-structural damage, stability is not affected
2	10÷30	presence of cracks in the walls
3	50÷60	major deformations, wide-open cracks, evacuation required
4	70÷90	partial subsidence in floors, wall breaches, disintegration of walls, immediate evacuation
5	100	structure destroyed, recovery impossible

As defined by *AEAI, Association des Etablissements cantonaux d'Assurance Incendie*, the damage corresponding to slow-moving landslides is due to changes in the speed and direction of movement within the landslide body. In the case of a deep, low-velocity, homogeneous landslide, the entire building is dragged down by the landslide as the horizontal and vertical components of the movement undergone by the building remain unchanged. If, however, the landslide has a somewhat higher and heterogenous velocity, the sliding becomes more rapid with horizontal and vertical components of the movement, undergone by the construction, showing significant variations. Based on velocity, the following is a breakdown of damage assessed according to both low and homogeneous velocity landslides, first 3 classes, and higher and heterogeneous velocity landslides, fourth class.

Table 17: Damage assessment, based on speed, proposed in this work for cases A, B and C

CLASSES	VELOCITY (cm/year)	DAMAGE DESCRIPTION
1	<10	No building damage or crack's formation depending on construction material, foundation; slight settlements and ground elevation
2	10÷30	Formation of many cracks and/or tilting of the building; compaction and compression phenomena lead to visible changes in the soil
3	30÷100	Formation of many cracks and/or tilting of the building; settling and compression phenomena cause lasting changes in the soil;
4	> 100	Severe structural damage, loss of foundation load-bearing capacity

For case D, on the other hand, reference is made to the impact pressure that buildings are able to withstand. Wooden and masonry buildings already suffer severe damage at impact pressures of between 15 and 30 kPa, while reinforced concrete buildings, which are more resistant, withstand up to 100/110 kPa of pressure above which they are severely damaged structurally. A classification of damage based on impact pressure is proposed in *Table 18*.

Table 18: Damage assessment, based on impact pressure, proposed in this work for cases D

CLASSES	IMPACT PRESSURE (kPa)	DAMAGE DESCRIPTION
1	0÷25	Major structural damage, loss of functionality for timber and masonry buildings
2	25÷60	Less than 50% of the brick-concrete building's framework survives, or two or more storeys are buried
3	60÷110	A great number of columns and beams are broken, most walls are broken and part of the roof falls in. Loss of some functionality, minor structural damage could be repaired with major effort
4	>110	Major structural damage, loss of functionality for reinforced-concrete buildings

Chapter 5: METHODOLOGY

Unlike other natural processes such as floods and earthquakes, it is very difficult to assess vulnerability to landslides due to complexity and wide range of landslide processes which may develop. In the current and available literature, there are several studies that relate vulnerability and intensity to different parameters concerning landslides and buildings. A brief review of the existing literature on landslide vulnerability assessment is presented below.

Within the quantitative risk analysis, *Gomes, et al. (2003)*, considered the vulnerability assessment to landslides by assigning the major weight, within the set of risk elements as industries, infrastructures, public and residential buildings, to human life. Another important study about physical and social vulnerability to landslides is carried out by the Department of Hydrology and Meteorology of Nepal: physical vulnerability is expressed as a combination of physical exposure of people, infrastructure agricultural land and danger, while social vulnerability considers elements such as hospitals, banks, sensitive facilities, etc. This article emphasises the importance of analysing vulnerability that has increased due to reduced adaptive capacity and higher physical exposure of the elements at risk, (*Shrestha 2005*). Landslide vulnerability assessment is also addressed in the study conducted by Glade and Crozier (2005), analysing the physical vulnerability related to the position of people in space, e.g., inside buildings, vehicles, workplaces. Uzielli, et al. (2008) developed a methodology based on quantitative estimation of physical vulnerability to landslides defined as a product between landslide intensity and susceptibility of vulnerable elements (people roads infrastructure, etc.). Li, et al. (2010) made available a new quantitative model for the vulnerability estimation of people and structures exposed to landslide hazard. Vulnerability is expressed as a function of the hazard intensity and the resistance of vulnerable elements.

All of the methodologies mentioned before, are to be considered preliminary to the quantitative study of landslide vulnerability as they must be adapted and calibrated on the basis of actual landslide events or data collections from in-situ investigations. Research in this field is proceeding in this direction in order to refine the methodologies and make them more realistic.

The present work mainly refers to four articles, which analyse intensity and vulnerability as follows:

1. Li et al. (2010) proposed a methodology where vulnerability depends on both the characteristics of the element at risk and the landslide intensity; **vulnerability** is defined as a complex function of intensity and resistance parameter of the elements at risk subjected to hazardous event. In this study, the landslide **intensity** is a function of two factors: the dynamic intensity factor referring to the landslide velocity and the geometric intensity factor considering the dimensional characteristics of the landslide elements.
2. Uzielli et al. (2014) adopted the analytical structure of the function used to describe vulnerability by Li et al. (2010) but replaced the resistance factor with the resilience index; thus, **vulnerability** is quantitatively defined as a function of intensity and the resilience index. Resilience, defined as the ability of a material to absorb an impact without breaking, is parameterised as the intrinsic ability of risk-exposed elements to preserve their performance during the development of the hazardous event.
3. Chen, et al. (2020) used as a main parameter for the quantitative estimation of physical vulnerability the calculation of the force acting on the building foundation. For the methodology developed in the following work, the focus is based on the calculation of the inclination and rotation of the building, defined by the ratio of horizontal difference between the observation point at the top and at the bottom of the building, and the vertical height of the building after tilting.
4. Miteva et al. (2022) propose a methodology where the intensity is defined as a function of the impact pressure, which in turn is estimated by considering the density and height of the debris flow; the intensity thus defined is used, in the present work, in case D where the damaged building is located at the toe of the landslide.

5.1 Intensity

“Intensity is the measure of geometrical and/or mechanical parameters, as maximum movement velocity, total displacement, differential displacement depth

or volume of the moving mass, kinetic energy per unit area, relate to the destructive potential of a landslide”, (Bonnard, Forlati and Scavia 2003). The intensity may be expressed qualitatively or quantitatively and varies according to the position of the element at risk on the landslide body or according to the evolution of the landslide itself. In the present work, intensity is quantitatively estimated with equations adapted to the case of a slow-moving landslide.

In this work, two equations will be given for the intensity assessment:

- The first equation is used to estimate the intensity in cases **A**, **B** and **C**, where buildings are located above the landslide body and move with the landslide itself; in these three cases, the impact of the moving mass is not considered because the effect of a slow-moving mass is visible only at the foundations level with subsidence, fractures, ground uplift and building inclinations.
- The second equation is used to estimate the intensity in case **D** where the building is located at the foot of the landslide body; in this case, a moving mass hitting a building with a certain pressure is taken into account, so as for debris flows, here the impact is considered.

The following paragraphs report the equations used to define intensity and parameters (used in the formulas with their ranges of variability).

5.1.1 Evaluation of Landslide Intensity and parameters used in the proposed methodology

The evaluation of landslide intensity in cases **A**, **B** and **C** refers to the general expression defined by Li, et al. (2010):

$$I = f(I_{dyn}, I_{gem}) \quad \text{Equation 3}$$

Where:

- I_{dyn} : is the dynamic intensity factor and it is based on landslide velocity
- I_{gem} : is the geometric intensity factor

The simplified intensity equation, proposed in this paper (Li, et al. 2010), is expressed through the product of 2 factors below and adapted for buildings constructed on the body of a slow-moving landslide:

$$I = I_{dyn} * I_{dpt} \quad \text{Equation 4}$$

Where:

I_{dyn} : is the dynamic intensity factor for structures, calculated using the following formula:

$$I_{dyn} = \frac{1}{16} (\log_{10} C + 0.30)^2 \text{ with } C > 5 * 10^{-1} \quad \text{Equation 5}$$

Where:

- C : is the average velocity of the sliding mass in mm/s; in *Table 19* are shown 4 velocity classes used for the development of vulnerability curves.

Table 19: 4 speed ranges used for the construction of vulnerability curves

CLASSES	VELOCITY (cm/year)	VELOCITY (mm/s)
1	<10	<3.17*10 ⁽⁻⁶⁾
2	10÷30	3.17*10 ⁽⁻⁶⁾ ÷9.51*10 ⁽⁻⁶⁾
3	30÷100	9.51*10 ⁽⁻⁶⁾ ÷3.17*10 ⁽⁻⁵⁾
4	>100	3.17*10 ⁽⁻⁵⁾ ÷1.27*10 ⁽⁻⁴⁾

I_{dpt} is the debris-depth factor used to evaluate structures on the body of a slow-moving landslide, calculated using the following formula:

$$I_{dpt} = 0.1 * D_{dpt} \quad \text{Equation 6}$$

Where:

- D_{dpt} is the debris depth expressed in meters, at the location of the building; considering a slow-moving landslide, the debris-depth also represents the depth of the failure surface. In *Table 20* are indicated 4 depth classes used for the development of vulnerability curves.

Table 20: 4 debris depth ranges used for the construction of vulnerability curves

CLASSES	DEPTH (m)
1	<2
2	2÷5
3	5÷30
4	>30

Intensity obtained will subsequently be used for vulnerability assessment and, as defined in Li's methodology, it will be expressed in nondimensional terms; in *Table 21* is proposed an intensity classification based on the structure damage degree.

Table 21: Intensity classification provided by this work, cases A,B and C

CLASSES	INTENSITY	DAMAGE
1	<0.1	Low
2	0.1÷0.3	Medium
3	0.3÷1	High
4	>1	Very high

The evaluation of landslide intensity in case **D** refers to the general expression defined by Kang, et al. (2015); intensity is expressed as the impact pressure that the slowly moving landslide applies when it strikes structural elements. The impact pressure mainly consists of dynamic overpressure and hydrostatic pressure. These forces depend on the peak discharge, velocity, volume and sediment–water ratio. The first part of the equation refers to hydrostatic pressure while the second one to dynamic overpressure.

$$P_t = \frac{1}{2}\rho_{df}gh + \rho_{df}v^2 \quad \text{Equation 7}$$

Where:

- ρ_{df} is the mean density of the material. The density of a debris flow is in the range 1500÷2500 kg/m³, and typically 2000÷2200 kg/m³. Hu, et al. (2012) derived a density of 2000 kg/m³ by analyzing sediment samples taken from debris flow deposits in Western China. *AEAI* (*Association des Etablissements cantonaux d'Assurance Incendie*) defines a density of 1800 kg/m³ for a muddy debris flow and 2200 kg/m³ for a granular one. In this work the density is assumed equal to 2000 kg/m³.
- g is gravity acceleration equal to 9.8 m/s²
- h is the height of the moving mass or the depth of the debris flow.

Table 22: Height values and their sources

HEIGHT (m)	SOURCE
0.5÷3	VKF/AEAI
5.84	Case study
2.70	Case study
0÷8.5	This Work

In this work the range of values considered includes both those provided by AEAI and the values relating to the 2 case studies (*Table 22*); considering, moreover, that since this is a slow-moving landslide, the heights may be greater than those assumed for a debris flow.

- v is the velocity of the moving mass;

Table 23: Velocity ranges and their sources

VELOCITY (m/s)	SOURCE
2÷7 and 15÷20	VKF/AEAI
40÷60	Erika Prina Howald
0÷9	This Work

In this work, the second line (*Table 23*) concerning the range of velocity variation relative to AEAI was considered by adapting it to the case of a slow-moving landslide. Therefore, the range of variation with which the vulnerability curves were constructed is that in the last line of the *Table 23*.

The intensity obtained will subsequently be used for the calculation of vulnerability; in *Table 24* is proposed an intensity classification based on the structure damage degree, (*Miteva e Prina Howald 2022*). This classification takes up the subdivision of debris flows intensity because by adopting the necessary simplifications, case **D** is considered similar to the debris flow impact on a building.

Table 24: Intensity classification provided by this work, case **D**

CLASSES	INTENSITY (kPa)	DAMAGE
1	0÷25	Low
2	25÷60	Medium
3	60÷110	High
4	>110	Very high

5.2 Vulnerability function

Vulnerability is a dynamic element that should be assessed considering spatial and temporal aspects. According to the glossary of risk-assessment terms of the International Society of Soil Mechanics and Geotechnical Engineering, vulnerability refers to the degree of loss to a given elements or set of elements within the area affected by the landslide hazard. Vulnerability depends on both the characteristics of the element at risk and the landslide intensity.

In this thesis vulnerability is analysed in average and is a function of intensity and resistance: the analytical structure is given by Li's model (*Li, et al. 2010*), but the resistance formulation is adapted to the case of slow-moving landslides. In Li's model the resistance index is the resistance ability of the elements/persons to withstand a hazardous event; for structural elements it is a resilience indicator to danger, while for people represent the ability to deal with hazardous event. The model used in this study is shown below, defining vulnerability in the range [0,1].

$$V = \begin{cases} \frac{2I^2}{R_B^2} & \frac{I}{R_B} < 0.5 \\ 1 - \frac{2(R_B - I)^2}{R_B^2} & 0.5 \leq \frac{I}{R_B} \leq 1 \\ 1 & \frac{I}{R_B} > 1 \end{cases} \quad \text{Equation 8}$$

Where:

- **I** is the intensity parameter. The expressions used for intensity have already been defined above, *paragraph 5.1.1*.
- **R_B** is the strength index. The expression defining this parameter will be specified later as it vary depending on which position of the building is considered, (**A, B, C, D**).

The resistance formulation used and adapted to this case study, is shown below. It is an equation expressing the resistance as a function of factor's summation:

$$R = \left(\prod_{i=1}^{n_s} \xi_i \right)^{\frac{1}{n_s}} \quad \text{Equation 9}$$

Based on Li's model, the proposed formulation of resistance considers only structural elements and is meant as follows: resistance to slow landslide movement for cases A, B and C and impact resistance for case D. Resistance (R) has been replaced by building resistance (R_B) in this work; the definition of the resistance index R_B for each of the 4 cases analysed will be given below, also including values and weights used for each of the formula components.

▪ RESISTANCE INDEX R_B CASES A, C:

The resistance index R_B for cases A and C where buildings are located in the crown and central part of the landslide respectively, is calculated using the following equation (*equation 9* modified for the case under study):

$$R_B = \sqrt[2]{2 * \xi_{fd} * \xi_{cm}} \quad \text{Equation 10}$$

Where:

- ξ_{fd} is the parameter concerning foundation depth
- ξ_{cm} is the construction material parameter

Within the *equation 10*, the parameters will be weighted according to their influence on the building's resistance capacity. The depth of building foundation has a greater influence on the building's vulnerability to slow-moving landslides than the construction material of his section above the ground level. This last section is supposed to be an integral part of the building's resistance as it interacts with the foundations by undergoing deformations in relation to its construction material. The construction material of the foundations is always considered to be concrete: as the score does not change from one building to another, this factor is worth 1; *equation 10* does not include this factor because being 1 does not change resistance index. Therefore, the weights assigned to these two factors are: 2 for the depth of building foundation (ξ_{fd}) and 1 for the construction material (ξ_{cm}).

Table 25 shows the failure surface depth ranges considered in this thesis.

Table 25: Failure surface depth ranges considered in this work

DEPTH OF THE FAILURE SURFACE(m)
1.5÷2
2÷5
5÷30
>30

For each failure surface depth range, a score is assigned to the factor concerning depth of the building foundation. This depends on the foundation depth compared to that of the sliding plane: it will be the greater the shallower the foundation depth compared to that of the failure surface. This procedure is performed for all building materials considered, whose score is shown in *Table 26*.

Table 26: Scores relating to the type of building construction material used in this work

TYPE OF STRUCTURE	TYPE OF MATERIAL	SCORE
Chalet	Timber	0.6
	Timber + Concrete	0.4
Residential Building	Masonry	0.2
	Reinforced Concrete	0.6
Residential Villa	Masonry	0.2
	Concrete + Masonry	0.3

These scores were given on the basis of tensile strength of the material under study:

- Timber is the most tensile-resistant material: 10÷30 N/mm²
- Masonry is the least tensile-resistant material: 0.6÷2.1 N/mm²
- Concrete has a tensile strength that can be approximately 10 % of its compressive strength: 3÷5 N/mm²
- Reinforced Concrete is a fibre-reinforced concrete mix in which the addition of steel fibre modifies its mechanical and physical properties and improves its tensile behaviour by preventing the progressive opening of cracks

▪ RESISTANCE INDEX R_B CASE B:

This case represents a simplification of an extreme situation of a building location. The resistance index R_B for case B where buildings are located on the lateral edge of the landslide body, is calculated using the following equation (*equation 9* modified for the case under study):

$$R_B = \sqrt[3]{3 * \xi_{cm} * 2 * \xi_{bi} * \xi_{nf}} \quad \text{Equation 11}$$

Where:

- ξ_{cm} is the construction material parameter
- ξ_{bi} is the parameter concerning building inclination
- ξ_{nf} is the parameter concerning the number of floors

Within the *equation 11*, the parameters will be weighted according to their influence on the building's resistance capacity. The construction material has a greater influence on the building's vulnerability to slow-moving landslides than building inclination and number of floors. Therefore, the weights assigned to these three factors are: 3 for the construction material (ξ_{fd}), 2 for the building inclination (ξ_{bi}) and 1 for the number of floors (ξ_{nf}).

Concerning the construction material parameter, scores assigned according to the type of buildings are the same used in cases A and C previously analyzed.

ξ_{bi} is a parameter identifying the building inclination due to the structure's rotation at the boundary between the landslide body and the stable slope. According to the 'Code of Deformation Measurement of Building and Structure' we can calculate the inclination of a building as follow:

$$i = \tan \alpha = \frac{y_m}{H} \quad \text{Equation 12}$$

Where

- i is the inclination of a building
- α is the incline angle of the building
- y_m is the horizontal difference between the top and bottom of the building, maximum deformation
- H is the vertical height of the tilted building calculated from the ground level

Scores about building inclination are assigned on the basis of threshold values provided by 'Ministry of Housing and Urban–Rural Development of PRC, 2016'; buildings with an inclination that exceeds the threshold values are considered to be dangerous and uninhabitable, (Chen, et al. 2020); the present work proposes 3 inclination classes from very low to very high, shown in Table 27.

Table 27: Scores relating to the building inclination used in this work

HEIGHT (m)	(i_m)THRESHOLD VALUE	CLASSES	SCORE
$H \leq 24$	0.01	$i < 50\%(i_m) \rightarrow$ very low	1.2
$24 < H \leq 60$	0.007	$50\%(i_m) < i < 100\%(i_m) \rightarrow$ medium	0.7
$60 < H \leq 100$	0.005	$i > 100\%(i_m) \rightarrow$ very high	0.1

Given these threshold values, if we assume 10 m as the building height, the critical horizontal distance between the top and bottom of the building is approximately 10 cm. In the developed methodology for creating vulnerability curves, the first row of Table 27 will be used, as buildings with more than 6 floors are not considered.

Concerning the indicator 'number of floors/height' 4 different ranges were distinguished, the scores (Table 28) provided by Li will mainly be used in this work, considering buildings up to 5/6 floors, (Li, et al. 2010).

Table 28: Scores relating to the number of floors/height used in this work

NUMBER OF FLOORS	SCORE
1	0.1
2	0.3
3,4	0.9
>4	1.1

▪ RESISTANCE INDEX R_B CASE D:

The resistance index R_B for case D where buildings are located at the toe of the slope, is calculated using the following equation (*equation 9* modified for the case under study):

$$R_B = \sqrt[3]{3 * \xi_{cm} * 2 * \xi_{nf} * \xi_{ms}} \quad \text{Equation 13}$$

Where:

- ξ_{cm} is the construction material parameter
- ξ_{nf} is the parameter concerning the number of floors
- ξ_{ms} is the parameter concerning the maintenance state

Within the *equation 13*, the parameters will be weighted according to their influence on the building's resistance capacity. The construction material has a greater influence on the building's vulnerability to slow-moving landslides than the number of floors and the maintenance state respectively. Therefore, the weights assigned to these three factors are: 3 for the construction material (ξ_{fd}), 2 for the number of floors (ξ_{nf}) and 1 for the maintenance state (ξ_{ms}). The score assigned to the construction material according to the building considered, can be seen in *Table 29*. Li's model is adopted for the attribution of this score by adapting it to the case of a moving mass hitting a structure with a certain pressure, (*Li, et al. 2010*).

Table 29: Scores relating to the type of building construction material used in this work

TYPE OF STRUCTURE	TYPE OF MATERIAL	SCORE
Chalet	Timber	0.2
	Timber + Concrete	0.6
Residential Building	Masonry	0.8
	Reinforced Concrete	1.5
Residential Villa	Masonry	0.8
	Concrete + Masonry	1.2

These scores were given on the basis of the compressive strength of the material under study:

- Timber is the least compressive-resistant material: $2 \div 5 \text{ N/mm}^2$
- Concrete is the most compressive-resistant material: $30 \div 80 \text{ N/mm}^2$
- Masonry has a compressive strength that can vary in a range of $6 \div 15 \text{ N/mm}^2$
- Reinforced Concrete is a fibre-reinforced concrete mix in which, the compressive strength does not change significantly compared to concrete

Concerning the indicator 'number of floors/height', the subdivision into 4 classes is the same as in case B.

The maintenance state describes the change in building's performance; it is expressed in 5 classes from very poor to very good (*Table 30*), following the classification proposed by Li, et al. (2010).

Table 30: Scores relating to the maintenance state used in this work

MAINTENANCE STATE	SCORE
very poor	0.1
poor	0.4
medium	0.8
good	1.2
very good	1.5

Chapter 6: VULNERABILITY CURVES

The vulnerability curve represents, changing intensity due to the development of the landslide event, the probability that the building will reach a certain state of damage. An example of a vulnerability curve, with vulnerability (y-axis) function of intensity (x-axis), is given in *Figure 23*.

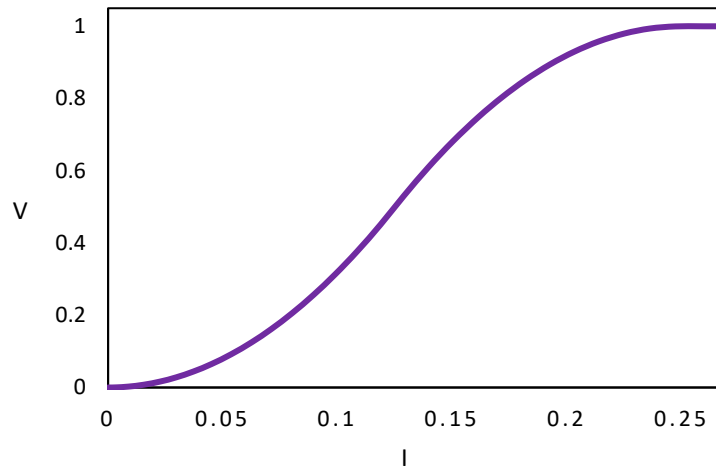


Figure 23: An example of a vulnerability curve

Vulnerability curves were developed for each type of vulnerable structure in each of the 4 corresponding positions (**A, B, C, D**) defined in *Chapter 4*. The function used for the construction of vulnerability curves is that presented in *Chapter 5, Equation 8* with the hazard intensity calculated according to *Equations 4* (**A, B, C**) and *5* (**D**), and the building resistance determined with *Equation 9*. The obtained curves are shown in *Chapter 6.1*. Each curve is characterized by a legend explaining the type of building considered and the parameters used in its construction. The legend explanation is given in *Tables 31 (CASES A, C), 32 (CASES B), 33 (CASES D)*.

Table 31: Explanation of the vulnerability curve legend cases **A** and **C**

TYPE OF STRUCTURE	FOUNDATION DEPTH	CONSTRUCTION MATERIAL
Chalet → CH	1 metre → 1m	Timber → T
	> 1 metre → >1m	Timber + Concrete → T+C
Residential Villa → RV	1 metre → 1m	Masonry → M
	> 1 metre → >1m	Concrete + Masonry → C+M
Residential Building → RB	< 2 metres → <2m	Masonry → M
	between 2 and 10 metres → 2÷10m	Reinforced Concrete → RC
	> 10 metres → >10m	

Table 32: Explanation of the vulnerability curve legend case B

TYPE OF STRUCTURE	NUMBER OF FLOORS	CONSTRUCTION MATERIAL	INCLINATION
Chalet → CH	1 floor → 1	Timber → T	Very low → VL Medium → M Very high → VH
	2 floors or > 2 floors → 2, >2	Timber + Concrete → T+C	
Residential Villa → RV	2 floors → 2	Masonry → M	
	3 floors → 3	Concrete + Masonry → C+M	
Residential Building → RB	4 floors → 4	Masonry → M	
	> 4 floors → > 4	Reinforced Concrete → RC	

Table 33: Explanation of the vulnerability curve legend case D

TYPE OF STRUCTURE	NUMBER OF FLOORS	CONSTRUCTION MATERIAL
Chalet → CH	1 floor → 1	Timber → T
	2 floors or > 2 floors → 2, >2	Timber + Concrete → T+C
Residential Villa → RV	2 floors → 2	Masonry → M
	3 floors → 3	Concrete + Masonry → C+M
Residential Building → RB	4 floors → 4	Masonry → M
	> 4 floors → > 4	Reinforced Concrete → RC

6.1 Results

Vulnerability curves obtained for each type of structure are shown in the following *figures*; each figure will be preceded by a brief description regarding its construction and followed by an analysis of what has been gained.

▪ CASE A, C

Vulnerability curves is constructed using the same intensity; considering the depth of the sliding surface as the key parameter, the foundation depth scores are given. In the legend of each curve, the abbreviation corresponding to the foundation depth is indicated in the central position.

The first two graphs refer to Case A: *Figure 24* considers a failure surface depth of less than 2 metres while *Figure 25*, assumes a depth between 2 and 5 metres. The two plots in the *Figures 26, 27* instead, refer to Case C: the first takes up a failure surface depth between 5 and 30 metres, while the second considers a depth greater than 30 metres. The depth was divided as described before, because an increase in

the sliding surface depth from the crown to the central part of the landslide body is assumed.

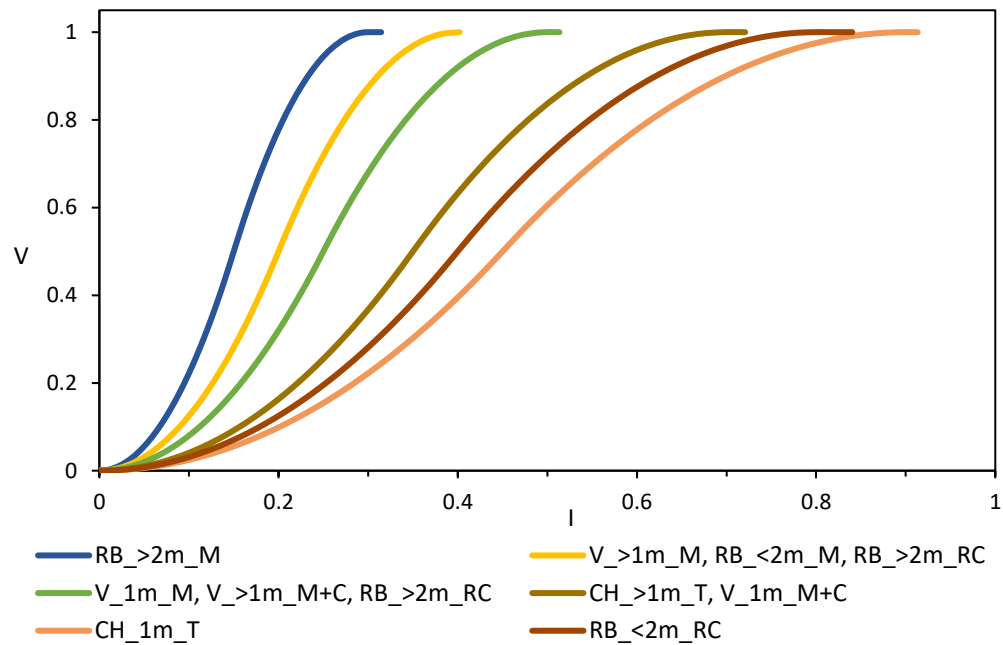


Figure 24: Vulnerability curves obtained for case A when the depth of the sliding surface is less than 2 metres

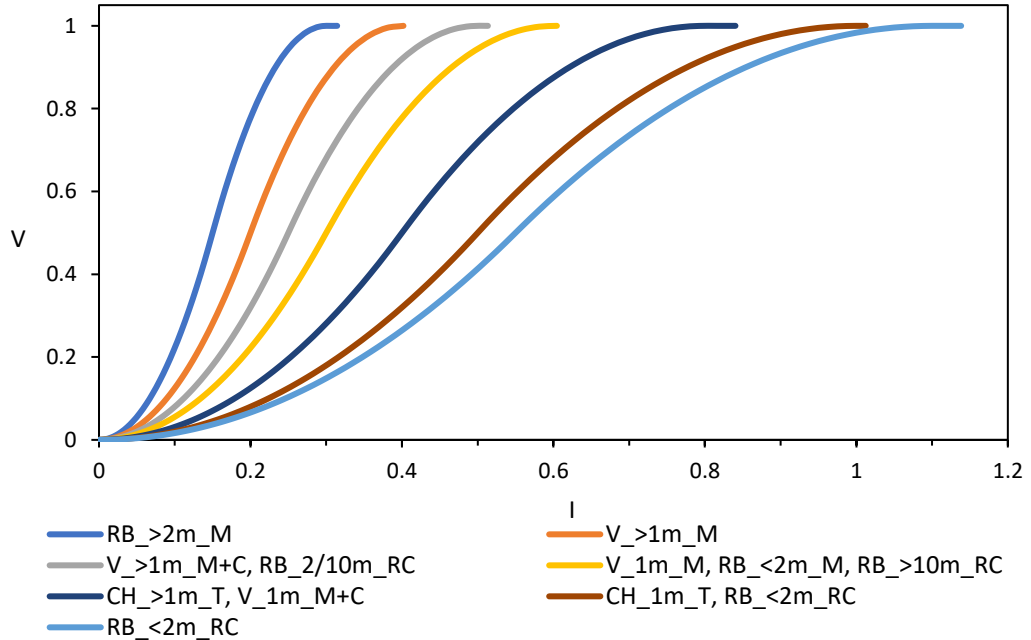


Figure 25: Vulnerability curves obtained for case A when the depth of the sliding surface is assumed between 2 and 5 metres

Both cases analysed in the two figures above, show that the most vulnerable buildings are those where the foundations are crossed by the sliding surface of the

landslide body. Concerning materials for the reasons explained in *Chapter 5, Section 5.2*, masonry is the least resistant material compared to timber and reinforced concrete.

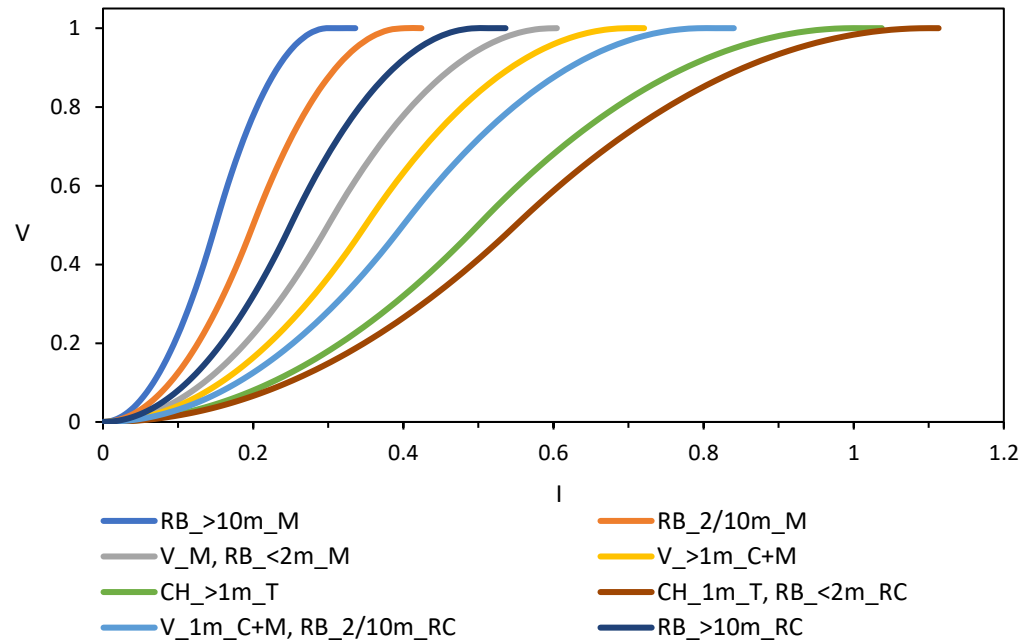


Figure 26: Vulnerability curves obtained for case C when the depth of the sliding surface is assumed between 5 and 30 metres

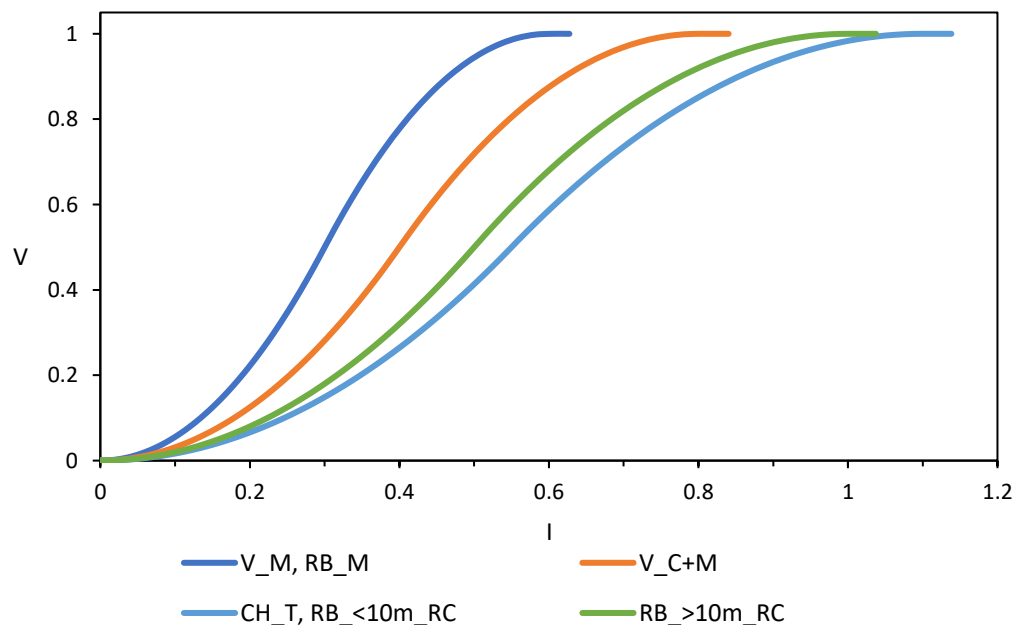


Figure 27: Vulnerability curves obtained for case C when the depth of the sliding surface is higher than 30 metres

Figure 26 shows that the most vulnerable buildings are masonry residential buildings with a foundation depth greater than 10 metres. On the other hand, chalet with foundations of 1m is the most resistant because, for low movement velocities, it moves with the landslide body without sustaining large deformations.

■ CASE B

Vulnerability curves is constructed using the same intensity applied in cases A and C. The three graphs given in the following *figures* are divided by building type: Chalet in *Figure 28*, Residential Villa in *Figure 29* and Residential Building in *Figure 30*. This case is the most critical since the building is located on the boundary between the landslide body and the stable slope: adopting the necessary simplifications it assumed that the key parameter is that concerning inclination and rotation of the building due to the movement of the unstable body. In the legend of each curve, the abbreviation corresponding to the key parameter is indicated in the third position (VL, M, VH).

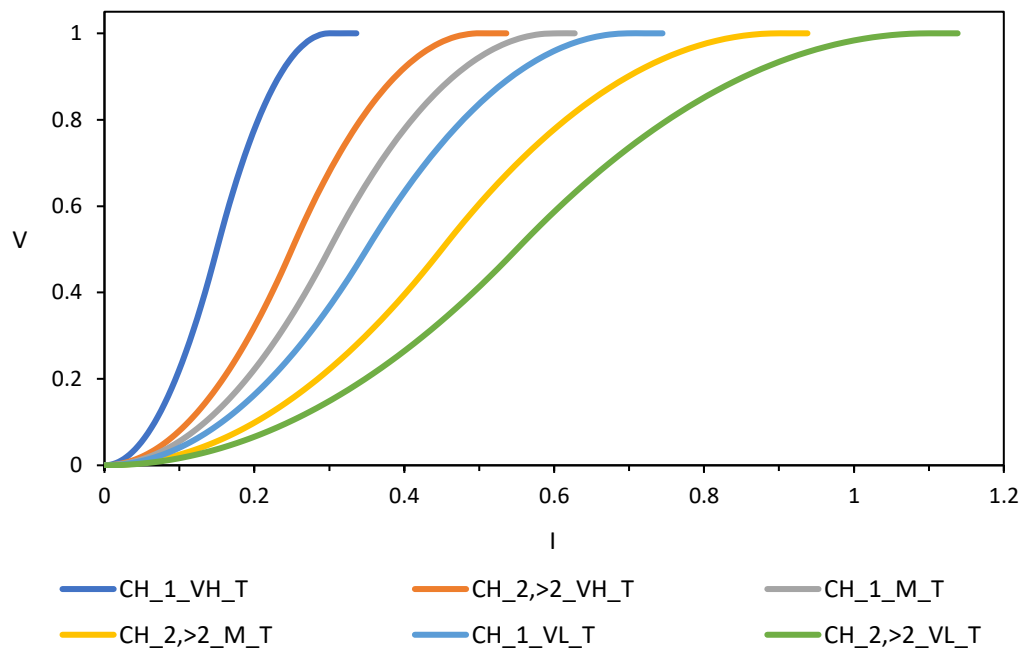
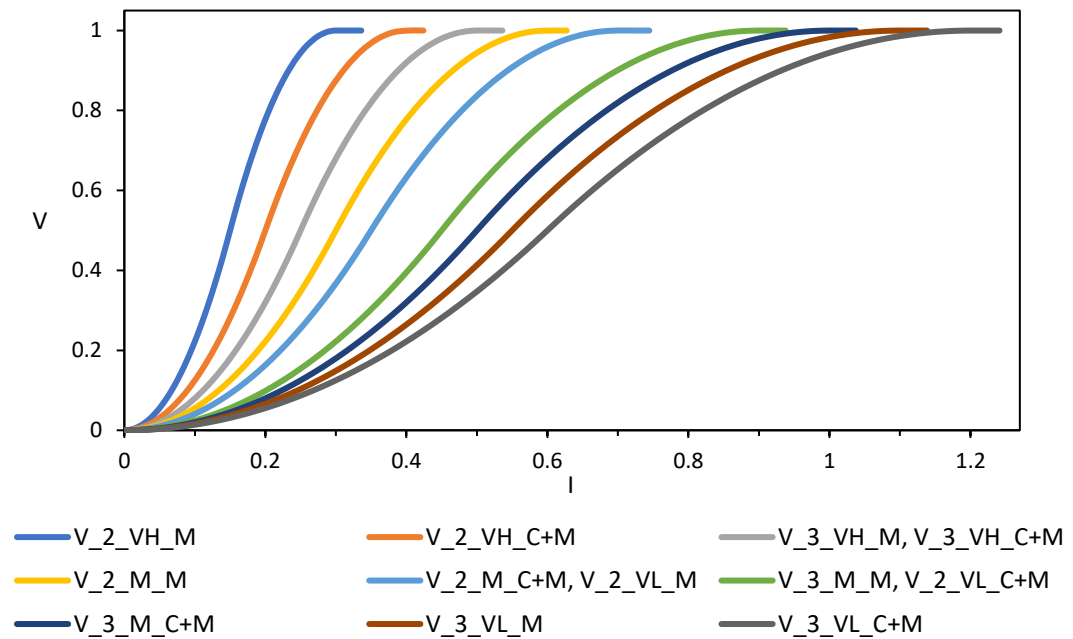
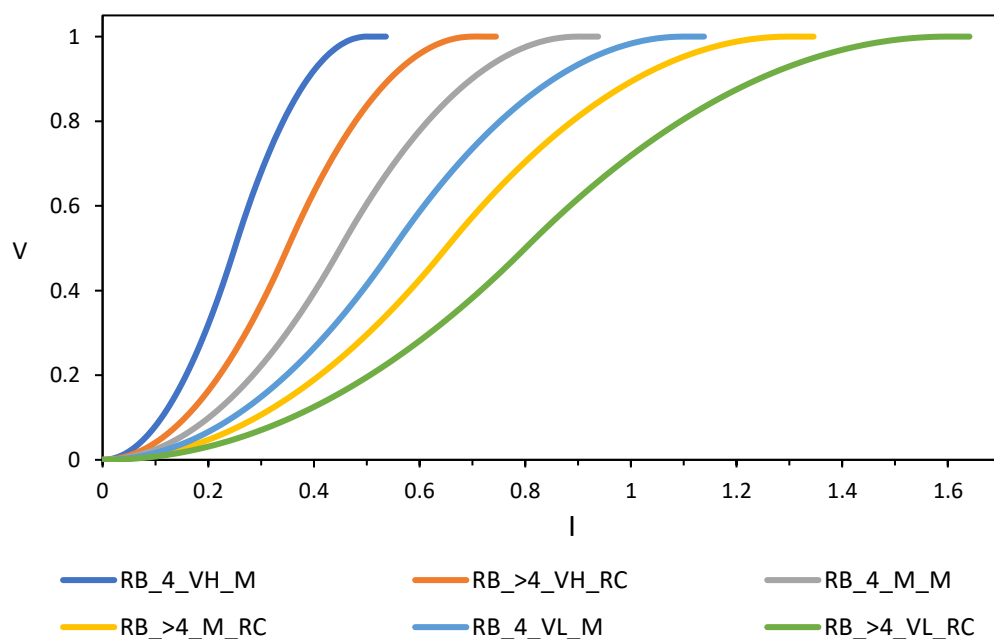


Figure 28: Chalet vulnerability curves obtained for case B

The most vulnerable building turns out to be the 1-storey chalet with a very high (VH) inclination while the 2, >2-storey chalet with a very low inclination results the least vulnerable, (the definition of the parameter was given in *Chapter 5*).

Figure 29: Residential villa vulnerability curves obtained for case **B**Figure 30: Residential building vulnerability curves obtained for case **B**

Even for vulnerability curves shown in the *Figure 28, 29* the most vulnerable buildings are those with the highest inclination, keeping in mind that threshold values regarding inclination and rotation of the building vary depending on the height and therefore the number of floors (*Chapter 5*), a parameter considered within the curves and shown in the legend in second position.

▪ CASE D

Vulnerability curves are constructed using a different equation of intensity from the previous cases: it is expressed through the pressure that the moving mass applies when it impacts on a building. The key parameter is the construction material because the building resistance depends on the compressive strength of the material. In the legend of each curve, the abbreviation corresponding to the construction material is indicated in the final position.

The other 2 parameters are the number of floors then the height of the building, and the maintenance state; the three graphs are structured as follows: in *Figure 31* vulnerability curve were constructed on the basis of a very low maintenance state, in *Figure 32* based on an average maintenance state and in *Figure 33* with a very high maintenance state.

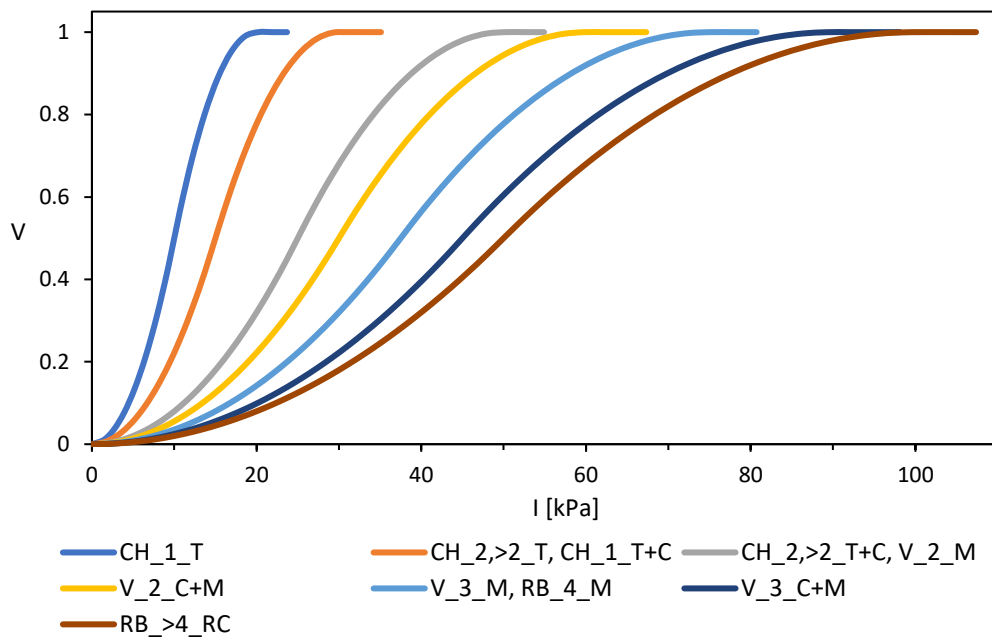


Figure 31: Vulnerability curves obtained for case **D** when the maintenance state is very poor

In *Figure 31* the most vulnerable building is the one-storey wooden chalet while the strongest building is the reinforced concrete residential building; it is observed that the curves constructed for wood + concrete or masonry buildings have a very similar vulnerability because although masonry has a higher compressive strength than wood, being wood + concrete the values are very similar.

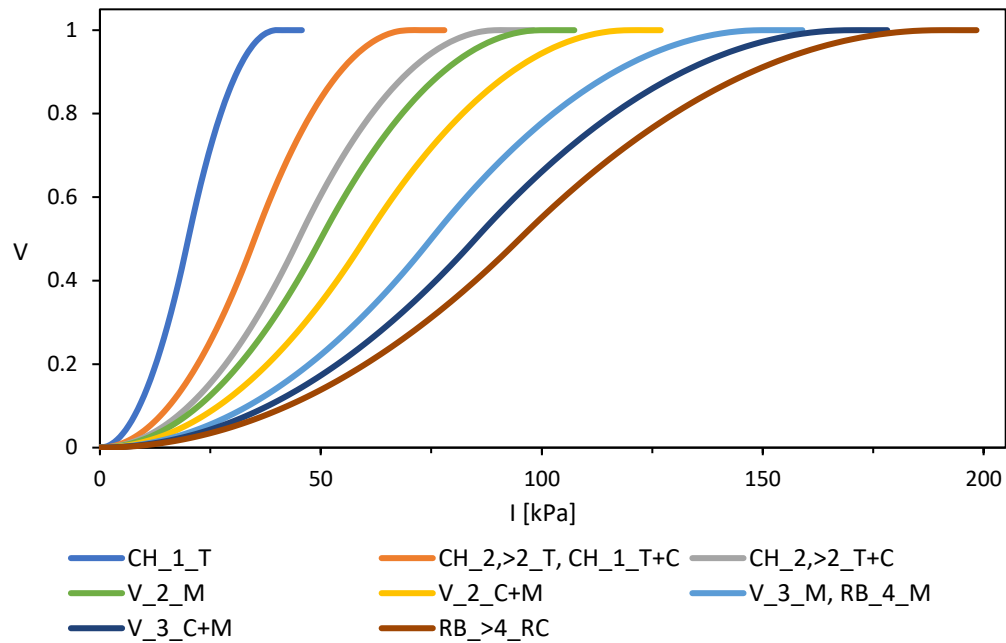


Figure 32: Vulnerability curves obtained for case **D** when the maintenance state is medium

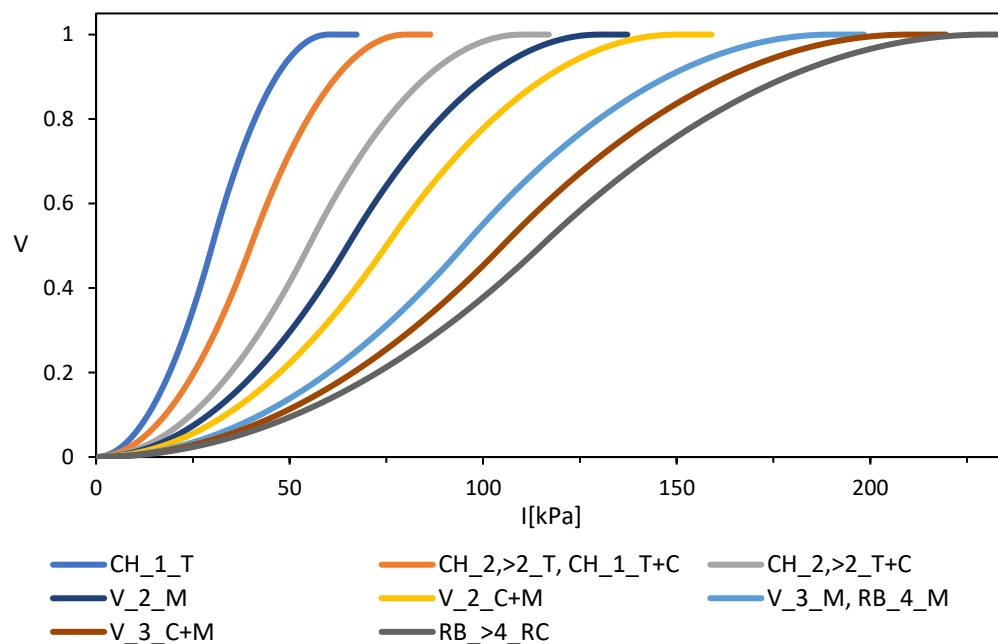


Figure 33: Vulnerability curves obtained for case **D** when the maintenance state is very high

Even for vulnerability curves shown in the *Figure 32, 33* the most vulnerable buildings are those construct in wood, while the most resistant one are those with more than four storeys made of reinforced concrete. It is possible to detect that in *Figure 33* vulnerability curves are more smeared than the previous two graphs, since being in good maintenance state they have less vulnerability.

Chapter 7: CASE STUDIES

In this chapter, 4 case studies are analysed: Hohberg Landslide, Converney-Taillepiéd Landslide, Pont Bourquin Landslide and La Frasse Landslide. These are permanent landslides that occasionally develop into debris flows or rockfall phenomena and are located in the NORTH-WEST part of Switzerland. Each case study will be presented as follows:

- Introduction on the landslide 's geographical area with available data used to apply the proposed methodology, followed by a brief review of past events and monitoring measures applied to avoid similar phenomena
- Hydrogeological context
- Results obtained from the methodology's application: case studies are visualised in the graphs showing the vulnerability curves, with indicators; it was decided to display 1 plot per case study highlighting the indicators against the vulnerability curves, which were left in transparency. Each graph will analyse one of the 4 building positions (**A, B, C, D**) on the landslide body; the other plots will be shown in *Appendix 1*.

7.1 Hohberg Landslide (FR)

7.1.1 Study area and available dataset

Hohberg landslide is located in the Fribourg Pre-Alps, about 2 km north-east of Lac Noir. Hohberg landslide extends from the northern Hohmattli slope, approximately 1780 metres high, to the southern border of Ättemberg, about 1500 m high; it moves forward into the morphological depression crossed by the Hohbergbach and stops to eastern edge of the Rohrmoos plain, in the residential area of Rohr (1030 m).

The size between the top and bottom of the landslide exceeds 2500 metres. The landslide has a particular hourglass shape with a large feeding zone upstream, subdivided into a lot of active corridors between 50 and 300 m wide; it narrows towards the landslide central part to create space for a passage about 200 m wide that follows the morphological depression crossed by the Hohbergbach (1300 and 1150 m high). The lower zone widens from the mouth of the corridor and presents a rough morphology due to the accumulation of multiple landslide and mudflow deposits.

The Hohberg landslide activity has been monitored since 1994, when the upper part of the slide suddenly reactivated, affecting the middle and lower zones. Monitoring work began in 1995, with the installation of a network of GPS points and fixed laser distometers for continuous displacement measurements. By means of geophysical measurements, it was possible to reconstruct three-dimensional structure of the landslide body; the depth of the sliding plane was measured with the aid of inclinometer probes; boreholes also made it possible to collect several wood samples located deep in the Quaternary. As a result of monitoring work, remedial measures are implemented in 1999, mainly surface drainage in the central part of the landslide, later extending them to the lower and upper parts.

The highest velocities, exceeding one metre per month, were reached on the southern edge of the landslide, at the level of the road leading to the Lengmoos chalet; these velocities are measured over short time intervals since 1995, especially between June and August 1997. This area lies at the foot of the southern upper corridor, which is characterised by rapid movements linked to debris flow processes. In the spring of 1999, accelerations of the landslide movement in the upper and central parts of the landslide were recorded; these spread rapidly downstream with displacement rates of up to 5-10 cm per month, resulting in significant deformations in the structures of several buildings in the Rohr district. Subsequently, in 2009 and 2014, two more large reactivation events occurred, confined to the upper parts of the landslide, which extends from the Guglera Hohberg (altitude 1500 m) to the valley bottom (altitude 1000 m). Displacement is up to 1 m per day in the upper part and a few decimetres per day in the lower part. The volume of the entire unstable mass reaches 23 million of m³ with a surface area of over 20000 m². The depth of the main sliding plane varies between 15 and 20 m in the lower and central zones and gradually decreases in the upper part.

7.1.2 Geological Context

The highest part of Hohberg landslide, located on the northern slope of the Hohmattli, is on the north side of Nappe Median Pre-Alps Plastics. This nappe is made up of several units that begin in the Upper Triassic and extend into the Lower Cretaceous, exposing many different types of lithologies. A narrow band of Mélange, which represents the central and upper part of the landslide, separates the Gurnigel

Nappe from that of the Median Pre-Alps. This geological context is shown in *Figure 34*.

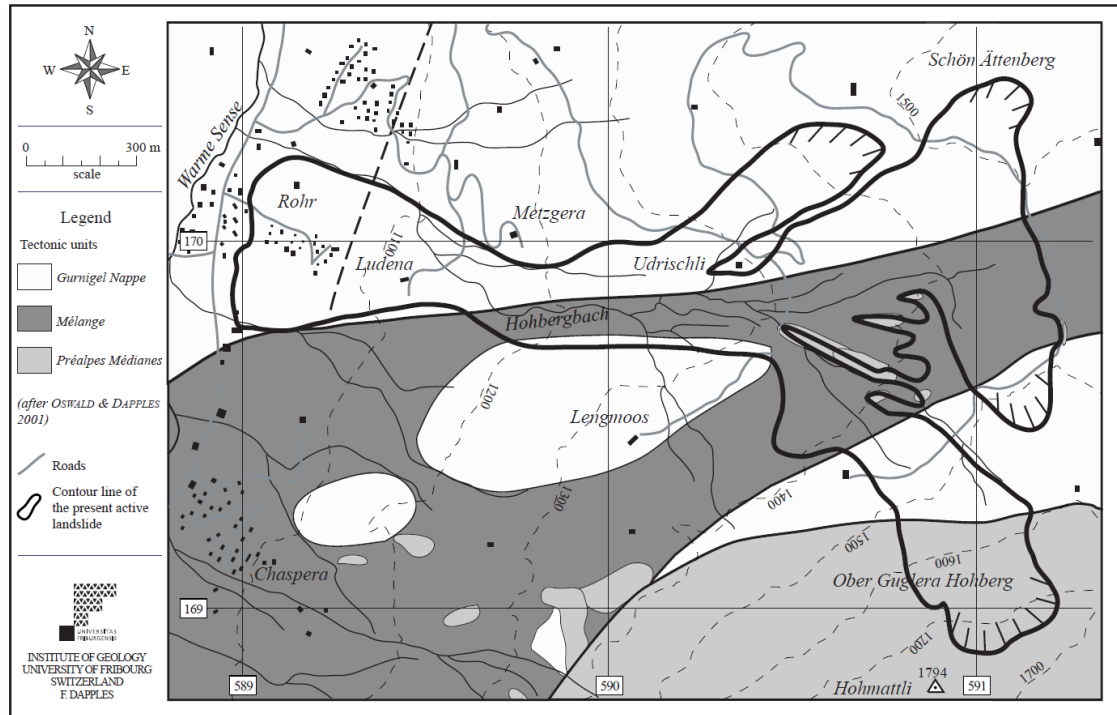


Figure 34: Local tectonic context of the Hohberg landslide area, (Dapples 2002)

Thus, the northern part of the landslide area is made up of different bio stratigraphic flysch units that vary in size and thickness. The shallowest materials contain a considerable amount of clayey and marly sediments from the several flysch units; the majority of fine and impermeable particles is an important factor for the formation of failure surfaces related to groundwater circulation. The movements only affect the shallow part of the Quaternary deposits that have accumulated over the millennia in the Hohbergbach watershed; in fact, the Quaternary materials lying on the bedrock show no signs of significant movement.

7.1.3 Results

The proposed methodology is applied to cases A and D, crown and toe of the landslide respectively. *Tables 34, 35* show the data used for the methodology application to the Hohberg landslide.

Table 34: Data used in the methodology application for case A , landslide crown

	HEIGHT (m)	VELOCITY (cm/year)	BUILDINGS CONSIDERED
CASE A	2 < H ≤ 5	60	Timber Chalet
		120	Timber + Concrete Chalet
		36500	

Table 35: Data used in the methodology application for case D , landslide toe

	DENSITY (kg/m ³)	HEIGHT (m)	VELOCITY	BUILDINGS CONSIDERED
CASE D	2200	H ≤ 5	V > 1m/month	Timber + Concrete Chalet
			V > 0.1m/day	Masonry Villa
				Masonry + Concrete Villa

The graph concerning case A, with indicators implemented on the basis of the obtained data from the analysis of this case study, is shown in *Figure 35*.

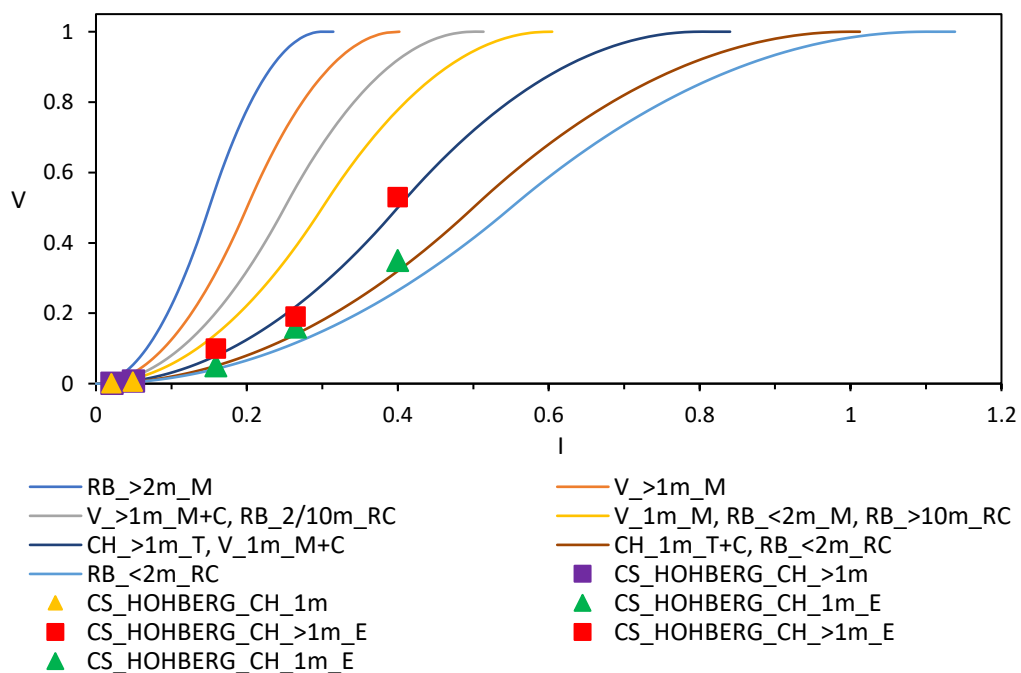


Figure 35: Vulnerability curves and indicators obtained for case A when the depth of the sliding surface is assumed between 2 and 5 metres

Since the crown of the landslide body is located in a mountainous area, the buildings considered are timber and concrete-timber chalets; the indicators are placed in the area next to vulnerability curves relative to these 2 building types. The purple squares as well as the yellow triangles represent buildings with very low

vulnerability because the intensity was calculated using velocity of a few centimetres per year and a relatively low soil thickness. While the red squares as well as the green triangles indicate buildings with a higher vulnerability calculated using a velocity that exceeds the range considered in this study because it is the maximum velocity reached within an event and not the average speed as the landslide body moves.

7.2 Converney-Taillepied Landslide

7.2.1 Study area and available dataset

Converney-Taillepied Landslide is an extended permanent sliding of glacial outwash material located in the Canton of Vaud between Lausanne and Chexbres, western Lavaux. It is a slow slide resulting in a progressive deformation of the ground partly due to soil geology. The landslide develops in the area including three cities: Belmont-Sur-Lausanne, the southern slope of Monts de Lutry and Paudex shores. Belmont Sur-Lausanne has only 20% of the total area affected by this movement, but that part of the city is in the most active portion of the landslide body. Lutry municipality, on the other hand, covers two-thirds of the total area of Converney landslide. The municipality of Paudex is less involved in the landslide area (only 15%) and is mainly covered by forests and hills. The landslide body intersects 4 important transport infrastructures: N9 Léman highway and Perraudettaz freeway in the top half of the landslide and the two railway lines Lausanne-Berne and Lausanne-Simplon in the bottom half.

Surface area of the entire unstable mass reaches 2.5 km²: from the slopes of Lavaux, with an altitude of 750 m above sea level, to the cities of Les Ecaravez and Corsy. The failure surface has an average depth between 10 and 40 m, while the characteristic velocity is 2 cm/year. Main triggering factors of landslide movement are: variations in the groundwater level, dry followed by periods of heavy rain, erosion caused by the rivers crossing the landslide and distributed load on the sliding mass.

The activity of the Hohberg landslide is dated 1618 with many building damages on the eastern side. In 1758 there was another reactivation of the landslide body, which

affected an area of 500000 m². The same movement destroyed a cottage in 1930. In 1962 the triggering factor the reactivation of the landslide was a slope cut 6 metres deep. Two other events are dated 1965 and 1980: they caused a distortion of the railway embankment and a lot of damages to a villa and a railway line respectively. The last recorded event (February 1990) is a fast landslide on the main slope of the Converney landslide triggering by heavy rainfall. This caused the sliding of a rock layer with a volume of 40000 m³ and a velocity of approximately 0.05 m/s. The rock layer had a depth of about 4 metres including 2 m of sandstone and 1.5 m of sandy and clayey marls. This phenomenon has destroyed four houses and damaged a road in the municipality of Belmont-sur-Lausanne. Recent monitoring shows that there may be reactivations at a depth of about 14 m below the city of Belmont where movements are still recorded.

7.2.2 Hydrogeological Context

The Converney-Taillepie slide must have been, in its initial and main phase, a giant layer-on-layer slide with weak internal dislocation. It is mainly located on the coal molasse that contains alternating levels of marl, mudstone and sandstone banks. Molasses is a rock with mechanically plastic behaviour and low cementation. Outcrops of molassic rocks are visible on the La Conversion and Corsy hills. The alternation of hard cracked and soft impermeable benches in addition the dip of the layers in the downstream direction of the slope, aid the development of the landslide. The inclination of the layers into downstream direction of the slope as well as the sequence of layers of hard, cracked and soft, impermeable banks, aid the development of the landslide. Straightening of rock layers and strong fracturing of the entire landslide mass reducing the quality of mechanical strength, are some of the triggering causes of ground movements.

Concerning the hydrological context, the landslide is crossed by the Flonzen river and lapped by Paudèze and Lutrive rivers, which join at the bottom of the landslide. In the Converney area, the presence of marls and sandstones in the moving body (highly porous sedimentary rocks) allows high water storage but low circulation (low permeability).

In the Taillepied region, water circulation is extremely high, with underground flows having a flow rate of about 100 l/s. Therefore, the landslide body contains 2 aquifers: a water flow within the landslide and a semi-confined aquifer inside the underlying sands.

7.2.3 Results

The proposed methodology is applied to cases C and D, central part and toe of the landslide respectively. *Tables 36, 37* show the data used for the methodology application to the Converney-Taillepied landslide.

Table 36: Data used in the methodology application for case C, landslide central part

	HEIGHT (m)	VELOCITY (cm/year)	BUILDINGS CONSIDERED
CASE B	10 < H ≤ 40	20	Timber Chalet
		50	Timber + Concrete Chalet

Table 37: Data used in the methodology application for case D, landslide toe

	HEIGHT (m)	VELOCITY (cm/year)	BUILDINGS CONSIDERED
CASE C	10 < H ≤ 40	20	Timber Chalet
			Masonry Villa
		50	Masonry + Concrete Villa
			Masonry Building Reinforced Concrete Building

The graph concerning case **B** (chalet vulnerability assessment), with indicators implemented on the basis of the obtained data from the analysis of this case study, is shown in *Figure 36*. It is complicated to have precise information about the buildings that lie on the boundary between the landslide body and the stable slope; therefore, using an assumed intensity the presence of Chalets, Villas and Residential Buildings is considered in order to assess their vulnerability. Below is shown the graph concerning chalets, the others can be viewed in *Appendix 1*.

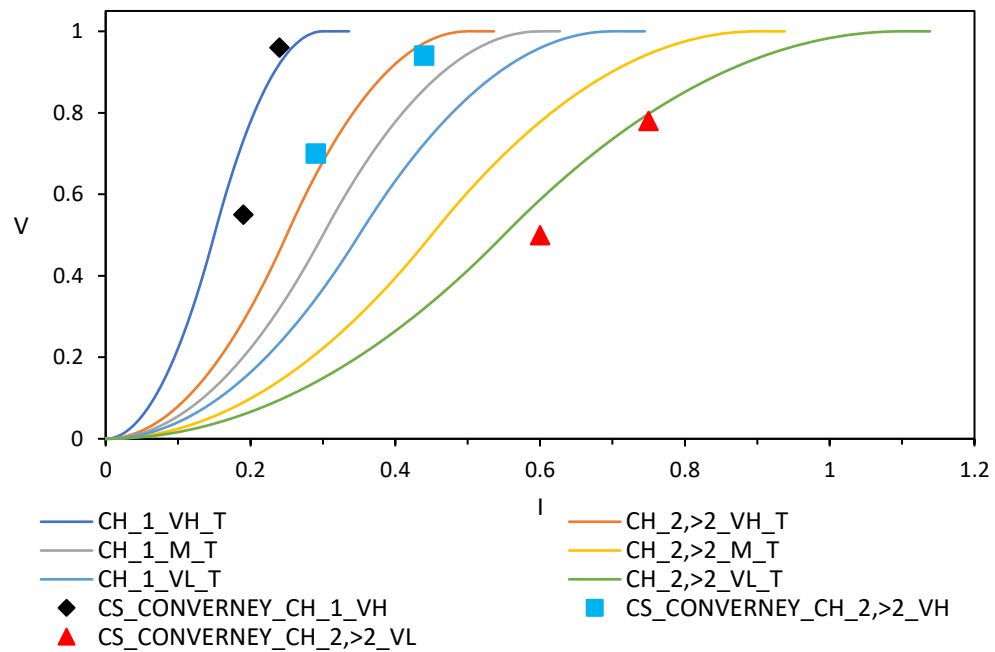


Figure 36: Chalet vulnerability curves and indicators obtained for case B

Chalets considered being on the edge between the landslide body and the stable slope, present high vulnerabilities compared to case A and C because even small movements would lead to severe structural damage due to shear failure.

7.3 La Frasse landslide

7.3.1 Study area and available dataset

Located in the Prealps (Vallée des Ormonts) of the Canton Vaud, Switzerland, near the Lemman Lake of Geneva, La Frasse landslide is a very large slide with the landslide toe continuously eroded by the Grande-Eau River. The most active part is the foot of the landslide crossed by the national road RC 705.

Total landslide area exceeds 1 km² with a length of approximately 2000 m-oriented NW to SE and a width varying between 500 m in the landslide crown to 1000 m at the toe of the landslide body. Although the total volume of the landslide is approximately 73 million m³, the volume of the active mass is 42 million m³ because some portions have been stabilised. The depth of the unstable mass varies between 40 and 80 m, although the depth of the entire landslide reaches 110 m in the central part. The slope has an inclination of 11° in the upper part reaching 20° in the lower part of the landslide. Concerning velocity, the landslide body could be divided in 5

main portions shown in *Figure 37*: Grand Glissement Supérieur, Lobe Sépey, Lobe Aigle, zone+ and zone ++, (Matti, Tacher et Commend 2012).

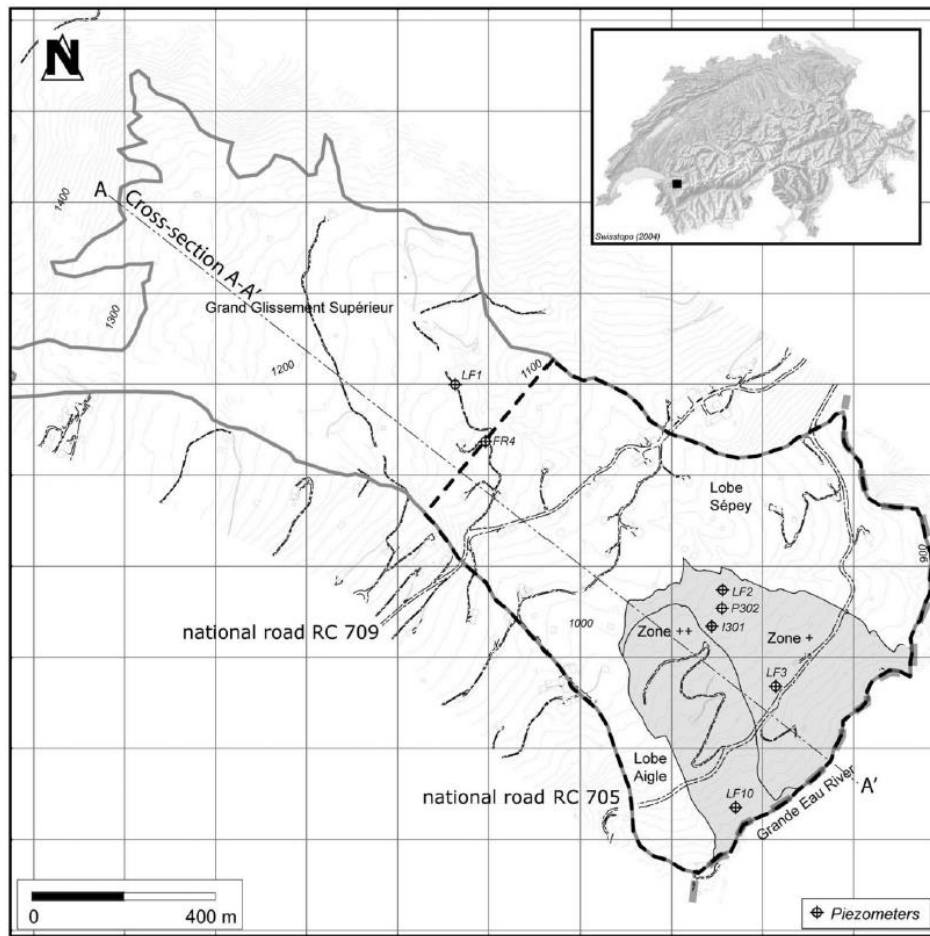


Figure 37: Location of La Frasse Landslide with subdivision in 5 main portions, (Matti, Tacher et Commend 2012)

The activity of La Frasse landslide dates back to 1863 with several reactivation phenomena, especially in the lower part, occurred in 1910, 1914, 1966, 1981-1982 and 1993-1994. The long-term velocity in the upper and central part of the landslide is not affected by these reactivation events, always varying between 10 to 15 cm/year. In the lower part, however, it varies between 20 to 60 cm/year with the maximum velocity reached of 1 m/week. With the application of monitoring measures as anchored piles or local pumping platform including drainage boreholes, the movement velocity decreased from 60 to 2.4 cm/year. The landslide's global behaviour is not yet completely secure as near the Cergnat hamlet, the landslide has been sliding at an average rate of about 13 cm/year for the past 200 years.

7.3.2 Hydrogeological Context

The geological structure of the La Frasse landslide is highly heterogeneous: it consists mainly of Tertiary flysch, which in turn is composed of sandstones and clay schists with sandy blocks, cretaceous siltstones and surface moraine fragments. C14 dating of wood fragments has shown that the landslide has been active for millennia with an average velocity of about 7 cm/year in the upper part; in the lower part, however, there are higher speeds as a result of the reduced thickness of the moving mass and the higher inclination.

At the regional scale, a single aquifer can be identified, while at the local scale the aquifer is discontinuous, limiting groundwater circulation and forming interconnected local aquicludes. The intense fracturing allows for a rapid groundwater flow fed not only by direct infiltration from the surface but also from the boundaries of the landslide body, which play an important role in the recharge process. From some boreholes it is derived that there are artesian inflows, i.e. pressure water not only at the level of the sliding surface, but also in the moving mass, (Matti, Tacher et Commend 2012).

7.3.3 Results

The proposed methodology is applied to cases C and D, central part and toe of the landslide respectively. Tables 38, 39 show the data used for the methodology application to La Frasse landslide.

Table 38: Data used in the methodology application for case C, landslide central part

	HEIGHT (m)	VELOCITY (cm/year)	BUILDINGS CONSIDERED
CASE C	40	10	Timber Chalet
	50	13	Timber + Concrete Chalet
	80	20	Masonry + Concrete Villa
		60	Masonry Villa

Table 39: Data used in the methodology application for case D, landslide toe

	DENSITY (kg/m ³)	HEIGHT (m)	VELOCITY	BUILDINGS CONSIDERED
CASE D	2200	7	< 0.05 m/s	Timber + Concrete Chalet
		5		Masonry Villa
				Masonry + Concrete Villa
				Reinforced Concrete Building

The graph concerning case **C**, with indicators implemented on the basis of the obtained data from the analysis of this case study, is shown in *Figure 38*.

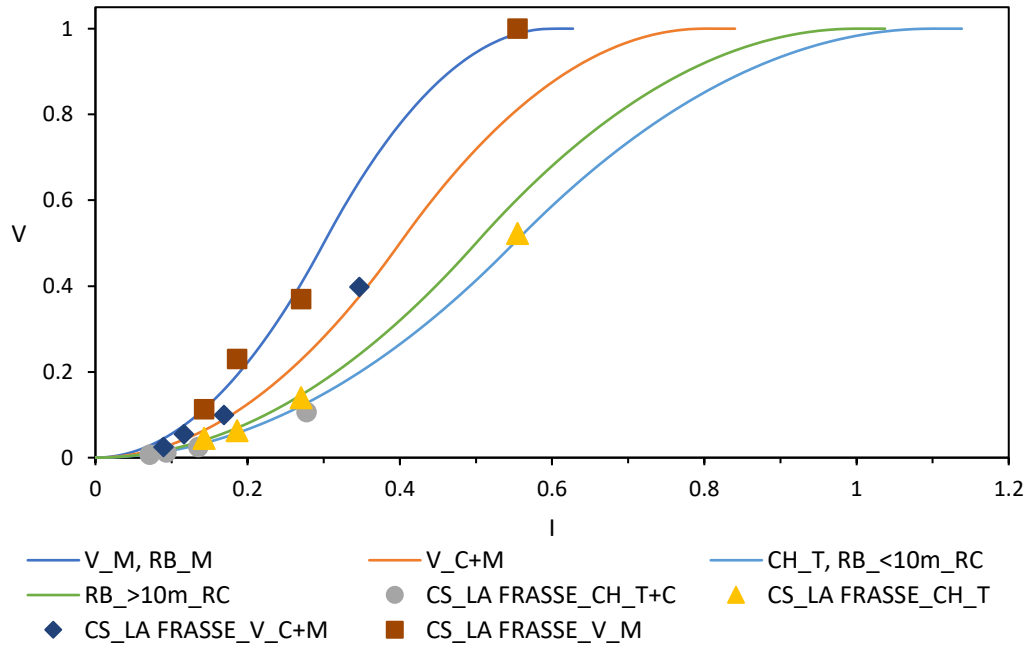


Figure 38: Vulnerability curves and indicators obtained for case C when the depth of the sliding surface is assumed to be higher than 30 metres

Since the central part of the landslide body is located in a mountainous area, the buildings considered are timber and concrete-timber chalets, masonry and concrete-masonry villas. In this case, the velocities used to calculate the indicators' vulnerability are relatively low, with a maximum of 60 cm/year, while the thickness of the landslide body is very high, reaching 80 m concerning the deepest sliding plane. The red square has a vulnerability value equal to 1 because, despite the failure surface being very deep, masonry is the least resistant material to tensile stress compared to concrete and wood. The grey indicators compared to the red squares have a considerably lower vulnerability calculated by referring to the higher strength parameters of timber and concrete.

7.4 Pont Bourquin landslide, Les Diablerets

7.4.1 Study area and available dataset

Pont Bourquin landslide is located in the Swiss Prealps, 40 km east of Lausanne city. We are dealing with a gravitational deformation appeared in the upper part of the

hill in 1990 and then developed along the slope over the next 10 years. The Pont Bourquin slope is affected by two main landslides: Pont Bourquin landslide and to the west of the latter, the Parchet landslide active since 2000s with a velocity of about 5-10 cm/year, shown in *Figure 39*.

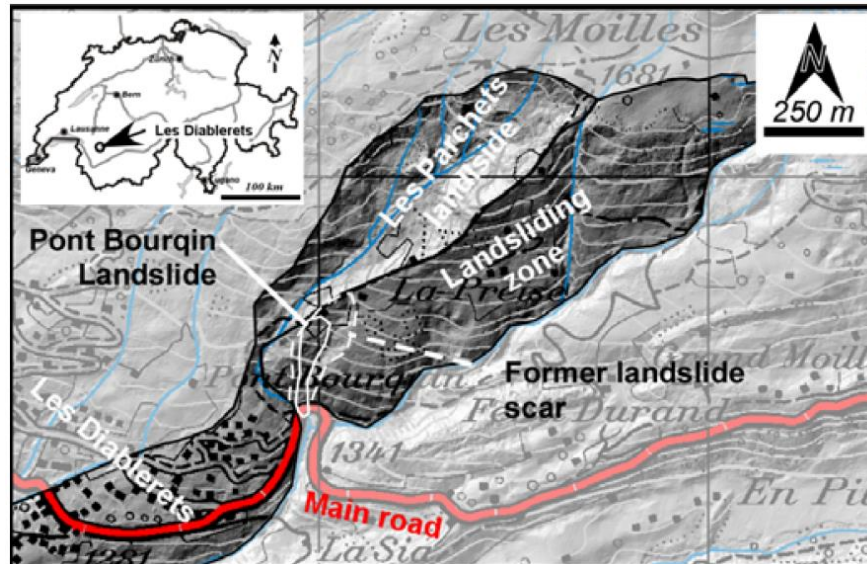


Figure 39: Pont Bourquin landslide area, near les Diablerets, (Jaboyedoff, et al. 2015)

The deepest part of the landslide has an average thickness of about 15-17 m and it is characterised by a subsidence at the top, which outlines the scar; while the shallowest landslide has a depth of about 5m with the landslide toe which lies above the cornieule. The deepest landslide has a volume reaching 40000 m³ and a total area of approximately 8200 m²; it has a length of approximately 244 m and a width varying between 12 and 60 m. The shallowest landslide, meanwhile, has a volume of approximately 11000 m³ and an area of up to 5000 m².

In September 2006, displacements of up to 80 cm is recorded, leading to the development of a translational landslide encompassing an area of 8000 m², having a width between 15 and 60 m. Another phenomenon occurred on 5 July 2007 after a period of heavy rainfall: an earth flow reached the Pillon Pass Road that connects two famous ski resorts of Les Diablerets in Gstaad (western Switzerland) at the point called Pont Bourquin. The landslide reached a maximum speed of 12 m/s approaching the road with a movement rate of 5 m/s and leaving an over two-metre accumulation of material. This earth flow has a volume ranging from 3000 to 6000 m³ and involves the upper 5 m of the deep landslide. Erosion processes, small translational or rotational surface landslides and earth flows led to material

accumulation at the foot of the landslide over the next three years, creating the collapse of the landslide toe between 18 and 20 August 2010.

Reactivation of this landslide is still possible and would bring damage to the nearby tourist site and to the previously mentioned road.

7.4.2 Geological Context

The Pont Bourquin landslide is defined a complex landslide because the events occurred start as a landslide and evolve as an earthflow due to the saturation of the surface material. The geological context of the Pont Buorquin landslide is extremely complex; three thrust faults with an inclination of approximately 35° northwards cross the landslide and separate geological formations. In the upper and lower part of the slope, the bedrock is composed of Triassic cargneule (cellular dolomite) associated with gypsum. These highly soluble and deformable rocks may have favoured the slope destabilisation at the landslide toe. Below the cargneule layer, the upper part of the slope consists of black schists of Alalenian origin, the erosion of which is the main source of clayey sliding material. In the central part of the slope, the landslide is overlain by flysch made up of thin-layered turbidites which include siltstones and conglomerates. The top of the hill is covered by several metres of moraine deposits. It is possible to define that the present-day landslide mass is mainly composed by four geological units: gypsum, more than 50 m of cargneule (high-permeability dolomite), 150 m of flysch formed by turbidites, siltstones and a few conglomerates, and 70 m of clay shales.

The main triggering landslide factor is surface erosion, which, together with the lack of vegetation, causes shallow earthflows. The rocks were heavily fractured by the Alpine orogeny and subsequently influenced by overturning phenomena; flexural toppling is another factor weakening shale rock which, when subjected to freeze-thaw cycles, deforms the rock mass in the first 10 cm, reducing the material's strength.

Regarding the July 2007 event, the dissolution of the gypsum and cornieule are the primary cause of the slope instability; this is due to increased pore water pressure leading to the complete liquefaction of the landslide mass with reduction in mechanical strength. This process is mainly triggered by heavy rainfall resulting in saturation of the unstable mass.

7.4.3 Results

The proposed methodology is applied to cases C and D, central part and toe of the landslide respectively. *Tables 40, 41* show the data used for the methodology application to Pont Bourquin landslide.

Table 40: Data used in the methodology application for case C, landslide central part

	HEIGHT (m)	VELOCITY (cm/year)	BUILDINGS CONSIDERED
CASE C	15	5	Timber Chalet
	17		Masonry Building
	20		Masonry Villa

Table 41: Data used in the methodology application for case D, landslide toe

	DENSITY (kg/m ³)	HEIGHT (m)	VELOCITY	BUILDINGS CONSIDERED
CASE D	1900	5	10 m/s	Timber + Concrete Chalet
				Masonry Villa
				Masonry + Concrete Villa
				Reinforced Concrete Building

The plots concerning case **D**, with indicators implemented on the basis of the obtained data from the analysis of this case study, is shown in *Figure 40, 41, 42*.

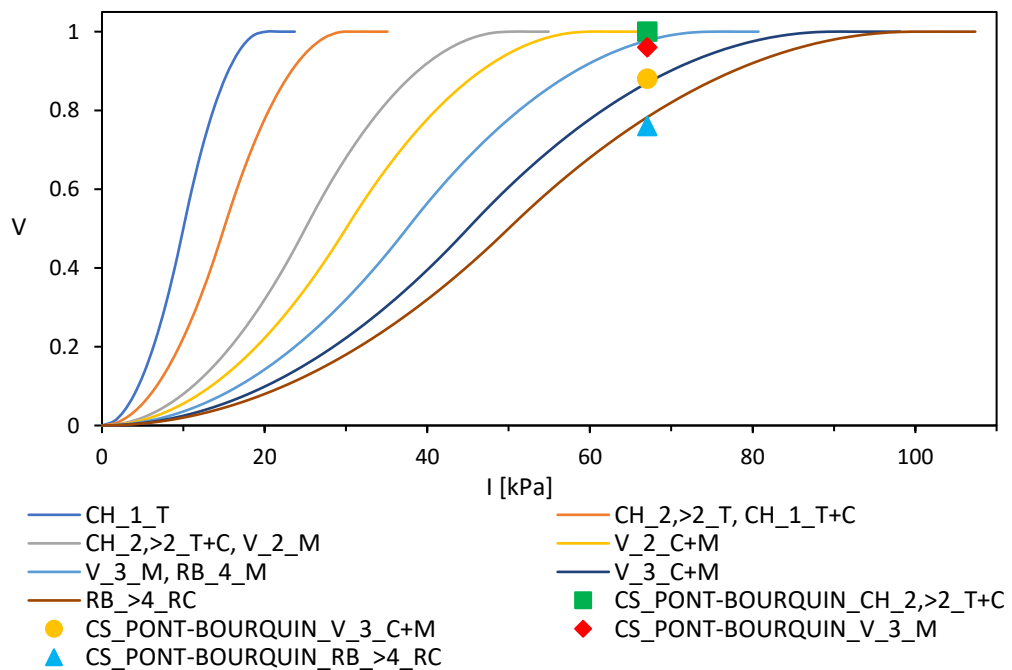


Figure 40: Vulnerability curves and indicators obtained for case **D** when the maintenance state is very poor

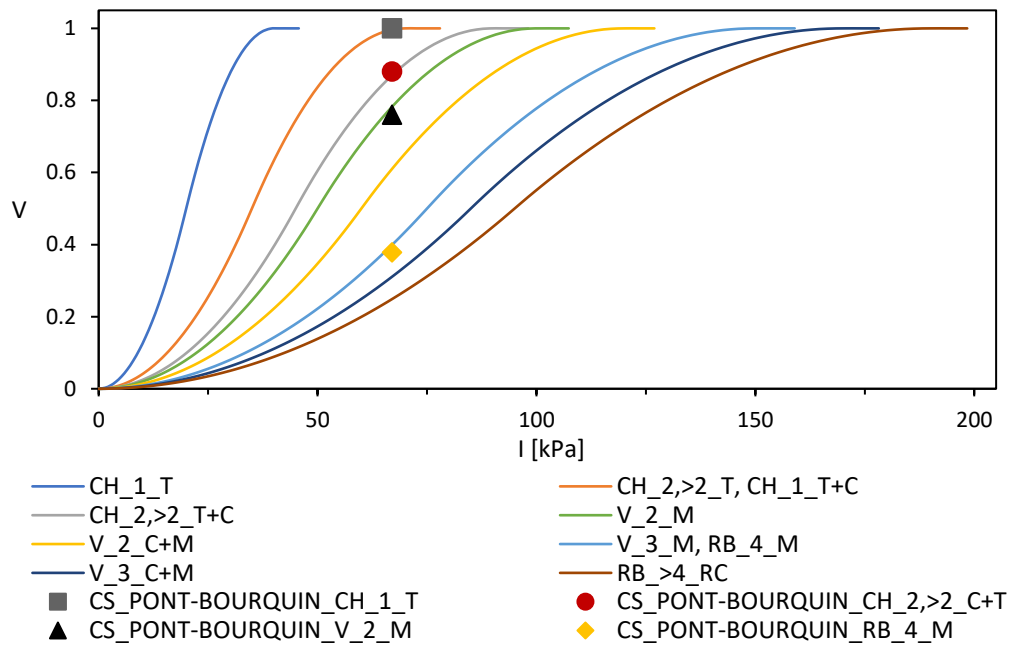


Figure 41: Vulnerability curves and indicators obtained for case **D** when the maintenance state is medium

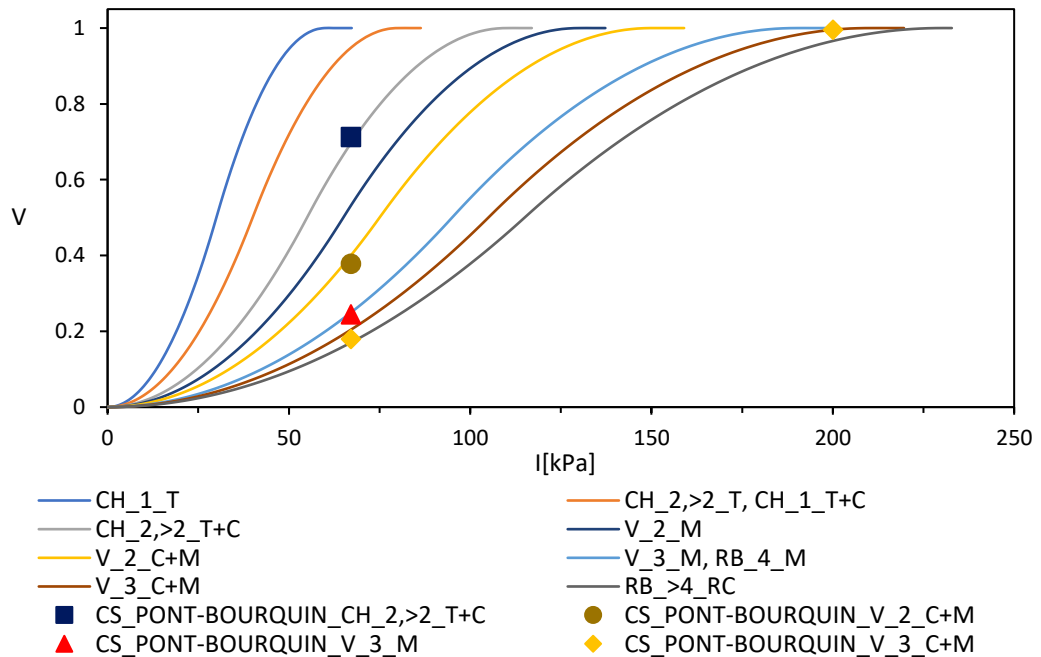


Figure 42: Vulnerability curves and indicators obtained for case **D** when the maintenance state is very high

The landslide toe is located in the area around Les Diableres, a mountain village and ski resort at an altitude of 1200 metres. The buildings considered, as shown in *Figure 43*, are timber and timber-concrete chalets, masonry and masonry-concrete villas and residential buildings with up to four storeys. In the third plots, it can be observed how, going from a low to a high state of maintenance, the vulnerability of

indicators representing buildings progressively decreases; the yellow rhombus indicates the buildings' vulnerability to an earth flow impact that reached a velocity of 12 m/s. All buildings considered at earthflow impact have vulnerability equal to 1 and are therefore all represented by a single indicator.



Figure 43: Les Diableres village, located in the municipality of Ormont-Dessus, Canton of Vaud, Switzerland

Chapter 8: CONCLUSIONS

This work introduced myself to scientific research from a base given by some courses held at the Polytechnic University of Turin such as Landslide and Slope Engineering, Consolidation of Rocks and Soils, etc. These topics were investigated at the Haute Ecole d'Ingénierie et de Gestion du Canton de Vaud- HEIG-VD, in Yverdon-Les-Bains, Switzerland. Starting from a state-of-the-art analysis of the existing literature, a methodology was developed concerning vulnerability assessment of buildings to landslides. The method developed aims to show how to analyse the impact of slow-moving landslides on buildings located in 4 different positions on the landslide body. Four positions were chosen by adopting the necessary simplifications in order to highlight the main areas where a building might be located.

The results of applying the above methodology are vulnerability curves constructed by means of function taking both the intensity of the landslide movement and the structural strength of the affected buildings. In all 4 cases analysed, intensity is calculated with reference to the slide of the landslide body understood as slow movement in cases A, B, C and as rapid movement impacting with a certain pressure on risk elements, in case D. Resistance, however, is evaluated as a product of weighted indicators based on the relevance given them in this work. The method's application to the case studies analysed allowed the following conclusions to be drawn:

- For cases A and C, concerning the crown and central part of the landslide respectively, the buildings are not very vulnerable, with a maximum V of 0.5 (out of a range between 0 and 1). An exception is provided by the data concerning La Frasse landslide, implemented on the vulnerability curves obtained for case C where: the high depth of the landslide body, relative to the deepest failure surface, together with a velocity of more than 1 metre per year, give a vulnerability of 1 for masonry buildings (material with the lowest tensile strength of those considered).
- Regarding case B, being the most difficult in terms of data retrieval and the most critical in terms of building vulnerability, due to the assumed position at the boundary between the landslide body and the stable slope, the

presence of chalets is supposed, resulting in a vulnerability of more than 0.5 in both low and high inclination conditions of the structure (out of a range between 0 and 1).

- Case D, however, showed that the most vulnerable buildings are timber chalets while the least one are reinforced-concrete buildings, taking the compressive strength of the different materials as the reference parameter.

Several studies and papers have dealt with building vulnerability to slow-moving landslides, some resulting in vulnerability curves similar to those presented in my work (vulnerability as a function of landslide intensity), others with fragility curves, (probability of exceeding a certain damage as a function of estimated cumulative displacement), (Peduto D. 2016), (Peduto, et al. 2017). The vulnerability curves presented by Chen, et al. (2020) use different parameters to calculate the intensity defined as the reverse of the building safety factor, constructing the curves by first varying the length (Figure 44, a) and then the width (Figure 44, b) of the building.

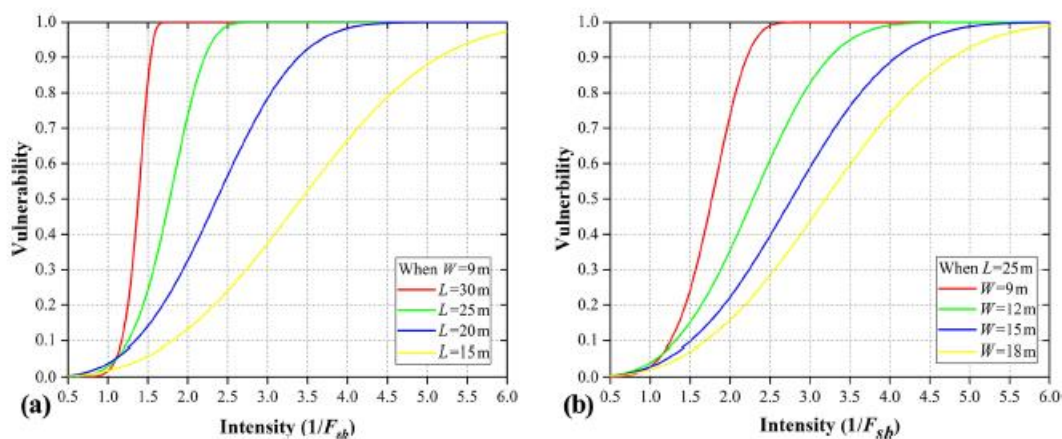


Figure 44: Physical vulnerability curves of buildings with different parameters: (a) length and (b) width, source (Chen, et al. 2020)

These curves indicate that independently from parameters used, for safety factors greater than 1 building's physical vulnerability with any length/width is very low (stable slope condition), whereas when F_s becomes less than 1 vulnerability increases depending on the length/width values considered. Making a comparison with my results, when the movements are minimal (i.e. very low velocities, a few cm/year and fracture surface relatively shallow) the vulnerability is low (condition of an approximately stable slope); whereas when the velocities are higher and the landslide event occurs (earthflow and sliding phenomena) vulnerability also

reaches high values, close to 1. These data can be reviewed in *Chapter 7* where the analysis of the 4 case studies considered is included.

Construction in areas affected by more or less stabilised and ancient landslides, or in geologically sensitive sites where stability is a key issue, can lead to situations whose severity is difficult to predict. A minor environmental impact, such as overburdening or rainfall, can cause greater damage due to density, value of buildings and structures exposed, and extent that a small landslide can reach beyond its initial limits. The development of practical methods that take slope instabilities and their evolution factors into account in the local planning of risk zones have to be considered. This work may open new perspectives to help spatial planning authorities select the most suitable areas for urbanisation. Furthermore, the presence of slope instability specialists should be required in the procedures for obtaining and granting building permits; this would be useful for both builders and local authorities to avoid building in geologically critical areas.

APPENDIX

- 1. TABLES WITH DATA USED FOR THE CONSTRUCTION OF THE VULNERABILITY CURVES**
- 2. GRAPHS CONCERNING VULNERABILITY CURVES AND CASE STUDIES**
- 3. GIS DRAWING BOARDS ABOUT LANDSLIDE ANALYSED IN THE CASE STUDIES**

REFERENCES

- Antronico, L., L. Borrelli, R. Coscarelli, e G. Gullà. «Time evolution of landslide damages to buildings: the case study of Lungro (Calabria, southern Italy).» (Springer-Verlag) March 2014: 47-59.
- Bonnard, Ch., F. Forlati, and C. Scavia. *Identification and Mitigation of Large Landslide Risks in Europe*. A.A. Balkema Publishers, 2003.
- Chen, L.X., K.L. Yin, e Y.X. Dai. «Building Vulnerability Evaluation in Landslide Deformation Phase.» (Science Press, CAS and Springer-Verlag) 2011: 286-295.
- Chen, Q., et al. «Assessment of the physical vulnerability of buildings affected by slow-moving landslides.» (Copernicus Publications) September 2020: 2547–2565.
- Coltorti, M., e D. Firuzabadì. «La Deformazione gravitativa profonda (DSGM) del versante orientale del Monte Amiata: un Geosito ed un itinerario geomorfologico in Toscana Meridionale.» January 2011.
- Dapples, F. *Instabilités de terrain dans les Préalpes fribourgeoises (Suisse) au cours du Tardiglaciaire et de l'Holocène: influence des changements climatiques, des fluctuations de la végétation et de l'activité humaine*. Thèse, Géosciences – Géologie et Paléontologie, Université de Fribourg, Fribourg: GeoFocus, 2002, 30-44.
- Egli, T. *Protection des objets contre les dangers naturels gravitationnels RTABLISSMENTS CANTONAUX D'ASSURANCE*. Traduzione di Nendaz H. Marro C. Berne: VKF/AEAI, 2005.
- Frodella, W., et al. «A method for assessing and managing landslide residual hazard in urban areas.» (The Authors) Landslide 15 (August 2017): 183-197.
- Froude, M. J., e D. N. Petley. «Global fatal landslide occurrence from 2004 to 2016.» *Natural Hazards and Earth System Sciences*, August 2018: 2161-2181.
- Highland, L., e M. Johnson. «Landslide Types and Processes, USGS science for a changing world.» 2014.
- Hill, B. V. «Analysis of the Parkway Drive Landslide, North Salt Lake, UT.» *All Graduate Plan B and other*, August 2018.
- Hungr, O., S. Leroueil, e L. Picarelli. «The Varnes classification of landslide types, an update.» (Springer-Verlag) Landslide 11 (November 2013): 167-194.

- Jaboyedoff, M., A. Pedrazzini, A. Loye, T. Oppikofer, e Güell i Pons M. «Earth flow in a complex geological environment: the example of Pont Bourquin, Les Diablerets (Western Switzerland).» July 2015: 131-137.
- Kang H., Kim Y. «The physical vulnerability of different types of building structure to debris flow events.» (Springer Science+Business) October 2015: 1475-1493.
- Keaton, J. R., et al. «The 22 March 2014 Oso Landslide, Snohomish County, Washington, Geotechnical Extreme Events Reconnaissance Turning Disaster into Knowledge.» (National Science Foundation) July 2014.
- Lacroix P., Handwerger A. L. and Bièvre G. «Life and death of slow-moving landslide.» *Nature Reviews Earth & Environment*, July 2020.
- Lacroix, P., A. Handwerger, e G. Bièvre. «Life and death of slow-moving landslide.» *Nature Reviews Earth & Environment*, July 2020.
- Li, P., e P. Mo. «A unified landslide classification system for loess slopes: A critical review.» *ELSEVIER* Volume 340 (April 2019): 67-83.
- Li, Z., F. Nadim, H. Huang, M. Uzielli, e S. Lacasse. «Quantitative vulnerability estimation for scenario-based landslide hazards.» (Springer-Verlag) *Landslides* 7 (January 2010): 125-134.
- Mainsant, G, e Brönnimann C., Jongmans D., Michoud C., Jaboyedoff M. Larose E'. «Ambient seismic noise monitoring of a clay landslide: Toward failure prediction.» *HAL open science*, June 2012: 1-12.
- Matti, B., L. Tacher, e S. Commend. «Modelling the efficiency of a drainage gallery work for a large landslide with respect to hydrogeological heterogeneity.» (NRC Research Press) July 2012: 968-985.
- Mavrouli, O., et al. «Vulnerability assessment for reinforced concrete buildings exposed to landslides.» (Springer-Verlag) February 2014: 265-289.
- Miteva, T., e E. Prina Howald. «Vulnerability assessment of different types of building structures to debris flow events.» (GEAM ambiente) april 2022: 14-21.
- Papathoma-Köhle, M., B. Neuhäuser, K. Ratzinger, H. Wenzel, e D. Dominey-Howes. «Elements at risk as a framework for assessing the vulnerability of communities to landslides.» (European Geosciences Union) December 2007: 765-779.
- Parkash, S. *Training Module on COMPREHENSIVE LANDSLIDES RISK MANAGEMENT*. First 2012, Second 2020. New Delhi, India: Author and National Institute of Disaster Management (NIDM), 2020.

- Peduto D., Pisciotta G., Nicodemo G., Arena L., Ferlisi S., Gullà G., Borrelli L., Fornaro G., Reale D. «A procedure for the analysis of building vulnerability to slow-moving landslides.» *Metrology for Geotechnics*, March 2016: 248-254.
- Peduto, D, et al. «A procedure for the analysis of building vulnerability to slow-moving landslides.» March 2016.
- Peduto, D., S. Ferlisi, G. Nicodemo, D. Reale, G. Pisciotta, e G. Gullà. «Empirical fragility and vulnerability curves for buildings exposed to slow-moving landslides at medium and large scales.» *Springer Landslides* 14 (April 2017): 1993-2007.
- Popescu, E. M. «Landslide causal factors and landslide remediatial options.» s.d.
- Tsironi, V., A. Ganas, I. Karamitros, E. Efstathiou, I. Koukouvelas, e E. Sokos. «Kinematics of Active Land-slides in Achaia (Peloponnese, Greece) through InSAR Time Series Analysis and Relation to Rainfall Patterns.» (MDPI) February 2022: 2-20.
- Uzielli, M., F. Catani, V. Tofani, e N. Casagli. «Risk analysis for the Ancona landslide—II estimation of risk to buildings.» *Springer Landslide* 12 (February 2014): 83-100.